Atmospheric Diffusion Experiments with SF_6 Tracer Gas at Three Mile Island Nuclear Station Under Low Wind Speed Inversion Conditions

GPU ELECTRIC POWER COMPANIES

ATMOSPHERIC DIFFUSION EXPERIMENTS WITH SF_6 TRACER GAS AT THREE MILE ISLAND NUCLEAR STATION UNDER LOW WIND SPEED INVERSION CONDITIONS

Pickard, Lowe, and Associates, Inc.
The Research Corporation of New England
General Public Utilities Service Corporation

January 1972

TABLE OF CONTENTS

TABLE OF CONTENTS (continued)

TABLE OF CONTENTS (continued)

TABLE OF CONTENTS (continued)

1407 006

LIST OF TABLES

LIST OF TABLES (continued)

LIST OF FIGURES

LIST OF FIGURES

LIST OF FIGURES

SECTION 1.0
INTRODUCTION

1.1 General

Weather data collected for several years at the Three Mile Island Nuclear Station site indicate considerable meander during low wind speed conditions. These conditions, which occur about 5% of the time, are observed on the wind direction recordings primarily during nighttime. Since many of these data are taken at very low wind speeds, near the threshold of the direction vane, it is important to determine whether the meander observed is truly representative of the wind conditions or is just an inaccuracy of the measurement due to characteristics of the vane.

Because of this potential inaccuracy, it has been the practice in recent reactor licensing cases to assume poor diffusion conditions both vertically and horizontally when these conditions exist during low wind speed conditions at night. Since it is required that the design basis accident diffusion conditions be such that site boundary concentrations are exceeded no more than 5% of the time, these conditions (which are usually assigned Pasquill F or G stability) play a significant role in the determination of accident diffusion estimates.

If the meander is real, however, the amount of effluent which would reach a stationary receptor during an accident would be considerably lower than the amount computed using a stable plume model in the Gaussian equation, as is customary in reactor licensing cases. It is the intent of this experiment to determine whether concentrations can be predicted conservatively but accurately during low wind speed inversion conditions, using meteorological data collected at the site. If the prediction procedure is validated, it is expected that these wind conditions would not appear among

those which yield the highest 5% of predicted concentrations.

The SF_6 gas tracer experiment discussed in this report was designed to accurately measure average concentrations during nighttime inversion and low wind speed conditions during a 45-minute release of tracer gas. Measurements were made in the "free field" and in the vicinity of large plant structures. Results are compared to predictions made using various models to determine the appropriate model for use with the Three Mile Island site weather data.

1.2 Experimental Procedure in Brief

1.2.1 General

The basic procedure involves the continuous release of a suitable tracer substance under controlled and monitored conditions at a given point on the site. This substance is then collected at constant rates in evacuated tanks for at least a 45-minute time period at various locations around the release point.

The requirements for the tracer were that it had to: (1) be essentially inert with respect to the environment; (2) be nontoxic, (3) have a low background in the site area; (4) be noncendensable; (5) be nonparticulate; (6) be non-buoyant in air; and (7) be detectable in poor visibility conditions at very low concentrations. Sulfur hexafluoride (SF_6) at very low concentrations meets all these requirements, and a detector having a threshold sensitivity of less than one-tenth of a part per billion is commercially available.

Each tank assembly consisted of an evacuated 16 liter chamber fitted with a vacuum gauge and constant flow rate apparatus. Gas samples were collected by permitting the tanks to fill simultaneously for a fixed period

of time. The tanks were returned to the field laboratory still partially evacuated, and then brought to ambient pressure by admitting clean bottled air. The resulting SF_6 tank concentrations was then measured with an Analog Technology Corporation Tracer-Gas Leak Detector. This detector was also used to measure elevated samples and to measure off-site downwind concentrations during mobile traverses.

Wind measurements were made at three locations during each test, and vertical temperature difference was measured at one location. Supplementary wind information was also obtained by releasing smoke candles and recording visual observations during the test.

1.2.2 Experimental Phases

The experimental program included three phases. In Phase I, an open field was used, with the tracer being released as a "point source" in the center of a 300 foot radius circular grid with 18 sample tanks spaced around the circumference. Elevated samples were also taken using a balloon system. The purpose was to measure concentrations at the samplers without the influence of building obstructions. Five tests were conducted in Phase

Phase 2 involved the release of gas in the wake of large structures already present in the nuclear plant complex. Releases were made near the Unit 1 containment building at or near grade level. These tests simulate as close as practicable the actual conditions that would exist in the event of the accidental release of radioactive material during periods of low wind speed, inversion conditions. Ideally the sample tanks should have been located at 2000 ft, which is the site exclusion boundary; however, the presence of the river made this impractical. The tanks were located as far

as possible from the release point, limited by the river's edge and other structures, to approximately an 800 ft circle. Vertical concentration profiles were again measured using a balloon during each Phase 2 test. Five tests were conducted in Phase 2.

The Phase 3 test was dedicated to collecting time-integrated elevated samples using four helium filled balloons to support tubing which terminated at several elevations. Integrated samples over a 45-minute period were collected in evacuated bottles connected to the tubing at grade level. Mobile traverses off-site were conducted during two of the tests in Phases 2 and 3.

1.2.3 Scheduling of Tests

Daily weather forecasts prepared specifically for the site by a private weather service were used for scheduling experiments. Personnel were put on alert if the prediction was for near calm conditions. The final decision for a test was made just prior to the scheduled time. Table 1 lists the test dates and summarizes the weather conditions.

1.3 Participants

This experiment was funded by the Metropolitan Edison Company (Met Ed), Pennsylvania Electric Company and Jersey Central Power and Light Company, who are the owners of the Three Mile Island Nuclear Station. On behalf of General Public Utilities Service Corporation (GPU), Pickard, Lowe and Associates, Inc. (PLA) directed the project in consultation with Dr. James Halitsky (University of Massachusetts). The Research Corporation of New England (TRC) was retained to develop the techniques for, and to conduct, the field measurements. Project planning, experimental design and data analysis was provided by Keith Woodard (PLA), Dr. Halitsky, George F. Collins (TRC), and George Kunder (GPU). The Metropolitan Edison Company, who will operate the nuclear station, provided additional personnel and equipment in the field where necessary.

SECTION 2.0

SUMMARY OF RESULTS

2.1 General

All tests were conducted during low wind speed inversion weather conditions, and the expected meander was observed during most of the tests. Measurements of pertinent weather parameters made at several locations on-site during the tests served as input to a series of models developed for predicting the tank concentrations. The "best" models were found to be those which accounted for the wind meander. Comparison of results with the model commonly used in reactor licensing showed the licensing model was very conservative. Following is a discussion of the results for each phase.

2.2 Phase 1

Table 1 summarizes the weather conditions during the Phase 1 tests. In almost all cases the tracer was detected over more than a 150° arc, demonstrating that the meander recorded on the wind instrument was real. In general, locations of the maximum concentrations corresponded to measurements of wind direction persistency during the tests.

Five point source or "P" models described in Section 4.2 were compared for each test. A summary of the Phase 1 model predictions versus measured concentrations is included in Table 12. The model which is commonly used in licensing cases, referred to as Model 1P ("AEC/DRL ΔT Model"), over-predicted the concentrations by an average factor of 21. The best

model, Model 4P ("Sector Average Model"); which takes into account the meander effect, had an average χ_{max}/χ_{model} ratio of 1.27 for the Phase 1 series. This constitutes excellent agreement for a diffusion study of this nature. Model 3P ("Split σ Model") was the next best (conservative) performer, while Model 2P ("Slade σ_θ Model"), underpredicted (non-conservative) by almost a factor of two for these weather conditions.

One further comaprison is of note. Using the AEC Safety Guide 4 meteorology of Pasquill F and 1.0 m sec^{-1} in the standard Gaussian equation (Model 1P), the results of Phase 1 tests (which had wind speeds less than 1.0 m sec^{-1}) were overpredicted by an average factor of 5.8.

2.3 Phase 2

As shown in Table 1, low wind speed inversion conditions prevailed for tests conducted in the vicinity of the reactor building complex. Phase 2 measured concentrations were considerably lower than in Phase 1 due to the aerodynamic turbulence of the buildings and greater distance to the samplers. The meander effect was observed in several tests and contributed, along with the building wake effect, to the very low measured concentrations.

Five building wake or "W" diffusion models were tested in Phase 2 (see Section 4.3) with the results being more difficult to correlate. In two of the tests (Tests 7 and 8) the models predicted sample concentrations very well; however, in the remaining three tests, the "best" models overestimated concentrations by a substantial factor. The "best" model was, however, the one which accounted for the meander condition as well as for the wake effects.

It is believed, as discussed later in this report, that for several

tests the building effect caused the maximum concentrations to occur above the tanks during very stable conditions. This belief was substantiated by qualitative visual observations of smoke plumes where it was commonly noted that, despite the low wind speed inversion conditions, the smoke was initially transported vertically in the region of the reactor building, and only after gaining considerable altitude did the plume acquire a horizontal trajectory. Quantitative evidence of this plume behavior was provided by a series of instantaneous vertical profiles of SF_6 concentrations measured from the ground to a height of 200 ft which show that the gas is initially distributed vertically by the building wake.

2.4 Phase 3

Because it was suspected that the maximum concentrations may have occurred above the ground samplers, it was decided to obtain time integrated samples of the vertical plume concentrations. This was accomplished in the single Phase 3 test where average concentrations at several elevations up to 250 ft were measured at four radial locations on the circumference of the 800 ft grid. Results showed a marked increase in concentration with height. However, the maximum measured concentration was lower than the predictions of all models.

Since the maximum concentration was aloft at a radial distance of 800 ft, it was considered necessary to determine concentrations at the site boundary and beyond. To accomplish this, a series of mobile traverses were made generally downwind to a distance of three miles. These results further validated the model proposed for use during low wind speed inversion conditions at Three Mile Island.

SECTION 3.0

CONCLUSIONS

The diffusion of the sulfur hexafluoride tracer gas over flat terrain within the valley and in the turbulent wake of large structures during low wind speed inversion conditions was shown to be satisfactorily described by models which account for plume meander. Model 1P ("AEC/DRL ΔT Model") which is the common Gaussian equation (corrected for wake effects) with Pasquill stability categories based on vertical temperature structure, is overly conservative during these conditions. This experimental program validated the use of Model 5W ("Sector Average Wake Model"), which is a more appropriate, yet conservative, model for prediction of diffusion during periods of low wind speed inversion (nighttime) conditions.

SECTION 4.0

THEORY AND MODELS

4.1 Diffusion Models

The purpose of this section is to test various diffusion models for comparison with experimental results. In particular, it is desired to find an expression which predicts χ/Q; where χ is the downwind maximum ground level concentration for a given release rate Q. This expression should be based on weather parameters collected during the test in the same manner as in the site weather program so that the expression can be applied using previously recorded data.

Many models have been developed in the past by experimenters for the prediction of diffusion. These are based on wind speed and some indication of atmospheric turbulence. The predictors of turbulence have included time of day, radiation to or from the ground, horizontal and/or vertical wind fluctuations, combinations of speed and horizontal fluctuations, and vertical temperature difference. In this section, models based on wind speed, wind direction fluctuation and vertical temperature difference are examined. A summary of all models considered in this study is included in Table 2.

Diffusion models which are generally accepted employ a Gaussian equation in which atmospheric turbulence is expressed in terms of the standard deviations of plume concentrations both vertically (using σ_z) and horizontally (using σ_y). Curves which give σ_y and σ_z as a function of distance for six Pasquill diffusion categories are shown in Figures 1 and 2. The G category used by the AEC/DRL is represented by a curve located the same distance below F as E is above F on the curves.

Several methods have been proposed for selection of the appropriate curves. Slade, in Meteorology and Atomic Energy[1], proposed the use of the

standard deviation of azimuthal wind direction angle (σ_θ) according to Table 3. For licensing cases, AEC/DRL has proposed the use of vertical temperature difference (ΔT) alone for selection of diffusion categories as given in Table 4. Others have used a combination of σ_θ and ΔT.

Models selected for this study are described below.

4.2 Diffusion from a Point Source (Phase 1)

4.2.1 The Gaussian Diffusion Equation

For a ground-level continuous point source, the equation which yields centerline ground-level concentrations is:

$$\chi = \frac{Q}{\pi \bar{u} \sigma_y \sigma_z} \qquad (1)$$

where χ is the centerline surface concentration (in parts per part), Q is the source strength (release rate of SF_6) in $m^3\ sec^{-1}$, $\bar{u}$ is the average horizontal wind speed in $m\ sec^{-1}$, and σ_y and σ_z are the horizontal and vertical dispersion coefficients from Figures 1 and 2 respectively, in meters.

Equation (1) is used to obtain the first three point source models (designated P) as follows:

Model 1P ("AEC/DRL ΔT Model"): Uses equation (1) with the ΔT groups given in Table 4 to define both σ_y and σ_z.

Model 2P ("Slade σ_θ Model"): Uses equation (1) with the σ_θ groups given in Table 3 to define σ_y and σ_z.

Model 3P ("Split σ Model"): Uses equation (1) with the ΔT groups of Table 4 and the σ_θ groups of Table 3 to define σ_z and σ_y respectively.

4.2.2 The Sector Average Equation

If equation (1) is integrated over all values of y and divided by the length of arc of angle θ (in radians) at distance x, we obtain the average concentration along the arc of:

$$\bar{\chi} = \frac{Q\left(\frac{2}{\pi}\right)^{1/2}}{\bar{u}\,\sigma_z\,x\,\theta} \qquad (2)$$

The fourth model is defined as follows:

Model 4P ("Sector Average Model"): Uses equation (2) with θ equal to the maximum wind direction meander (range) during the sample period, and σ_z based on the ΔT groups of Table 4.

4.2.3 Directional Frequency Model

Model 4P assumes that the plume meanders within the boundaries of the measured angular range. However, a variation of this maximum range model, also applicable to long-period stationary sampling, has been suggested. This fifth model assumes that the sampler is in the direct path of the plume for some fraction of the total sampling interval and that the remainder of time the plume makes no contribution to the measured concentration. The fraction of time is taken from the recordings of wind direction during the test interval. The relevant equation for the peak concentration is equation (1) modified by f, where f is the highest frequency of wind in any 10° sector during the test. The equation is as follows:

$$\chi = \frac{Qf}{\bar{u}\,\sigma_y\,\sigma_z} \qquad (3)$$

The fifth model is specified as follows:

Model 5P ("Directional Frequency Model"): Uses equation (3) with σ_y and σ_z based on ΔT in Table 4.

4.3 Diffusion in the Wake of Large Structures (Phase 2)

When material is released near large structures, the turbulence created by the wake provides additional mixing. Tests in wind tunnels have formed a basis for model development; however, few field experiments have been run, especially during low wind speed inversion conditions. Based on wind tunnel tests and theory, the following models were considered for comparison with the results of Phase 2 tests.

4.3.1 Building Wake Correction to the Gaussian Equation

To account for building wake effects, equation (1) is modified as follows:

$$\chi = \frac{Q}{\bar{u}\,(\pi\sigma_y\,\sigma_z + cA)} \qquad (4)$$

where

c = the shape factor, and

A = the cross sectional area of the building (m^2).

The AEC in Safety Guide Number 4[4] uses the same relationship with a shape factor c = 0.5 and building area equal to the smallest vertical cross section area of the reactor containment building. The AEC also imposes the restriction that the concentration calculated according to equation (4) not be less than 1/3 of that calculated according to equation (1).

There is some question as to whether c should be assigned the value of

0.5. Dr. J. Halitsky has published isopleths of non-dimensionalized concentration (K_c) based on wind tunnel experiments with a typical or complex as described in Meteorology and Atomic Energy[2], page 251 and reproduced as Figure 3 herein. K_c is related to the shape factor c by:

$$c = \frac{1}{K_c} - \frac{\pi \sigma_y \sigma_z}{A} . \qquad (5)$$

Using a sampler distance of 800 ft and a containment diameter of 150 ft, the non-dimensionalized distance, from the center of the containment to the sampler is 5.4. Therefore, from Figure 3, the value of K_c was about 0.5 value at the samplers. The turbulence intensity in the wind tunnel at the mid height of the model was about 4%, corresponding to a Pasquill F stability. Therefore, σ_y, σ_z at the sampler was about 50 m^2. Inserting these values into equation (5) with a TMI containment area A = 2000 m^2 yields $c \approx 2$.

This leads to two variations to the point source model forming four wake models (designated with a W) as follows:

Model 1W ("ΔT Wake Model"):	Uses equation (4) with cA based on area of containment with c=2, and ΔT groups in Table 4.
Model 2W ("Slade σ_θ Model with Wake Correction"):	Uses equation (4) with cA based on area of containment, c=2, and σ_θ group in Table 3.
Model 3W ("Split σ Wake Model"):	Uses equation (4) and both Tables 3 and 4 as for Model 3P, cA based on area of containment and c=2.
Model 4W ("AEC/DRL ΔT Wake Model"):	Uses equation (4) with cA based on containment area, c=0.5 and ΔT from Table 4. Maximum wake correction is 3.

4.3.2 Sector Averaging with Building Wake Included

Since the meandering wind effectively disperses the released material

in a wide area, a model was developed which would take both the building wake and the meander into account. The basic equation in a Gaussian form was suggested by Davidson and appears on page 112 of Meteorology and Atomic Energy[3] as follows:

$$\chi = \frac{Q}{\bar{u}\,\pi\,\Sigma_y\,\Sigma_z} \exp - \left(\frac{y^2}{2\,\Sigma_y^2} + \frac{h^2}{2\,\Sigma_z^2} \right) . \qquad (6)$$

For ground level releases h = 0. If this is integrated over all values of y and divided by the sector arc length θ at the sample distance x as in equation (2) above, the equation becomes:

$$\bar{\chi} = \frac{Q \left(\frac{2}{\pi}\right)^{1/2}}{\bar{u}\,\Sigma_z\,x\,\theta} , \qquad (7)$$

where

$$\Sigma_z = \left[\sigma_z^2 + \left(\frac{cA}{\pi} \right) \right]^{1/2} \text{ and}$$

θ = maximum wind direction meander (radians). The fifth building wake model is defined as follows:

Model 5W ("Sector Average Wake Model"): Uses equation (7) with c=2, A=2000 and σ_z from Table 4.

SECTION 5.0

EXPERIMENTAL TECHNIQUE

5.1 General

The first use of sulphur hexafluoride (SF_6) as a gas tracer took place at the Connecticut Yankee Atomic Power Plant in 1963 and 1964 (Collins et al, 1965)[5]. At that time elaborate laboratory analysis was required to measure the collected sample concentration. The gas chromatographic technique used was refined and reported on again by Turk et al, 1968[6]. The study at Three Mile Island introduces significant improvements in both the sampling and analytical techniques.

The SF_6 sampling and analytical procedure is described in detail in Appendix A. Following is background information attesting to the suitability of SF_6 as a tracer gas.

5.2 The Suitability of SF_6

As discussed in Section 2, SF_6 is ideally suited to gas tracer experiments. To quote Turk et al[6], "SF_6 is particularly useful because it is amenable to ultra sensitive analysis by electron-capture detection, is convenient to handle and dispense into air, is odorless and non-toxic, is chemically and thermally stable, and does not usually occur in significant concentrations in outdoor air". Additional advantageous properties are its low solubility in water and its density which is somewhat heavier than air.

The Three Mile Island site environs were thoroughly checked for SF_6 background concentrations. It was found that some switchgear was leaking which was repaired. After this repair, no further problem with background was encountered.

5.3 SF_6 Detection Technology

The principal of electron capture is briefly described by Collins et al[5]. The measurement of SF_6 concentrations was recently vastly simplified by the introduction on the market of a portable tracer-gas leak detector manufactured by Analog Technology Corporation. This instrument, according to the manufacturer, responds to SF_6 with a sensitivity of greater than one part in 10^{11}. The Model 112B has a continuous sampling mode and a discontinuous or columnar mode for high-sensitivity measurements. The latter mode was used for tank sampling in this study. Two such instruments were on-site during each test.

The availability of this gas-leak detector greatly facilitated the measurement of sample concentrations since samples could be analyzed directly by inserting the detector probe into the collection tank. It was found that concentrations could be reliably measured over a range of values from 0.01 to about 3000 parts per billion. This was verified by shop calibration using standard SF_6 sources prepared especially by the laboratories of Axton-Cross.

An additional feature is that the battery-operated instrument could be utilized to measure real-time instantaneous concentrations of SF_6 present in the air. This feature was used in the field to locate the plume, to conduct mobile traverses, and to obtain both vertical profiles of SF_6 concentrations.

5.4 Sampling Equipment

The sampling tanks used were first described by A. Turk[6]. However, it was found that more reliable measurements could be taken if a vacuum gauge were installed at the end opposite to the constant flow controller (see Appendix A). The complete tank assembly is shown schematically in Figure 4.

The sampling method was improved after several trial runs to achieve a calibrated flow on each tank of 0.2 liters min^{-1} which would provide a 45 minute sample interval. Twenty such tank assemblies were available for each test. In both Phases 1 and 2, eighteen of these tanks were arranged as close as possible to the circumference of a circle and were spaced 20° apart.

5.5 Release Equipment

The SF_6, which was released at the center of the grid, was discharged at a constant rate through a rotameter. A schematic of the release system is shown in Figure 5. The gas was released for about 15 minutes prior to sample tank opening to establish steady-state conditions. Samplers were all opened simultaneously at the established time. The rotameter was continuously checked by the person assigned to the release point, and periodic entries were made in a log including comments on general weather conditions, the measured flow rate of gas and the trajectory of smoke from smoke candles released periodically during the test.

5.6 Sample Analysis

After the tanks were shut off, they were returned to the field lab, brought to a pressure of 1 atmosphere, and sampled. Accurate determination of the sample volume was made, as indicated in Appendix A, for use in accurately finding the sample concentration.

The gas detectors could be set at any one of four sensitivity ranges. The output was read in volts, and then converted to concentration in ppb from calibration curves. An example of the gas analyzer trace produced by the strip chart recorder is shown in Figure 6. The voltage produced varies linearly with the sample concentration such that only one known concentra-

tion of SF_6 was required to draw the calibration curve. When possible, a second concentration was used to increase the reliability. Each of the recorders was calibrated on all four ranges at the TRC labs using standard concentration sources.

SECTION 6.0

ON-SITE METEOROLOGICAL DATA

6.1 General

Measurements of pertinent meteorological parameters were recorded at several locations on the Three Mile Island site throughout the test. These data were reduced for periods coinciding with the tests and the results are summarized in Table 1 and in Appendix B. Data reduction techniques are also discussed in Appendix B. Details of the monitoring program are discussed below.

6.2 Temperature Data

There are two permanent micrometeorological towers installed on the site, one north and the other south of the power plant (see Figure 7). The north tower is instrumented with thermistors housed in Geotech aspirated radiation shields which provide values of the temperature difference between the 150-foot and the 25-foot levels. The average value of ΔT during each test, expressed in degrees Centigrade per 100 meters, served as the basis for determining the Pasquill Stability Category from Table 4. A typical recorder trace of the temperature difference data is shown in Appendix B.

6.3 Wind Data

Wind speed and direction were recorded at three locations during the tests. For the Phase 1 tests, a Weather Measure Model W1034-540 low threshold recording wind system with three-cup anemometer, 0-10 mph full scale speed range, and a 0-540 degree directional range was used. This instrument was installed to record the wind speed and direction at the 30 ft level above the SF_6 release point (see Figure 7). The Weather Measure instrument yielded the direction data which were used in conjunction with Table 3 for

Phase 1 models.

For Phases 2 and 3, the wind data were obtained primarily from the 100 ft level on the north tower. This information was supplemented by wind records from the 100 ft level on the south tower. Data from both towers are summarized in Appendix B. Both tower locations are shown on Figure 7. The equipment used for these installations are Beckman and Whitley short vane anemometers with a starting threshold of 0.6 mph; the recorders are manufactured by Esterline-Angus.

Examples of typical recorder traces of the wind data and a description of the data reduction appears in Appendix B.

6.4 Smoke Candles

It was also found that smoke candles were an important source of additional wind information, yielding not only surface wind direction, but also providing some qualitative indication of plume behavior. For example, during the Phase 2 tests in the building wake, the smoke exhibited a marked tendency to be transported vertically; candles ignited at the reactor building base (i.e., at the SF_6 release point) often revealed the presence of wind currents which carried the smoke upward along the reactor wall and over the roof. Where relevant, the observers' comments of the smoke plume behavior are included in the discussions of the individual tests.

SECTION 7.0

DESCRIPTION OF PHASE 1 TESTS

(OPEN FIELD SITE)

7.1 General

In this portion of the study the site consisted of a relatively level plowed field south of the construction area. The 18 sampling tanks were suspended from stakes five ft above ground arranged approximately in a circle centered on the 30 ft Weather Measure tower which was the SF_6 release point. The location of the Weather Measure is shown in Figure 7. The exact positions of the sampling tanks relative to the release point are given in Table 4.

7.2 Summary and Results of the Five Phase 1 Tests

Table 6 is a summary of the basic test data including observed and derived weather parameters from the 30 ft tower. These data were used in the prediction calculations shown for Models 1P through 5P in Table 7 through 11 respectively. Wind direction range divided by 6 was used to predict σ_y which is conservative compared to the calculated values of σ_θ also shown in Table 6. Table 12 summarizes and compares the results of each model with the Phase 1 test results. Note that Test 1 served as a shakedown test and did not yield meaningful data.

Figures 8 through 12 inclusive are polar projections centered on the SF_6 release point for each of the 5 tests. The "range rings" are designed to be used with three different scales. As a distance scale, they indicate the location of the sampling tanks from the release point. Their second function is to indicate the concentrations of SF_6 in ppb measured in the collected samples. Note that this is an exponential scale, with marked values of 100, 400, 900 and 1600 ppb. In essence, the concentrations are

depicted in a bar-graph form where each bar extends a radial distance outward from the tank position corresponding to the concentration. Note that, because the sample tanks are not located on a perfect circle, the concentration around the release point is indicated by the end of the bar and not the length of the bar. The increasing width with length of the concentration bars are intended merely to dramatize the variations in the values, and have no quantitative meaning.

The third use of the concentric rings is to provide a linear scale for the time duration, in minutes, of each wind direction during the course of the sampling time. These data are indicated by straight lines which emanate from the center. Angular resolution was chosen to be 10°. Solid segments indicate that the corresponding wind speeds were measurable by an anemometer, while dashed portions are used for periods of calm. Dotted lines denote data inferred from visual observations of smoke candle plumes and the wind vane. The bearing at which a given wind duration is drawn indicates the direction from which the wind was blowing.

7.3 Individual Tests

7.3.1 Test 2

On the basis of the vertical temperature profile, Test 2 was the most stable test in Phase 1 with an observed increase in temperature with height of 4.26 C/100 m. However, as was the case for all five tests in this phase, the wind meandered through more than 150° which would indicate there was considerable lateral spread.

Highest sample concentrations were measured at tank positions 13 (260°), 14 (280°) and 15 (300°) where the values were 2610, 1797 and 840 ppb respectively (see Figure 8). This is in good agreement with the wind direction

data. Both the 120° and the 100° durations of 6.7 min and 8.3 min respectively fit the concentrations well at positions 14 and 15. The highest concentration, which was at position 13, was downwind from the 80° wind for only 1.7 min. However, if the 90° wind duration is added to this value, the total duration becomes 10 min. The overall average speed was 0.62 m sec^{-1}, the highest of any test in this phase.

High sample concentrations were measured at all positions between bearings of 200° and 20°. The average sample tank concentration for this sector was 711 ppb, and the maximum tank concentration was a factor of 3.7 higher. This quantity is referred to hereafter as the peak-to-mean ratio. Although this was the highest for this phase, it must be noted that (as shown in Table 5) the sample grid for this test was not a uniform circle as for the remainder of Phase 1 tests.

Considering the prediction models for downwind concentration (Table 12) Model 1P ("AEC/DRL ΔT Model") fit the data poorest of all with a value for χ_{max}/χ_{model} of 0.096, while Model 3P (Split σ Model") gave the best agreement with a value for the ratio of 0.7.

7.3.2 Test 3

This test took place with a lapse rate of 2.97 C/100 m and again the direction meandered through more than 165°. Although the highest concentration, 1788 ppb, was measured at position 17 (340°), concentrations of over 100 ppb were measured in all the samples between bearings of 100° and 20° inclusive, a range of 280° (see Figure 9). This is in qualitative agreement with the high variability of the horizontal wind direction, which ranged from 60° to 235°, but does not explain the concentrations measured at positions 4 through 11. The wind record indicates no component toward

these positions. However, the longest duration was 10.2 min for the 106° wind, which is in direct line with the peak concentration.

Careful examination of the wind record indicates that, of the total sampling period of 50 min, a calm condition prevailed for about 36 min. Thus, usefulness of the corresponding measured wind vane directions, shown by dashed radials in Figure 9, is in question. Transcribed below are the notes made by field observers on the behavior of smoke plumes released at the test site.

Time (EDT)		Observed Smoke Plume Behavior
First Observer	Location:	SF_6 Release Point
0430		Toward W.
0445		Toward NW.
0500		Very little movement.
0505		Drift toward E, then toward SE. Previous smoke puff did 180° turn.
0525		Toward W, NW.
Second Observer	Location:	North of Release Point
0425		Drifting to W.
0448		Plume rose upward and with very slight drift to N, not very far.
0452		Smoke sitting just N of SF_6 release point, estimated height 100-150 ft. Smoke cloud not moving.
0456		Plume rises to about 25 ft, then drifts very slowly N.
0506		Smoke drifting slowly to SE.
0517		Drifting to W.
0525		Plume drifting W.
0530		Plume sitting about 75 ft W of SF_6 release point.

These comments tend to explain the concentration pattern on the polar diagram.

Turning now to the models, the maximum observed concentration of 1788 ppb yielded a χ_{max}/χ_{model} of 1.28 for Model 4P ("Sector Average Model"). This model showed best agreement, not only in Test 3, but in Tests 5 and 6 as well.

7.3.3 Test 4

The lapse rate was again stable at 2.83 C/100 m and the meander of 175° was the largest measured. Based on the previous discussion of meander effects, significant concentrations would be expected to occur at many sampling points, and this was indeed the case (see Figure 10). With the exception of location 16 (81 ppb), values exceeded 100 ppb between bearings of 120° and 340°. This high-concentration arc was 60° narrower than for Test 3, but the sector peak-to-mean concentration here was somewhat lower at 2.7 than for Test 3 which had a value of 3.4.

The two highest concentrations were at positions 8 (567 ppb) and 10 (439 ppb). These are reasonably well accounted for by the winds at 350° (6.0 min duration) and at 360° (13.5 min). However, there were a number of sample concentrations (locations 18 through 7) for which there were no corresponding winds. The average wind speed was only 0.19 m sec^{-1} and for 27 min out of the 45 min sampling period the wind speed was calm. Thus, there is reason to suspect the corresponding recorded wind directions. The record of smoke candle observations which follows does indicate the presence of a westerly wind on at least one occasion.

Time (EDT)	Observed Smoke Plume Behavior
Location:	SF_6 Release Point
0340	Straight up. Drifted a little to the E. Clear skies, but considerable low fog.
0410	Towards E at surface. Rose about 45 ft, turned to SW.
0428	Smoke right on ground.
0445	Dense fog.

The peak concentration predicted by Model 1P ("AEC/DRL ΔT Model") was very much higher than observed, with $\chi_{max}/\chi_{model} = 0.023$. The best fit was provided by Model 2P ("Slade σ_θ Model") with a ratio of 0.64. This was the only test for which this equation was best; however, Model 4P was very close at 0.6.

7.3.4 Test 5

This test was conducted under less stable conditions than others with a lapse rate of 0.7 C/100 m. The wind again displayed considerable meander over 167° of arc.

The polar diagram (Figure 11) reveals notable concentrations in a narrow sector bounded by positions 8 and 12 with the peak of 390 ppb at 220° (position 11). The peak-to-mean ratio was 3.4.

The prevailing wind directions are well correlated with the high measured concentrations. The overall average wind speed was 0.15 m sec^{-1}, the lowest of all the tests. Supplementary smoke candle observations follow.

Time (EDT)		Observed Smoke Plume Behavior
First Observer	Location:	SF_6 Release Point
0355		Drift toward NW to location 15.
0407		Drift toward W, WSW.
0421		Moderately strong SW wind. Smoke moved rapidly toward SW.
~ 15		Dead calm.
Second Observer	Location:	Near Tank 15
0408		Drifted slowly southward.
0428		Drifted to SW quadrant. Winds have been quite calm since 0400. From 0428 to 0438 winds toward SW at less than 1 mph.

Considering the prediction models, Model 4P ("Sector Average Model") was "best" with $\chi_{max}/\chi_{model} = 0.33$.

7.3.5 Test 6

As was the case in other tests, conditions were stable with a lapse rate of 2.05 C/100 m, and again the wind meandered through about 160°.

This last test in Phase 1 yielded a fairly uniform concentration pattern in a 180° sector bounded by tank positions 10 and 1 (see Figure 12). The peak-to-mean ratio was 2.5, the lowest thus far.

The wind direction durations in the polar diagram agree well with the concentration bars. The dotted radials represent visual observations of smoke candle plumes, when recorded winds were questionable. The average wind speed was 0.37 m sec^{-1}. Observations made during the test follow.

Time (EDT)	Observed Smoke Plume Behavior
2020	Drifted to SE, then to SE to N.
2100	Smoke drifts due W for about 30 ft, then to SW.
2102	Smoke goes upward for about 10 ft, then drifts to S. Cups on tower not moving.
2108	Plume still intact and standing just SSW of tower.
2112	Smoke plume is on road W of tower and drifting N.
2120	Drifting W. Winds calm on top of tower. Plume drifted out over river.
2135	Drifting N.
2139	Drifting to WSW.
2143	Drifting into tower area. Smoke odor is detectable. Winds on tower still remain calm.
2210	Plume moving to SW.

The peak concentration of 534 ppb was almost exactly predicted by Model 4P ("Sector Average Model"). The ratio of $\chi_{max}/\chi_{model} = 1.02$ was the best obtained in the entire study. This good agreement may be explained by studying Table 10 in conjunction with Figure 12. The value of θ used in the Sector model was 162° which almost agrees with the 180° sector width through which significant concentrations were measured. Furthermore, this model assumes a uniform dispersion of gas throughout the sector. As was noted earlier, Test 6 did indeed have a very low peak-to-mean ratio.

7.4 Conclusions

For each test the peak measured concentration was compared to that predicted by five diffusion models. Best agreement was obtained using Model 4P ("Sector Average Model") which takes into account plume meander. This is consonant with the preceding discussion. Model 4P had an average value of the ratio χ_{max}/χ_{model} for this phase of 1.27. The average value for Model 1P ("AEC/DRL ΔT Model") was 0.046. It thus may be concluded that, although very stable conditions accompanied by low wind speeds tend to inhibit the rapid dispersal of contaminants, the wide fluctuations in the horizontal wind direction cannot be neglected.

It is of interest to compare the measurements with the meteorological conditions specified for the first 8 hours in the AEC Safety Guide 4, i.e., Model 1P with Pasquill F Diffusion and 1.0 m sec^{-1} wind speed. The ratio χ_{max}/χ_{model} for this case varied between 0.06 and 0.31 with an average of 0.17 (see Table 12). Thus, the AEC model overpredicts the measured concentrations by an average factor of 5.8.

Looking briefly at the other models, Model 3P ("Split σ Model") is a significant improvement over Model 1P, but even here the concentrations are overestimated by a factor of more than 3. Model 5P ("Directional Frequency Model") performed about the same as Model 3P ("Split σ Model"). On the other hand, Model 2P ("Slade σ_θ Model") which assumes the same value of the Pasquill stability category for σ_z as used for σ_y (based on Range/6 per Table 3), underestimated the downwind concentrations by about a factor of 2. Although Model 2P underestimated concentrations for these tests, it is not considered that it would behave in this manner for higher winds or in cases where there is no meander.

SECTION 8.0

DESCRIPTION OF PHASE 2 TESTS

(REACTOR SITE)

8.1 General

The release point for Phase 2 testing was moved near the large structures comprising Unit 1. The purpose of this arrangement was to attempt to simulate, and hence assess the effects of, an accidental release of radio-active material. The geometry of the power plant site plays an important role in diffusing released material as will become evident in the discussion comparing the results of this phase to those of Phase 1.

The sampling tanks were now substantially further from the SF_6 release point than in previous tests. Distances from the center of the reactor building are provided in Table 13. Because the radial at a bearing of 60° (position 3) passes through cooling tower B, an additional tank, position 3A, was added (and is indicated in all future polar projection figures). Note that, in Phase 2, the distances of the sampling tanks from the center of the grid were not the same as their distances from the SF_6 release point. The grid center was the center of the Unit 1 reactor building, while the tracer gas release point was variable from test to test. The distance used in the models was always taken from the center of the reactor building.

Because of the larger radius of the sampling grid, a the desirability of depicting the SF_6 release point and the balloon location (used for vertical profiles) relative to the structures, a slightly modified polar display was used to present Phase 2 results as shown in Figures 13, 15,

17, 19 and 21. The radial distance scale is decreased; however, the scales for the sample concentrations and the wind direction durations remain unchanged from those used in Figures 8 through 12. Direction data from the south 100-foot tower are included in Figures 14, 16, 18, 20 and 22 which follow the polar display for each test.

8.2 Summary and Results of the Five Phase 2 Tests

The basic test data are summarized in Table 14. Weather conditions, summarized in Table 1, show that there was an inversion and low wind speed during all tests in Phase 2. To assure detectable concentrations of SF_6 in the sampling tanks with the additional dilution due to the wake and increased distance, the tracer gas release rate was increased above the Phase 1 rate. For Tests 4 through 6 the source strength Q was set at $1.59 \times 10^{-4} m^3 sec^{-1}$. Although this rate was doubled for the first Phase 2 test (Test 7), the highest tank sample concentration was only 63 ppb. The release rate was again doubled in Test 8 to a value of $6.34 \times 10^{-4} m^3 sec^{-1}$. The remainder of the tests used approximately this release rate.

Tables 15 through 19 contain the calculations which compare the peak concentrations predicted by the wake models (Models 1W through 5W) to those actually observed during Phase 2 testing. Tables 15 through 19 are based on north 100-foot tower data. Table 20 compares the results of each of the models using north 100-foot tower data. Table 21 is a summary comparison of models using the south 100-foot tower data. A detailed tabulation of south tower data appears in Appendix B.

8.3 Individual Tests

8.3.1 Test 7

The tracer gas release location for both Tests 7 and 8 was on the ground at the eastern wall of the turbine building, as indicated in Figures 13 and 15 for the respective tests.

Test 7 was characterized by a 4.4 C/100 m increase in temperature with height, and had the smallest value of Phase 2 direction range (31°). This was atypical of the meander condition which usually prevailed. The polar display of sample concentrations and wind direction durations (Figure 13) shows that significant concentrations were confined to a narrow 60° sector which includes positions 2, 3A, 3, 4, and 5 in consonance with the wind direction. The peak-to-mean ratio, i.e., the ratio of the highest measured value to the mean value is 2.3.

For Test 7, the longest duration of wind direction bearing 210° is displaced downwind by 30° from the location of the maximum concentration. However, because of the aerodynamic effects of the structures, it is difficult to extrapolate the surface wind patterns from those on the tower. Perhaps more relevant is the following transcription of visually observed smoke candle plumes released at the tracer gas release site. Also included are comments by a second observer on the winds at the Weather Measure tower, at the south end of the site.

Time (EDT)		Observed Smoke Plume Behavior
First Observer	Location:	SF_6 Release Point.
0155		Smoke start. Smoke path erratic; start in westerly direction moving N & S finally bouncing off building and toward E.

Time (LDT)		Observed Smoke Plume Behavior
First Observer	Location:	SF_6 Release Point.
0200		Most of smoke in area between building and transformer.
0210		Smoke stayed in vicinity of building.
0219		Moved slowly in N or NE direction. some smoke odor now noticeable.
0220		Smoke moving in a southerly direction; reached height of reactor building then to E and then to N. What air movement there is feels like from the S.
0230		Smoke release is in northerly direction initially for maybe one minute, then straight up to top of reactor building. Looping back to ground, spreading around building in N and S directions. Wind now noticeable from the E.
0240		Smoke release directly to reactor building up the side and looping back to ground; localized.
0250		Smoke release climbed straight up side of reactor building; looping back to ground and moved in northerly direction.
Second Observer	Location:	Weather Measure Tower
0155		Smoke drifting to NNE. Winds on (Weather Measure) tower from SSW.
0210		Smoke drifted to NE, then to N.
0214		Winds on tower from SW.
0220		Smoke moving to N. Winds on tower from S.
0223		Smoke still drifting to N.
0230		Smoke drifting to NNE, then to NE.

Time (EDT) (continued)	Observed Smoke Plume Behavior
Second Observer	Location: Weather Measure Tower, at Phase 1 Gas Release Point.
0235	Smoke drifting to NE.
0240	Drifting to N.
0248	Smoke drifting to NNE.

With the exception of Model 4W (AEC/DRL ΔT Wake Model") the Phase 2 models described in Section 4.3 (as shown in Tables 15 through 20) predicted values of χ_{max}/χ_{model} in the range 0.80 to .92. Using the south tower data, Table 21 shows that with the exception of Model 4W, the models underpredicted. This is attributed to the higher windspeed than was observed at the north tower. Model 4W overpredicted (was conservative) by a factor of about 40.

8.3.2 Test 8

The lapse rate for this test was 0.78 C/100 m, representing only a slight inversion. This was accompanied by a direction range of 56° and a wind speed of 1.79 m. sec^{-1}, the highest for all tests. The pattern of observed concentrations is shown in Figure 15, here it is seen that the highest concentrations were grouped in a fairly large sector, with values of over 10 ppb subtending 120° of arc between positions 13 and 1 respectively. The peak-to-mean ratio within this sector was 2.1.

The pattern of wind directions from the north tower agrees reasonably well with the location of the high concentration sector, but the samples at positions 2 through 14 inclusive, which include the peak value, show no associated winds from the north tower. However, as shown on the south tower wind rose (Figure 16), winds were considerably more easterly which would explain the peak values in the tanks on the west side of the grid.

Visual smoke plume observations appear below for the period including the test (2305 to 2350 EDT).

Time (EDT)		Observed Smoke Plume Behavior
First Observer	Location:	SF_6 Release Point.
2250		Smoke initially moved down road in northerly direction and then swung around building out of sight.
2305		Smoke started to head S, then shifted to N moving around building as before.
2320		Smoke release in northerly direction and around building.
2335		Release to north and around building.
2345		Smoke toward building and up to top; general swirling and then went to the N.
Second Observer	Location:	Weather Measure tower.
2305		Smoke rose straight up (Weather Measure) tower and drifted slowly W.
2308		Smoke still rising up tower and slowly drifting to SE.
2320		Smoke drifting to NW.
2324		Drifting N.
2335		Drifting NNE.
2339		Smoke still drifting N.
2345		Smoke drifted N.

With the exception of Model 4W, all models predicted χ_{max}/χ_{model} in the range of 0.84 to 1.57 with Model 5W, which accounts for the observed meander, yielding the higher ratio. Model 4W ("AEC/DRL ΔT Wake Model"), although it overestimated by a factor of 9, performed much better in Test 8 than in any

of the other tests in this series. In general, the above observations hold true using the south tower data in the models.

8.3.3 Test 9

The tracer gas release point was relocated for Test 9 to a point inside of the incomplete diesel generator building about 40 ft from the face of the reactor building at a bearing of 340° (see Figure 17).

An inversion of 5.2 C/100 m existed for Test 9, and the direction range was 165°, which was the largest in Phase 2. The average wind speed was 0.9 m/sec.

The effect of wind meander is notable in Figure 17 which shows significant sample concentrations at positions 2, 3A, 5, 8, and 13-17. The pattern of prevailing wind directions is in agreement with this. The longest duration wind, at 20°, is only counterclockwise 20° out of phase with the location of the peak concentration at position 11. The overall peak-to-mean ratio is 3.6. For the 140° high concentration sector bounded by positions 10 and 17 the ratio is 2.2. Supplemental visual observations on smoke plume behavior follows.

Time(EDT)		Observed Smoke Plume Behavior
First Observer	Location:	SF_6 Release Point.
0315		Initially smoke drifting from the SW, then drifting around the west side of the reactor building, then rising to the top of the reactor building, turning to the S, and drifting downwind of the reactor building.
0330		The smoke behaved the same as at 0315, except that the plume did not rise as high. Some drift to the W.

Time(EDT)		Observed Smoke Plume Behavior
First Observer	Location:	SF_6 Release Point.
0345		Good vertical rise with little horizontal movement at first. The plume rose the height of the reactor building and then slowly drifted to the S.
0400		Smoke dispersion pattern similar to that at 0345, slow rise followed by drift to the S.
0410		The smoke rose and drifted to the SW over and around the west face of the reactor building.
Second Observer	Location:	Weather Measure tower.
0330		Smoke drifted to SW.
0345		Smoke rose to a height of approximately 40 ft and drifted NW.
0348		Smoke drifted to the N for about 100 ft, then rose and drifted W.
0350		Smoke was stationary about 125 ft N of the (Weather Measure) tower. The smoke still persisted at about 250 ft NNW of the tower at 0352 at a height of approximately 50 ft and was drifting slowly to the NNW.

The diffusion equation which most closely predicted the maximum measured concentration for Test 9 was Model 5W ("Sector Average Wake Model") with a χ_{max}/χ_{model} of 0.679. Model 5W was also best with south tower data as shown in Table 21.

8.3.4 Test 10

The release point was the same for both Tests 10 and 11, i.e., 26 feet above grade on the roof of the auxiliary building. This point was 10 feet from the edge of the reactor building at a bearing of 240°.

For this test temperature increased with height at a rate in excess of 11.6 C/100 m, which represents full scale on the recorder, indicating extremely high stability. The wind was observed to have a direction range of 35° and the wind speed was 0.6 m sec^{-1}, lowest of all phase 2 tests.

The sampling grid here was slightly modified in an attempt to obtain a vertical wind profile. Positions 9 and 10 were not used; instead, samplers were located on top of the 7-foot high instrument shed for the north weather tower, and at the 100 and 150 foot levels of the north tower. However, no significant concentrations were measured at this location due to a wind shift during the test.

Significant sample concentrations were noted at positions 1 through 8 with the maximum of 3.4 ppb at positions 3 (Figure 19). This 140° sector had a peak-to-mean ratio of 2.4. The wind pattern was predominatly from the west, in agreement with the concentrations.

All of the models substantially overpredicted the measured maximum downwind concentration. Models 1W, 2W, 3W, and 5W all performed about the same with a χ_{max}/χ_{model} of about 0.013. Use of south tower data in the models showed even poorer model correlation with test results.

This first case of extreme over-prediction of the models is believed due to the plume remaining aloft at the sample tank locations as discussed later.

8.3.5 Test 11

Temperature differences were again full scale at 11.6 C/100 m and the wind meandered over a 60° arc with a wind speed of 0.87 m sec^{-1}. It should be noted that winds at the south tower meandered over a 175° arc, as shown on Figure 22. The tracer gas release point was also unchanged from the previous test.

The sampling grid was altered such that positions 3 and 10 were not used; instead, samplers were located at the 100 ft levels of both the north and south towers.

As shown on the polar diagram (Figure 21) very low concentrations were measured. Values above background were measured at locations 11 (0.26 ppb) and 14 (0.12 ppb) and values of between 1-2 ppb were measured at positions 12, 13 and the north tower. Observed concentrations were in agreement with the winds which were essentially from the east.

As in Test 10, the models overpredicted the results. The "best" model again was 5W with a χ_{max}/χ_{model} of only 0.0167. Model 4W ("AEC/DRL ΔT Wake Model") predicted concentrations 3000 times higher than measured for both tests 10 and 11. South tower data produced similar results, as seen in Table 21.

8.4 Conclusions

This phase demonstrated the powerfull effect of the building wake in reducing concentrations. Again, as in Phase 1, the effect of meander was observed to disperse the tracer over a wide arc in most cases.

Model 5W ("Sector Average Wake Model") was the "best" predictor for most of the tests. It was also "best" on the average when compared with the average performance of the other models. This was found to be true for both north and south tower data (see Tables 20 and 21). For the north tower, the χ_{max}/χ_{model} was 0.62 and for the south tower it was 0.90.

The reason for poor model correlation in tests 10 and 11 may be due to the failure of the gas to diffuse downward (after its initial rise due to the building wake effect) due to the extreme inversion conditions existing during the test. On many occasions the smoke was seen to rise up the sides of the reactor building and over the top, a height of 165 ft above the ground. If, as expected, the SF_6 followed the smoke trajectory concentrations less than the maximum would be detected by the surface sampling grid. Measurements of concentrations aloft which confirm this phenomenon were made, and are discussed in Sections 9 and 10.

SECTION 9.0

VERTICAL CONCENTRATION PROFILES

9.1 General

A major objective of these diffusion experiments was to obtain some understanding of the vertical distribution of plume concentrations during stable weather conditions. The data were used to explain observed results obtained from ground level samplers, and served as a basis for validating the diffusion models at distances beyond the fixed sample locations.

9.2 Phase 1 Open Field Vertical Measurements

A Kytoon balloon was introduced in Tests 3 and 4 to obtain concentration data aloft. This was accomplished by drawing air samples through tubing attached to the winch line for real-time sampling by a leak detector at the ground. For both of these tests, the balloon was located near position 6. The concentrations measured at the ground and at the 30 ft level are given in Table 22 for Test 3. As expected, concentrations aloft were, with one exception, lower than at the ground. In Test 4, lighter tubing was used such that the balloon rose to 100 ft. However, the wind did not blow in the direction of this balloon and no concentrations were measured.

Because of the limited lift capacity of the Kytoon, it was replaced from Test 5 on by a Kaysam balloon with a useful lift of the order of 15 lbs. For Test 5 and 6, two lines of tubing were attached to the winch cable; one at the balloon tether, and the other 100 ft. below. The balloon was raised to an altitude of 200 ft which permitted sampling at the 100 and 200 ft levels. By lowering the balloon, additional data were obtained at the 50

and 100 ft levels. By continuously lowering and raising the balloon, concentrations could be monitored at 50 ft increments up to 200 ft. Although the balloon location was such that there was no SF_6 detected on Test 5, vertical profiles were obtained in Test 6 with the balloon located near position 16.

The results shown for Test 6 in Table 23, as well as those which follow, were obtained by plotting concentrations as functions of time for each available level. These points were then joined to form a set of curves. Finally, vertical profiles were obtained by picking times which included as many sample levels as possible. Concentrations for remaining levels were interpolated whenever possible.

It is clear that concentrations are smaller aloft than at the ground, although the variation with height is irregular. The value at the ground (tank 16 below the balloon) was 111 ppb, whereas, the peak short-time values aloft were in the range of 8.5 to 27.

9.3 Phase 2 Vertical Measurements in the Building Wake

Attempts to obtain vertical concentration profiles were of limited success in Phase 1 primarily because of the inability to predict wind direction from one 10-minute period to the next. However, in the wakes of buildings, wind tunnel experiments have shown that near the buildings there was a good chance of being in some part of the plume, even for wind directions almost oblique to the sample location. Therefore, in Phase 2 (with the exception of Tests 7 and 8), the balloons were kept relatively close to the building complex.

During several Phase 2 tests, vertical measurements were taken close to the building to ascertain if the gas did indeed rise and distribute itself

over the building cavity, during low wind speed inversion conditions. If this were found to be the case, the use of conventional building wake compensated equations for such atmospheric conditions could be reasonably justified. Observations of smoke and measurements of concentrations aloft showed that for all six tests in Phases 2 and 3, the plume was radically affected by the building wake. A discussion of these tests follows.

Figure 23 shows a vertical cross section of the plant structures as viewed from the north and from the west. Location of the SF_6 release points are indicated for each test.

9.3.1 Tests 7 and 8

For Tests 7 and 8, it was decided that sampling time could be saved by attaching four lengths of tubing to the winch cable at 50 ft intervals; this allowed the balloon to remain fixed at the 200 ft level. However, Test 7 yielded no data because the wind direction was away from the balloon location. The vertical profiles obtained in Test 8 are documented in Table 24. In this series, surface data at the base of the balloon were also taken to provide five levels in all.

The balloon location in Test 8, indicated in Figure 15 by the solid dot marked B, was at about the same bearing as grid position 17, but was 60 meters farther from the reactor center. However, despite this 25% greater distance from the release point, concentrations aloft were occasionally a substantial fraction of the 48 ppb measured at the ground at position 17. For example, at 2339 EDT the 100-foot level showed a concentration of 25.5 ppb, almost the same as that measured on the ground. At 2349, values changed only slowly with height, while at 2350 the 100-foot value was almost twice

that at the surface. At 2353, the lowest value was at the surface; this tendency persisted through 2355 when the 100-foot value was larger than at the ground by a factor of 3. The maximum concentrations were 7.8 ppb at 50 ft; 25.5 ppb at 100 ft; 13.0 ppb at 150 ft; and 6.5 ppb at 200 ft. Thus $\chi_{ground}/\chi_{aloft}$ ratios were in the range of 1.9 to 7.4, somewhat lower than for Test 6 where they ranged from 4.1 to 13. Thus, there seems to be some tentative evidence to indicate greater transport aloft of the tracer gas in Test 8 as a result of aerodynamic effects of the structures than in Test 6 which was carried out in the open field.

9.3.2 Test 9

For Test 9, a new technique was introduced which was intended to substantially reduce the need for interpolating profile data. Plenum chambers were fitted such that four samples could be collected simultaneously using vacuum pumps, and retained for analysis with the leak-detector in the following few minutes. This necessitated a decrease in the number of sampled levels to four: surface, 50, 125 and 200 ft.

As shown in Figure 17, the balloon in Test 9 was located about 57 meters from the center of the reactor building at a bearing of 300°. This was close to the release point, in contrast to Test 8 where the balloon was well beyond the grid perimeter. The profiles obtained are given in Table 25.

Here we find evidence of high concentrations aloft. The most striking are: (1) the values of 89.1 ppb at 50 ft (0340 EDT); (2) the gradual increases with height to maxima of 17.3 ppb and 7.8 ppb at 125 ft (0400 EDT and 0405 EDT respectively), and (3) the value of 30.0 ppb at 50 ft (0415 EDT). These high values aloft support the suggestion made earlier that the building wake did

induce rapid vertical transport of the material. This is in good agreement with the smoke plume observations in which the smoke was noted to rise up and over the roof of the reactor building.

9.3.3 Test 10

The balloon was moved again and placed at a bearing of about 25° halfway between the release point and grid location 1. Its position is indicated in Figure 19 and the results are given in Table 26. It is seen that concentrations of about the same magnitude as at the ground were observed at elevations up to 125 ft.

9.3.4 Test 11

This last test in Phase 2 was unique in that an attempt was made to move the balloon location while the test was in progress to follow changes in the prevailing wind direction. Three locations were used as indicated in Figure 21 by the solid dots marked B_1, B_2 and B_3. Position 1 yielded data inadequate for profiles, and one profile each resulted from positions 2 and 3. These data are summarized in Table 27.

The profile for 0449 at position 2 shows a large increase from 0.057 ppb at the ground to 123 ppb at 200 ft. The profile for 0514 also shows a steady increase of concentration with height.

9.4 Phase 3 Time Averaged Vertical Measurements

9.4.1 General

Because of the frustrations involved in trying to place the balloon and vertical sample apparatus within the plume boundary, an "all out" attempt was made to sample the plume vertically. Four balloons were positioned in a 180° arc, each one having sample tubes which terminated at the following

heights: surface, 75, 150 and 250 ft. An improvement in the vertical sample technique was made to enable collection of integrated samples aloft. This was done by fitting each balloon apparatus with 16 liter evacuated sample bottles connected to each of the four tubes. The tubes were prepurged and were all the same length such that during the 45 minute period each would draw simultaneous samples from each level.

9.4.2 Test 12

Only one test (Test 12) was conducted using the configuration described above. The weather conditions were characterized by an inversion of 3.14 C/100 m with wind meander of 75° and wind speed of about 0.91 m sec^{-1}. The sample locations are shown on the polar diagram of Figure 24. A south tower wind rose is given in Figure 25. Results for each position are given in Table 28 and shown graphically in Figure 26. The balloon position 3 profile indicated a maximum of 2.26 ppb at the 150 foot level. At position 4, the concentration steadily increases with height to a maximum of 32.4 ppb at 250 ft. Positions 1 and 2 were outside of the plume and yielded no information.

9.4.3 Comparison of Maximum Concentration With Models

The maximum value of 32.4 ppb at position 4 was compared with the five wake models described in Section 4.3. A summary of this comparison using both north and south weather tower data is given in Table 29. The range of χ_{max}/χ_{model} for models 1W, 2W, 3W and 5W with north tower wind data was 0.19 to 0.67. Model 5W ("Sector Average Wake Model") was "best" based on the north tower data, with a ratio of 0.67. Based on south tower data, the models also overpredicted, with Models 1W, 2W and 3W being "best". Model 5W over-

predicted considerably due to the direction range of only 11° measured on the south tower. The χ_{max}/χ_{model} ratios for Model 4W (AEC/DRL ΔT Wake Model") were 0.02 and 0.04 for the north and south towers, respectively.

9.5 Conclusions

The vertical concentration profiles lend support to the conclusion that, in the presence of low wind speed inversion conditions, the aerodynamic effect of structures is to induce inital vertical transport of the diffusing material to altitudes comparable to the height of the nearest building, with subsequent advection downwind with the greatest concentration at some higher elevation.

For Test 12, where average tank samples were collected over a 45 minute sample period, the χ_{max}/χ_{model} was less than 0.67 for all models even though the maximum was at an elevated position. Thus, the models overpredicted concentrations at the 800 ft distance with Model 5W ("Sector Average Wake Model") being the "best". The concentration predicted by the Safety Guide 4 model (identical to Model 4W) using Pasquill F and 1.0 m/sec yields a χ_{max}/χ_{model} of 0.046 when compared to the maximum Test 12 concentration of 32.4 ppb. Therefore, it is concluded that the Safety Guide 4 model is very conservative.

SECTION 10.0

MOBILE OFF-SITE TRAVERSES

10.1 General

One of the major objectives of the experiment was to validate a diffusion model which could be used to predict site boundary concentrations. Since models were validated at a distance of 800 ft, and the site boundary is at 2000 ft, a series of mobile traverses were conducted to test the behavior of the models at distances beyond 800 ft.

During two tests, a road vehicle was equipped with a leak detector and recorder; and in one of these tests, a boat was also used. For each traverse the vehicle was driven along local highways downwind of the release point taking instantaneous readings of concentration at various locations.

10.2 Test 10 Road Traverse

Following the tank sampling portion of Test 10, the mobile SF_6 analyzer was mounted in a truck and samples were taken for almost two hours off the site. During this period, release of gas was continued at 1/2 the initial flow rate, or 3.17×10^{-4} m^3 sec^{-1}.

The locations where readings were taken and the corresponding time and concentrations are plotted in Figure 27. The prevailing wind speeds and directions on the north and south towers during the traverse period are shown in Figure 28. As shown in Figure 27, concentrations were observed to be relatively uniform along Route 441 over about a two mile stretch. The wind direction traces are consistent with those observations. Thus, the SF_6 was spread over a wide area at a distance of about 2000 ft.

10.3 Test 12 Road and River Traverses

For Test 12, the wind was blowing generally from the south. This required the use of a boat for close-in measurement and a car for measurements at greater distances downwind. The concentrations and locations for the road traverse are shown in Figure 29 and in Figure 30 for the river traverse. North and south tower winds are shown in Figure 31. The SF_6 release rate was 3.17×10^{-4} m^3 sec^{-1}.

10.4 Correlation of Results with Models

10.4.1 Test 10 Traverse

From Figure 27, the maximum concentration measured was 1.87 ppb at 0631 EDT. This value is compared (in Table 30) with predicted values using the "W" models in Table 2 and the meteorological conditions measured at the north and south towers during the traverses. As shown in Table 30, Model 5W ("Sector Average Wake Model") at 2000 ft resulted in an χ_{max}/χ_{model} of 0.26 using the north tower data. The use of the same model at the 800 ft distances showed generally poor correspondence of observed versus predicted tank concentrations at ground level. This is shown in Table 20 for Test 10 where χ_{max}/χ_{model} was 0.013.

However, it has been demonstrated that the maximum concentration in the plume is generally aloft at the 800 ft distance. This readily explains the poor correspondence. At greater distances, general streamline descent in the far wake is to be expected, and the concentrations near the ground should more closely approximate those predicted by the models. This was evident for Test 10 at 2000 ft where the χ_{max}/χ_{model} was 0.26. However, insufficient data were available to determine if the maximum concentrations were really at ground level. If the plume was still somewhat aloft at a 2000 ft distance,

the poorer correspondence could be attributed to this condition.

The agreement for Test 10 at 2,000 ft is not as good (with the same model) as was observed at 800 ft for the 250 ft level in Test 12 (0.67) but is still considered reasonable for a test of this nature and it is still on the conservative side.

10.4.2 Test 12 Traverses

Figure 32 shows a calculated curve of concentration versus distance, using Model 5W ("Sector Average Wake Model") with the approximate wind conditions which existed during Test 12 (see Table 14). The experimental observations made during the Test 12 land and river traverses are taken from Figures 29 and 30, and are plotted in Figure 32. The maximum value for Test 10 at a distance of 2,000 ft and the tank samples taken at the 250 ft level during Test 12 are included in Figure 32. It is seen that the Model 5W predicted curve is in excellent agreement with the measured concentrations.

Some scatter is noted but it must be remembered that the calculated curve is intended to represent an average concentration over a time period of approximately 45 minutes while mobile observations represent approximately 5 second samples. According to Turner[7] an inverse one-fifth power law describes variation of concentration with sampling time. The ratio of concentrations corresponding to a decrease of sampling time from 45 minutes to 5 seconds results in an increase in concentration by a factor of about 3.5. It is seen that all the individual observations at distances greater than 2,000 meters fall within a factor of 3.5 of the Model 5W curve in Figure 32.

The group of river observations show concentrations markedly less than predictions made by the model. Those observations were taken at about the same distance from the plant as the road traverse observations in Test 10. It was concluded in that discussion that the plume may still have been aloft at that distance and this explanation may serve here with the levels

of concentrations observed. Note that all of the observed data points fall below the computed curve for the Safety Guide 4 meteorology (Pasquill F stability and 1.0 m sec^{-1}) shown in Figure 32.

10.5 Conclusions

It is concluded that Model 5W is an accurate and conservative method of predicting the maximum concentration at a specified distance downwind of a source near a reactor building surface without specifying the height at which it occurs. It is conservative, of course, to assume that the maximum occurs at the ground even though it probably remained aloft for distances that ranged to at least 1000 meters during the tests.

Table 1

Weather Condition Summary Table

Phase	Test	Date	Time of Day (EDT)	Wind Speed (m/sec)	* ΔT (°C/100 m)	Wind Direction Range
I	2	8/25/71	0500	0.62	4.26	150
	3	9/08/71	0445	0.20	2.97	168
	4	9/09/71	0400	0.19	2.83	175
	5	9/23/71	0415	0.15	0.70	167
	6	9/24/71	2125	0.37	2.05	162
II**	7	10/06/71	0205	1.12	4.40	31
	8	10/08/71	2305	1.79	0.78	56
	9	10/13/71	0330	0.90	5.20	165
	10	10/15/71	0420	0.60	11.60+	35
	11	10/16/71	0400	0.87	11.60+	60
III**	12	11/12/71	0035	0.91	3.14	75

* All ΔT data from north tower.
** Wind data from north tower.

Table 2

Summary of Models

PHASE 1 MODELS

Model 1P ("AEC/DRL ΔT Model"):	Uses equation (1) with the ΔT groups given in Table 4 to define both σ_y and σ_z.
Model 2P ("Slade σ_θ Model"):	Uses equation (1) with the groups given in Table 3 to define σ_y and σ_z.
Model 3P ("Split σ Model"):	Uses equation (1) with the ΔT groups of Table 4 and the σ_θ groups of Table 3 to define σ_z and σ_y respectively.
Model 4P ("Sector Average Model"):	Uses equation (2) with θ equal to the maximum wind direction meander (range) during the sample period, and σ_z based on the ΔT groups of Table 4.
Model 5P ("Directional Frequency Model"):	Uses equation (3) and σ_y and σ_z based on ΔT in Table 4.

PHASE 2 MODELS

Model 1W ("ΔT Wake Model"):	Uses equation (4) with cA based on area of containment with c=2, and ΔT groups in Table 4.
Model 2W ("Slade σ_θ Model With Wake Correction"):	Uses equation (4) with cA based on area of containment with c=2, and σ_θ group in Table 3.
Model 3W ("Split σ Wake Model"):	Uses equation (4) and both Tables 3 and 4 as for Model 3P, cA based on area of containment and c=2.
Model 4W ("AEC/DRL ΔT Wake Model"):	Uses equation (4) with cA based on containment area, c=½ and ΔT from Table 4. Maximum wake correction is 3.
Model 5W ("Sector Average Wake Model"):	Uses equation (7) with c=2, A=2000 and σ_z from Table 4.

Table 3

Pasquill Stability Classes Based on Wind Data

Slade Pasquill Stability Class	Standard Deviation of the Horizontal Wind Direction,
A	$\sigma_\theta \geq 22.5^o$
B	$22.5^o > \sigma_\theta \geq 17.5^o$
C	$17.5^o > \sigma_\theta \geq 12.5^o$
D	$12.5 > \sigma_\theta \geq 7.5^o$
E	$7.5^o > \sigma_\theta \geq 3.8^o$
F	$3.8^o > \sigma_\theta$

Table 4

Pasquill Stability Classes Based on Temperature Data

AEC/DRL Pasquill Stability Class	Vertical Temperature Gradient T (C^o/100 m)
A	$-1.9 \geq \Delta T$
B	$-1.7 \geq \Delta T > -1.9$
C	$-1.5 \geq \Delta T > -1.7$
D	$-0.5 \geq \Delta T > -1.5$
E	$+1.5 \geq \Delta T > -0.5$
F	$+4.0 \geq \Delta T > +1.5$
G	$\Delta T > +4.0$

Table 5

Positions of Sampling Tanks: Phase 1

Sampling Tank Position Number	Bearing (Degrees)	Distance From Center of Grid (Meters)*	
		Test 2	Tests 3-6
1	20	183 (600)	101 (330)
2	40	190 (625	101 (330)
3	60	158 (518)	101 (330)
4	80 (East)	116 (382)	101 (330)
5	100	96 (314)	101 (330)
6	120	94 (310)	98 (322)
7	140	119 (390)	101 (330)
8	160	134 (440)	101 (330)
9	180(South)	150 (492)	94 (310)
10	200	171 (560)	98 (320)
11	220	165 (540)	88 (290)
12	240	120 (393)	101 (330)
13	260 (West)	94 (310)	98 (322)
14	280	94 (310)	101 (330)
15	300	109 (357)	107 (350)
16	320	143 (470)	98 (320)
17	340	146 (478)	101 (330)
18	360(North)	174 (570)	101 (330)

* Values in parentheses are equivalent feet.

Test 6

Summary of Basic Test Data: Phase 1

Test Number	Date	Start Test EDT	Duration (min)	SF_6 Release Rate, Q (m^3 sec^{-1})	30 ft. Wind Speed, $\bar{u}$ (m sec^{-1})	Lapse Rate, ΔT (^oC/100 m)	30 ft. Direction Range θ	Range/6	σ_θ*	Pasquill Stability Group Based On AEC/DRL ΔT	Pasquill Stability Based On Range/6
2	8/25/71	0500	50	2.38(-4)	0.62	4.26	150°	25.0	37.3°	G	A
3	9/08/71	0445	50	2.38(-4)	0.2	2.97	168°	28.0	49.4°	F	A
4	9/09/71	0400	45	1.59(-4)	0.19	2.83	175°	29.2	46.7°	F	A
5	9/23/71	0415	45	1.59(-4)	0.15	0.7	167°	27.8	40.1°	E	A
6	9/24/71	2125	45	1.59(-4)	0.37	2.05	162°	27.0	55.4°	F	A

*Computed (See Appendix B)

Table 7

Concentration Calculations Based on Model 1P ("AEC/DRL ΔT Model"): Phase 1

Test	Observed Sample χ_{max} (ppb)	Tank Sample Number	Distance From SF_6 Release Point (m)	AEC/DRL Pasquill Stability Category	Q (m^3 sec^{-1})	$\bar{u}$ (m sec^{-1})	σ_y (m)	σ_z (m)	χ_{model} (ppb)	χ_{max}/χ_{model}
2	2610	13	94	G	2.38(-4)	0.62	3.0	1.5	27,200	0.096
3	1788	17	101	F	2.38(-4)	0.20	4.7	2.3	35,000	0.051
4	567	8	101	F	1.59(-4)	0.19	4.7	2.3	24,600	0.023
5	390	11	88	E	1.59(-4)	0.15	5.9	2.8	20,400	0.019
6	534	18	101	F	1.59(-4)	0.37	4.7	2.3	12,700	0.042
									Average	0.046

Note: Model 1P:

$$\chi_{model} = \frac{Q}{\pi \bar{u} \sigma_y \sigma_z}$$

σ_y, σ_z based on ΔT and Table 4.

Table 8

Concentration Calculations Based On Model 2P ("Slade σ_θ Model"): Phase I

Test	Observed Sample χ_{max} (ppb)	Tank Sample Number	Distance From SF_6 Release Point (m)	Slade Pasquill Stability Category	Q (m^3 sec^{-1})	$\bar{u}$ (m sec^{-1})	σ_y (m)	σ_z (m)	χ_{model} (ppb)	χ_{max}/χ_{model}
2	2610	13	94	A	2.38(-4)	0.62	22.0	12.0	463	5.64
3	1788	17	101	A	2.38(-4)	0.20	23.0	13.0	1270	1.41
4	567	8	101	A	1.59(-4)	0.19	23.0	13.0	891	0.64
5	390	11	88	A	1.59(-4)	0.15	21.9	11.0	1400	0.28
6	534	18	101	A	1.59(-4)	0.37	23.0	13.0	457	1.17
									Average	1.83

Note: Model 2P:

$$\chi_{model} = \frac{Q}{\pi \bar{u} \sigma_y \sigma_z},$$

σ_y, σ_z both based on R/6 and Table 3.

Table 9

Concentration Calculations Based on Model 3P ("Split Model"): Phase 1

Test	Observed Sample χ_{max} (ppb)	Tank Sample Number	Distance From SF_6 Release Point (m)	Slade Pasquill Stability Category For σ_y	AEC/DRL Pasquill Stability Category For σ_z	Q (m^3 sec^{-1})	$\bar{u}$ (m sec^{-1})	σ_y (m)	σ_z (m)	χ_{model} (ppb)	χ_{max}/χ_{model}
2	2610	13	94	A	G	2.38(-4)	0.62	22.0	1.5	3700	0.70
3	1788	17	101	A	F	2.38(-4)	0.20	23.0	2.3	7160	0.25
4	567	8	101	A	F	1.59(-4)	0.19	23.0	2.3	5040	0.11
5	390	11	88	A	E	1.59(-4)	0.15	21.9	2.8	5500	0.07
6	534	18	101	A	F	1.5-(-4)	0.37	23.0	2.3	2590	0.21
										Average	0.27

Note: Model 3P:

$$\chi_{model} = \frac{Q}{\pi \bar{u} \sigma_y \sigma_z},$$

σ_y based on R/6 and Table 3

σ_z based on ΔT and Table 4.

Table 10

Concentration Calculations Based on Model 4P ("Sector Average Model"): Phase 1

Test	Observed Sample χ_{max} (ppb)	χ_{avg} (ppb)	AEC/DRL Pasquill Stability Category	$\bar{u}$ (m sec^{-1})	σ_z (m)	θ	χ_{model}	χ_{max}/χ_{model}	χ_{avg}/χ_{model}
2	2610	710	G	0.62	1.5	150°	832	3.14	0.85
3	1788	478	F	0.20	2.3	168°	1400	1.28	0.34
4	567	290	F	0.19	2.3	175°	944	0.6	0.31
5	390	113	E	0.15	2.8	167°	1180	0.33	0.10
6	534	209	F	0.37	2.3	162°	524	1.02	0.40
							Averages:	1.27	0.40

Note: Model 4P:

$$\chi_{model} = \frac{\sqrt{2/\pi}}{\bar{u} \times \sigma_z \times \theta}$$

σ_z based on Table 4 (ΔT).

Table 11

Concentration Calculations Based On Model 5P ("Directional Frequency Model"): Phase 1

Test	Observed Sample χ_{max} (ppb)	Distance From SF_6 Release Point (m)	Pasquill Stability Category	Q (m^3 sec^{-1})	$\bar{u}$ (m sec^{-1})	σ_y (m)	σ_z (m)	f Fraction Of Total Interval	χ_{model} (ppb)	χ_{max}/χ_{model}
2	2610	94	G	2.38(-4)	0.62	3.0	1.5	0.17	4510	0.58
3	1788	101	F	2.38(-4)	0.20	4.7	2.3	0.20	7010	0.25
4	567	101	F	1.59(-4)	0.19	4.7	2.3	0.13	3200	0.18
5	390	88	E	1.59(-4)	0.15	5.9	2.8	0.19	3880	0.10
6	534	101	F	1.59(-4)	0.37	4.7	2.3	0.066	835	0.64
									Average	0.35

Note: $\chi_{model} = \chi_{model\ 1P} \times f$

Table 12

Summary of Phase 1 Results

X_{max}/X_{model}

Test	Observed Sample X_{max} (ppb)	Model 1P "AEC/DRL ΔT Model"	Model 2P "Slade σ_θ Model"	Model 3P "Splitσ Model"	Model 4P "Sector Average Model"	Model 5P "Directional Frequency Model"	Model 1P With Type F & 1 m sec^{-1}
2	2610	0.096	5.64	0.7	3.14	0.58	0.312
3	1788	0.051	1.41	0.25	1.28	0.25	0.255
4	567	0.023	0.64	0.11	0.60	0.17	0.121
5	390	0.019	0.28	0.071	0.33	0.10	0.061
6	534	0.042	1.17	0.21	1.02	0.64	0.114
Averages:		0.046	1.83	0.27	1.27	0.35	0.173

Model 1P: Table 7
Model 2P: Table 8
Model 3P: Table 9
Model 4P: Table 10
Model 5P: Table 11

Table 13

Positions of Sampling Tanks: (Phase 2)

Sampling Tank Number	Bearing (Degrees)	Distance from Center of Grid* (Meters)** Tests 7-11
1	20	244 (800)
2	40	238 (780)
3	60	149 (490)
3A(See Text)	60	317 (1040)
4	80 (East)	244 (800)
5	100	244 (800)
6	120	259 (850)
7	140	244 (800)
8	160	244 (800)
9	180(South)	244 (800)
10	200	244 (800)
11	220	244 (800)
12	240	244 (800)
13	260 (West)	204 (670)
14	280	177 (580)
15	300	186 (610)
16	320	201 (660)
17	340	244 (800)
18	360(North)	244 (800)

* For Phase 1, the grid location was the field about 0.5 mi. south of the actual site; there, the center of the grid corresponded to the SF_6 release point. For Phase 2, however, the grid was centered on the exact center of the northernmost reactor building; now the SF_6 release point was not the center of the grid. See the individual polar projection figure for each test for the release location.

**Values in parentheses are equivalent feet.

Table 14

Summary of Basic Test Data: Phases 2 and 3

Test Number	Date	Start Test EDT	Duration min.	SF_6 Release Rate Q (m^3 sec^{-1})	100 ft Wind* Speed $\bar{u}$ (m sec^{-1})	Lapse Rate ΔT (°C/100 m)	Range (°)	Range/6	σ_θ** (°)	Pasquill Stability Group Based On AEC/DRL ΔT	Pasquill Stability Group Based On Slade Range/6
7	10/06/71	0205	45	3.17(-4)	1.12	4.4	31	5.2	7.6	G	E
8	10.08.71	2305	45	6.34(-4)	1.79	0.78	56	9.3	14.2	E	D
9	10/13/71	0330	45	3.17(-4)	0.90	5.2	165	27.5	67.8	G	A
10	10/15/71	0420	45	6.34(-4)	0.60	11.6 +	35	5.8	9.6	G	E
11	10/16/71	0400	45	7.93(-4)	0.87	11.6 +	60	10.0	18.2	G	D
12 (Phase 3)	11/12/71	0035	45	6.34(-4)	0.91	3.14	75	12.5	19.1	F	C

* From north tower at 100 ft
** Computed, see Appendix B

Table 15

Concentration Calculations Based On Model 1W ("ΔT Wake Model"): Phase 2

Test	Observed Sample χ_{max} (ppb)	Tank Sample No.	Distance From Center of Grid (m)	Pasquill Stability Category Based On AEC/DRL ΔT	Q (m^3 sec^{-1})	$\bar{u}$ * (m sec^{-1})	σ_y(m)	σ_z(m)	χ_{model} (ppb)	χ_{max}/χ_{model}
7	63.0	3	149	G	3.17(-4)	1.12	4.6	2.3	70.2	0.898
8	71.0	14	177	E	6.34(-4)	1.79	10.4	5.8	84.5	0.84
9	7.6	11	244	G	3.17(-4)	0.90	7.2	3.4	86.4	0.088
10	3.4	3	149	G	6.34(-4)	0.60	0.6	2.3	262	0.013
11	1.59	13	204	G	7.93(-4)	0.87	0.87	2.9	225	0.007

Model 1W:

$$\chi_{model} = \frac{Q}{\bar{u}\,(\pi\sigma_y\,\sigma_z + cA)},$$

σ_y, σ_z based on Table 4 (ΔT).

$cA = 4000$

*Based on north 100 ft tower data.

Table 16

Concentration Calculations Based On Model 2W ("Slade σ_θ Model with Wake Correction"): Phase 2

Test	Observed Sample χmax (ppb)	Tank Sample No.	Distance From Center of Grid (m)	Pasquill* Stability Category Based On Slade σ_θ	Q (m^3 sec^{-1})	$\bar{u}$ * (m sec^{-1})	σ_y (m)	σ_z (m)	χmodel (ppb)	χmax/χmodel
7	63.0	3	149	E	3.17(-4)	1.12	9.0	5.0	68.3	0.922
8	71.0	14	177	D	6.34(-4)	1.79	14.2	8.8	80.6	0.881
9	7.6	11	244	A	3.17(-4)	0.90	55.0	41.0	31.8	0.239
10	3.4	3	149	E	6.34(-4)	0.60	9.0	5.0	255	0.0133
11	1.59	13	204	D	7.93(-4)	0.87	16.5	9.8	202	0.0078

Model 2W:

$$\chi_{model} = \frac{Q}{\bar{u}\,(\pi\sigma_y\,\sigma_z + cA)}$$

σ_y, σ_z both based on Table 3 (Range/6)

cA = 4000

* Based on north 100ft tower data.

Table 17

Concentration Calculations Based on Model 3W ("Splitσ Wake Model"): Phase 2

Test	Observed Sample χmax (ppb)	Tank Sample No.	Distance From SF_6 Release Point (m)	Pasquill Stability Category Based On Slade σ_θ	Pasquill Stability Category Based On AEC/DRL ΔT	Q (m^3 sec^{-1})	$\bar{u}$ (m sec^{-1})	σ_y (m)	σ_z (m)	χmodel (ppb)	χmax/χmodel
7	63.0	3	149	E	G	3.17(-4)	1.12	9.0	2.3	69.6	0.905
8	71.0	14	177	D	E	6.34(-4)	1.79	14.2	5.8	83.2	0.854
9	7.6	11	244	A	G	3.17(-4)	0.90	55.0	3.4	76.8	0.099
10	3.4	3	149	E	G	6.34(-4)	0.60	9.0	2.3	260	0.0131
11	1.59	13	204	D	G	7.93(-4)	0.87	16.5	2.9	220	0.0072

Model 3W:

$$\chi_{model} = \frac{Q}{u\,(\pi\sigma_y\,\sigma_z + cA)}$$

σ_y based on Table 3
σ_z based on Table 4

$cA = 4000$

* Based on north 100 ft tower data

Table 18

Concentration Calculations Based on Model 4W ("AEC/DRL ΔT Wake Model"): Phase 2

Test	Observed Sample χ_{max} (ppb)	Tank Sample No.	Distance From Center Of Grid (m)	Pasquill Stability Category Based On AEC/DRL ΔT	Q (m^3 sec^{-1})	$\bar{u}$* (m sec^{-1})	σ_y (m)	σ_z (m)	χ_{model} (ppb)	χ_{max}/χ_{model}
7	63.0	3	149	G	3.17(-4)	1.12	4.6	2.3	28,400	0.022
8	71.0	14	177	E	6.34(-4)	1.79	10.4	5.8	623	0.114
9	7.6	11	244	G	3.17(-4)	0.90	7.2	3.4	1,530	0.005
10	3.4	3	149	G	6.34(-4)	0.60	4.6	2.3	10,600	0.0003
11	1.59	13	204	G	7.93(-4)	0.87	6.4	2.9	5,210	0.0003

Model 4W:

$$\chi_{model} = \frac{Q}{\bar{u}\,(\pi\sigma_y\,\sigma_z + cA)}$$

σ_y, σ_z based on Table 4 (ΔT)

$cA = 4000$

*Based on north 100 ft tower data.

Table 19

Concentration Calculations Based On Model 5W ("Sector Average Wake Model"): Phase 2

Test	Observed Sample χ_{max} (ppb)	Distance From Center Of Grid (m)	Pasquill Stability Category Based On AEC/DRL ΔT	Q (m^3 sec^{-1})	$\bar{u}$ * (m sec^{-1})	σ_y (m)	σ_z (m)	θ*	χ_{model} (ppb)	χ_{max}/χ_{model}
7	63.0	149	G	3.17(-4)	1.12	4.6	2.3	31	78.6	0.802
8	71.0	177	E	6.34(-4)	1.79	10.4	5.8	56	45.3	1.57
9	7.6	244	G	3.17(-4)	0.90	7.2	3.4	165	11.2	0.679
10	3.4	149	G	6.34(-4)	0.60	4.6	2.3	35	260	0.013
11	1.59	204	G	7.93(-4)	0.87	6.4	2.9	60	95.4	0.016

Model 5W:

$$\chi_{model} = \frac{Q\sqrt{2/\pi}}{\pi \bar{u} \Sigma_z \theta}, \quad \Sigma = \sqrt{\sigma_z^2 + \frac{cA}{\pi}}$$

σ_z based on Table 4 (ΔT)

cA = 4000

*Based on north 100 ft tower data.

Table 20

Summary of Results Using North Tower Data: Phase 2

χ_{max}/χ_{model}

Test	Date	Observed Sample χmax (ppb)	Model 1W "ΔT Wake Model"	Model 2W "Slade σ_θ Model With Wake Correction"	Model 3W "Split σ Wake Model"	Model 4W "AEC/DRL ΔT Wake Model"	Model 5W "Sector Average Wake Model"	Model 4W With Type F & 1 (m sec-1)
7	10/06/71	63.0	0.898	0.922	0.905	0.022	0.802	0.039
8	10/08/71	71.0	0.84	0.881	0.854	0.114	1.57	0.030
9	10/13/71	7.6	0.088	0.239	0.099	0.005	0.679	0.01
10	10/15/71	3.4	0.013	0.0133	0.013	0.0003	0.013	0.001
11	10/16/71	1.59	0.007	0.0078	0.0072	0.0003	0.017	0.0007
Averages:			0.369	0.413	0.376	0.028	0.621	0.016

Model 1W: Table 15
Model 2W: Table 16
Model 3W: Table 17
Model 4W: Table 18
Model 5W: Table 19

Table 21

Summary of Results Using South 100 ft Tower Data: Phase 2

			χ_{max}/χ_{model}				
Test	Date	Observed Sample χ_{max} (ppb)	Model 1W "ΔT Wake Model"	Model 2W "Slade σ_θ Model With Wake Correction"	Model 3W "Split σ Wake Model"	Model 4W "AEC/DRL ΔT Wake Model"	Model 5W "Sector Average Wake Model"
7	10/06/71	63.0	1.23	1.32	1.25	0.03	2.31
8	10/08/71	71.0	0.61	0.715	0.641	0.083	1.73
9	10/13/71	7.6	0.063	0.173	0.071	0.0036	0.446
10	10/15/71	3.4	0.0032	0.0037	0.003	0.00008	0.0076
11	10/16/71	1.59	0.0045	0.005	0.0045	0.00019	0.031
Averages:			0.383	0.443	0.394	0.023	0.9

Table 22

Vertical Concentration Profiles: Test 3

SF6 Concentration (ppb)*		
Time (EDT)	Ground	30 ft.
0507	8.5	14.6
0512	13.6	1.9
0519	1.8	0.53
0523	0.93	0.40
0527	0.28	0.11
0533	0.13	0.058

*Underscored values are interpolated from graphs of instantaneous concentration vs. time.

Table 23

Vertical Concentration Profiles: Test 6

SF_6 Concentration (ppb)*				
Time (EDT)	50 ft	100 ft	150 ft	200 ft
2150	6.4	11.2	2.6	12.7
2153	27.3	12.0	2.7	9.5
2156	6.0	12.8	2.2	7.2
2200	0.88	1.1	1.8	1.4
2203	0.21	0.53	3.6	0.36
2215	5.7	6.5	8.5	2.9
2218	4.5	2.4	6.2	3.5

*Underscored values are interpolated from graphs of instantaneous concentration vs. time.

Table 24

Vertical Concentration Profiles: Test 8

SF_6 Concentration (ppb)*					
Time (EDT)	Sfc.	50 ft.	100 ft.	150 ft.	200 ft.
2337	33.7	1.0	4.5	5.8	6.5
2339	29.0	1.8	25.5	13.0	3.4
2341	24.0	3.3	6.2	4.2	1.8
2344	15.0	7.8	0.72	0.55	0.48
2347	1.5	1.4	0.20	0.1	0.13
2349	0.35	0.38	0.25	0.1	0.05
2350	0.16	0.22	0.29	0.1	0.06
2353	0.08	0.20	0.41	0.11	0.11
2355	0.18	0.40	0.54	0.12	0.16
2357	2.5	0.75	0.68	0.15	0.18
2358	2.5	1.05	0.76	0.17	0.2

*Underscored values are interpolated from graphs of instantaneous concentration vs. time.

Table 25

Vertical Concentration Profiles: Test 9

SF_6 Concentration Profiles: (ppb)				
Time (EDT)	Sfc.	50 ft.	125 ft.	200 ft.
0335	0.62	0.20	0.16	1.01
0340	2.2	89.1	0.18	0.07
0353	12.1	4.4	0.64	0.46
0400	2.2	2.9	17.3	0.15
0405	0.73	2.2	7.8	0.42
0415	5.0	30.0	1.82	3.6

*Underscored values are interpolated from graphs of instantaneous concentration in time.

Table 26

Vertical Concentration Profiles: Test 10

Time (EDT)	Sfc.	SF_6 Concentration (ppb) 50 ft	125 ft	200 ft
0449	0.25	0.086	0.028	0.027
0455	1.0	1.0	1.62	0.15
0503	6.0	1.0	0.27	0.18
0512	1.65	1.39	1.53	0.11
0521	1.36	1.29	0.61	0.071
0530	1.63	0.84	0.73	1.0

Table 27

Vertical Instantaneous Concentration Profiles: Test 11

Time (EDT)	Sfc.	50 ft	125 ft	200 ft
Position 2				
0449	0.057	0.10	4.9	123.0
Position 3				
0514	0.16	0.18	0.40	0.64

Table 28

Vertical Average Concentration Profiles: Phase 3 (Test 12)

Location	Sfc.	SF_6 Concentration (ppb)* 75 ft	150 ft	250 ft
1	0.12	M	0.10	M
2	0.10	0.08	0.11	M
3	0.46	1.72	2.26	0.46
4	0.13	4.0	17.8	32.4

* M denotes missing data.

Table 29

Concentration Calculations Using Wake Models for Test 12

χ_{max}/χ_{model}

Test	Observed Maximum (ppb)	Weather Tower	$\bar{u}$ (m sec^{-1})	R_θ	T (^oC/100 m)	Model 1W "ΔT Wake Model"	Model 2W "Slade σ_θ Model With Wake Correction"	Model 3W "Split σ Wake Model"	Model 4W "AEC/DRL ΔT Wake Model[5]"	Model 5W "Sector Average Wake Model[4]"
12	32.4	North	0.91	75^o	3.14	0.193	0.219	0.200	0.021	0.668
12	32.4	South	1.80	11^o	3.14	0.382	0.382	0.382	0.042	0.194

Table 30

Summary of Wake Model Performance for Traverses: Tests 10

Test	Distance of χ_{max} From Release Point (meters)	Tower Data From	Wind Speed $\bar{u}$ (m sec^{-1})	Pasquill Stability Category Based On Slade R/6	Pasquill Stability Category Based On AEC/DRL ΔT	Observed χ_{max} Location (ppb)	Model 1W "ΔT Wake Model"	Model 2W "Slade σ_θ Model With Wake Correction"	Model 3W "Splitσ Wake Model"	Model 4W "AEC/DRL ΔT Wake Model"	Model 5W "Sector Average Wake Model"	Model 4W With Pasquill F & 1 m sec
10	620	North	0.5	A	G	1.87	0.0129	0.217	0.019	0.0032	0.26	0.0065
10	620	South	0.2	A	G	1.87	0.0051	0.086	0.0078	0.0013	0.084	0.0065

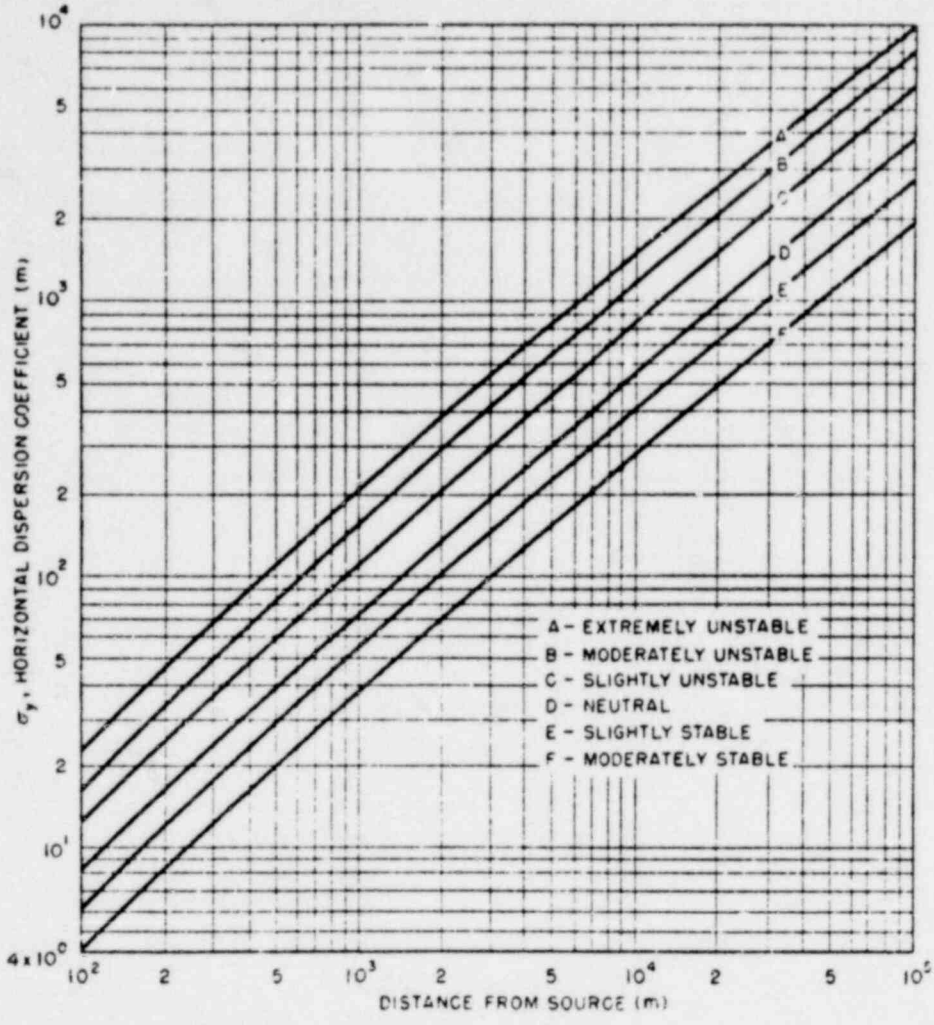

Figure 1
Lateral Diffusion, σ_y, versus Downwind Distance from Source for Pasquill's Stability Classes

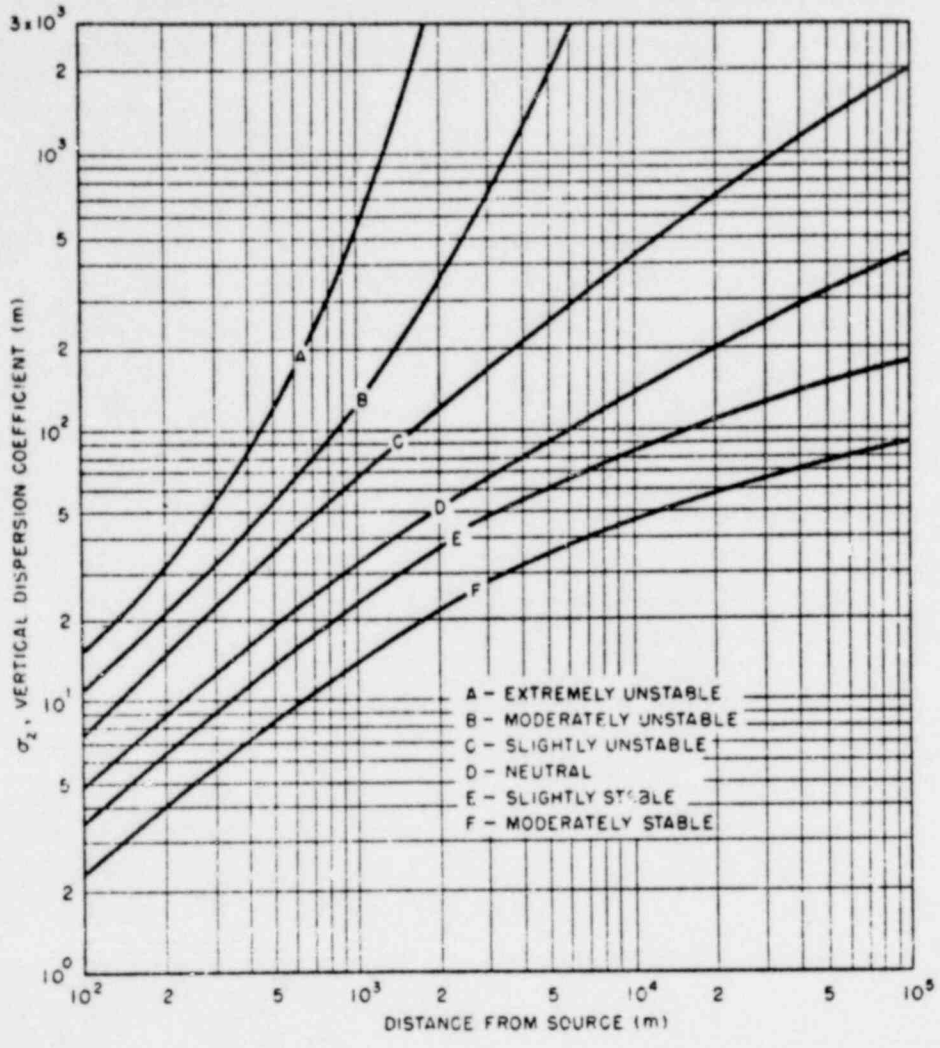

Figure 2
Vertical Diffusion, σ_z, versus Downwind Distance
from Source for Pasquill's Stability Classes

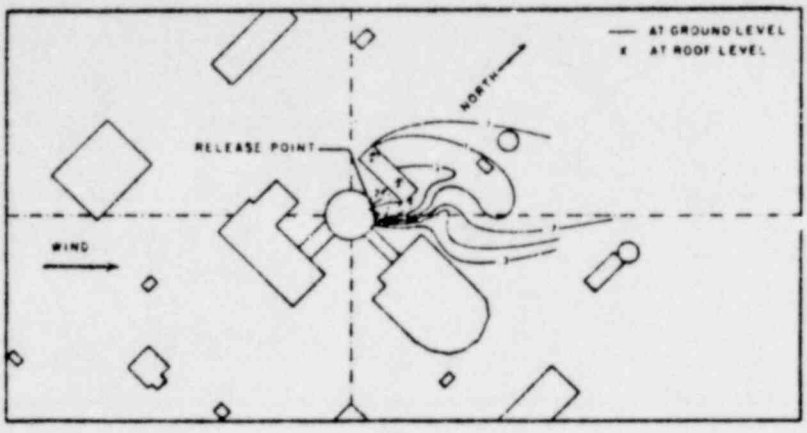

(a)

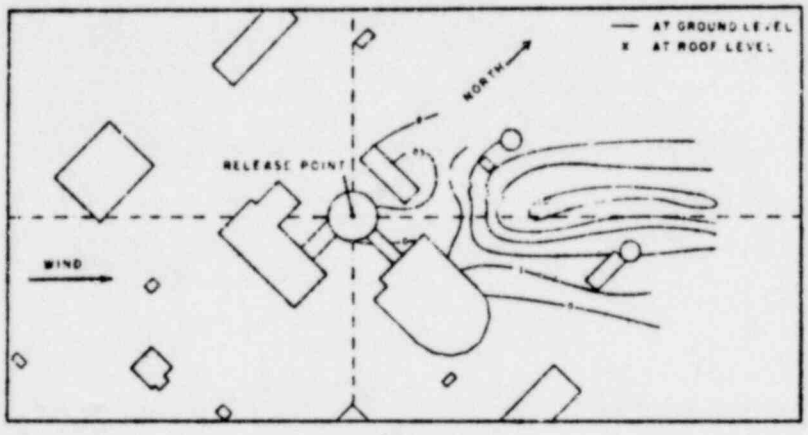

(b)

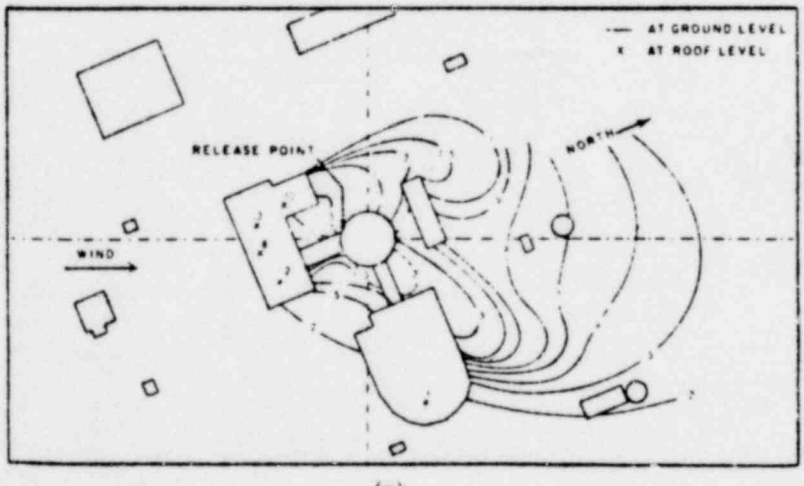

(c)

Figure 3

K_c Isopleths for Reactor Complex. (a) Downwind Release (b) Top Release (c) Upwind Release

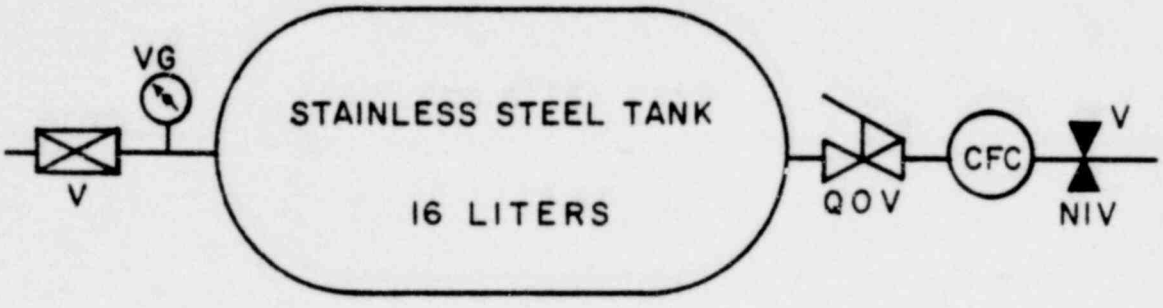

LEGEND

QOV: QUICK OPENING VALVE
CFC: CONSTANT FLOW CONTROLLER
NIV: NEEDLE INLET VALVE
VG: VACUUM GAUGE
V: VALVE

Figure 4
Sampling Tank Assembly

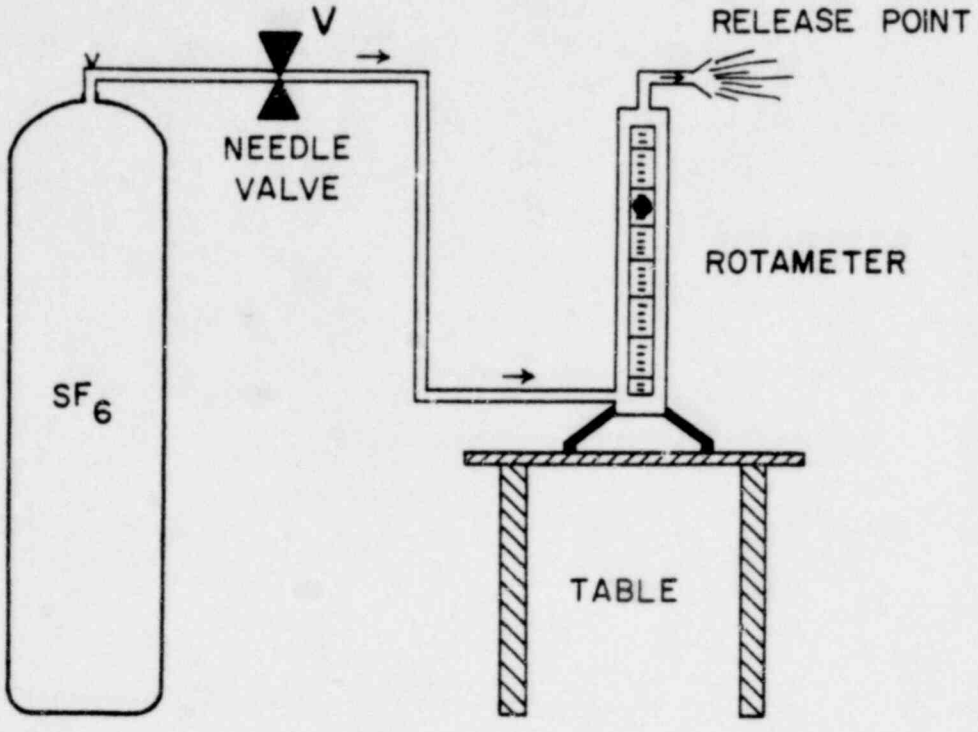

Figure 5
Tracer Gas Release Apparatus

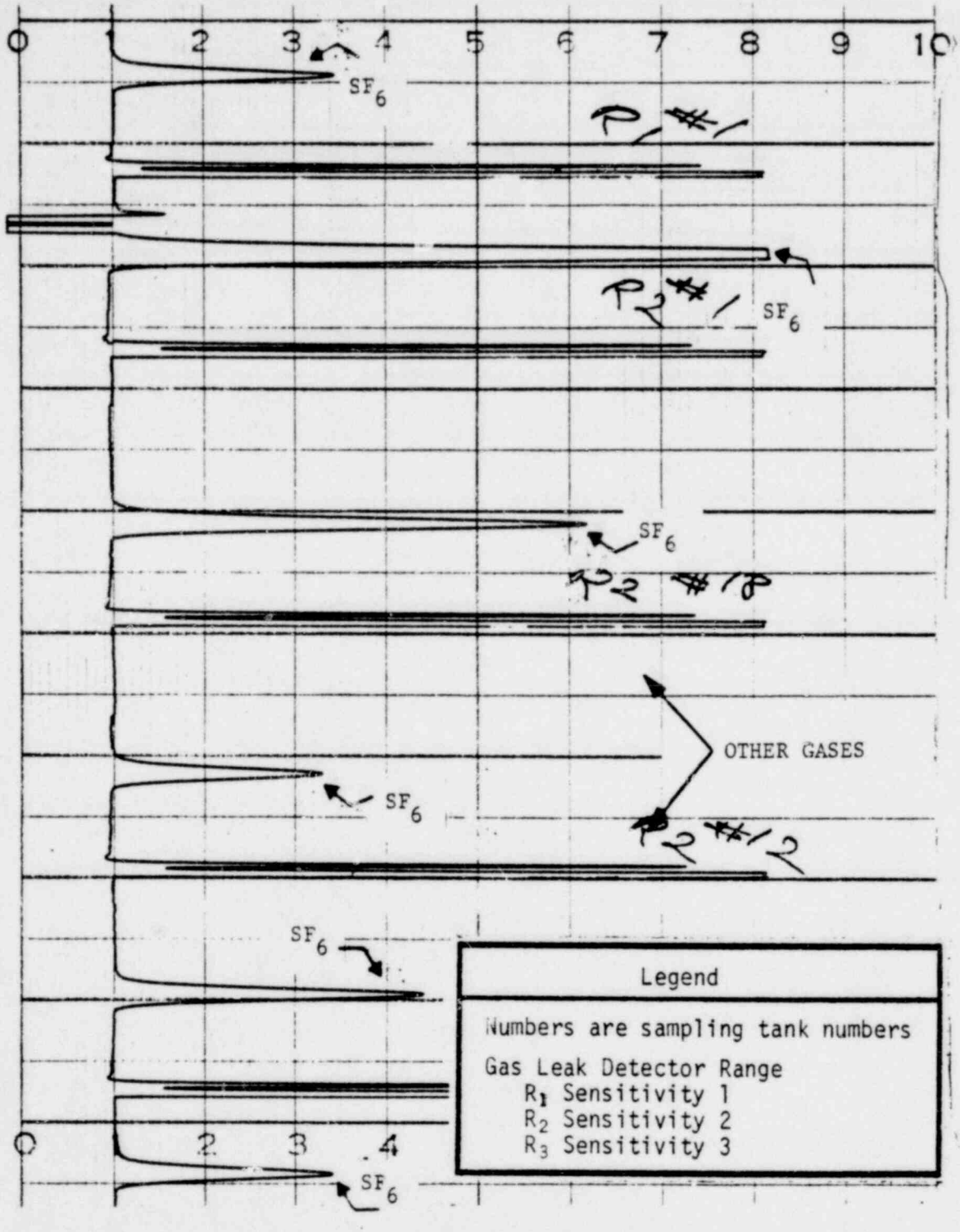

Figure 6
Strip Chart Record From Gas-Leak Detector

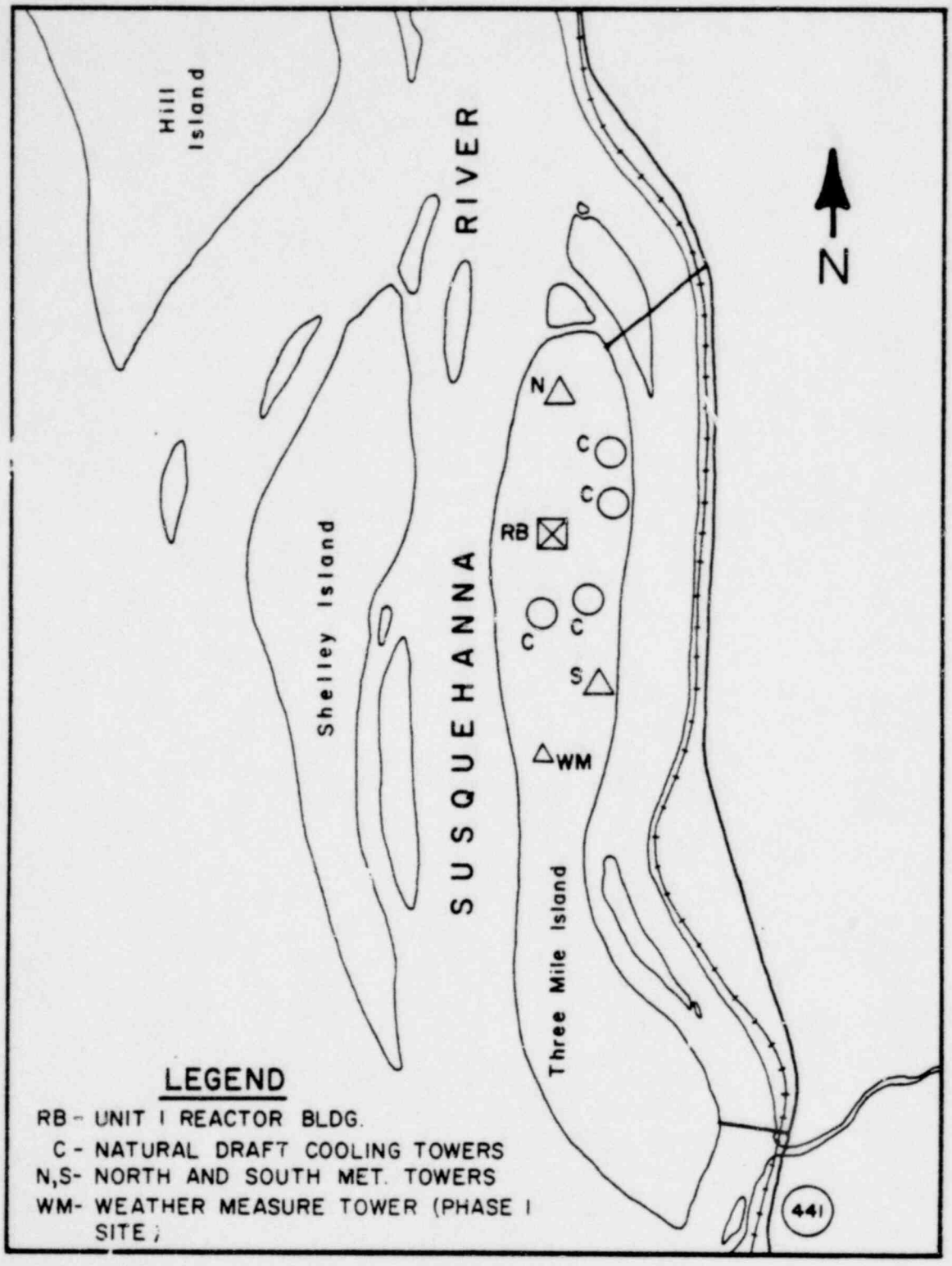

Figure 7
Three Mile Island Site Area

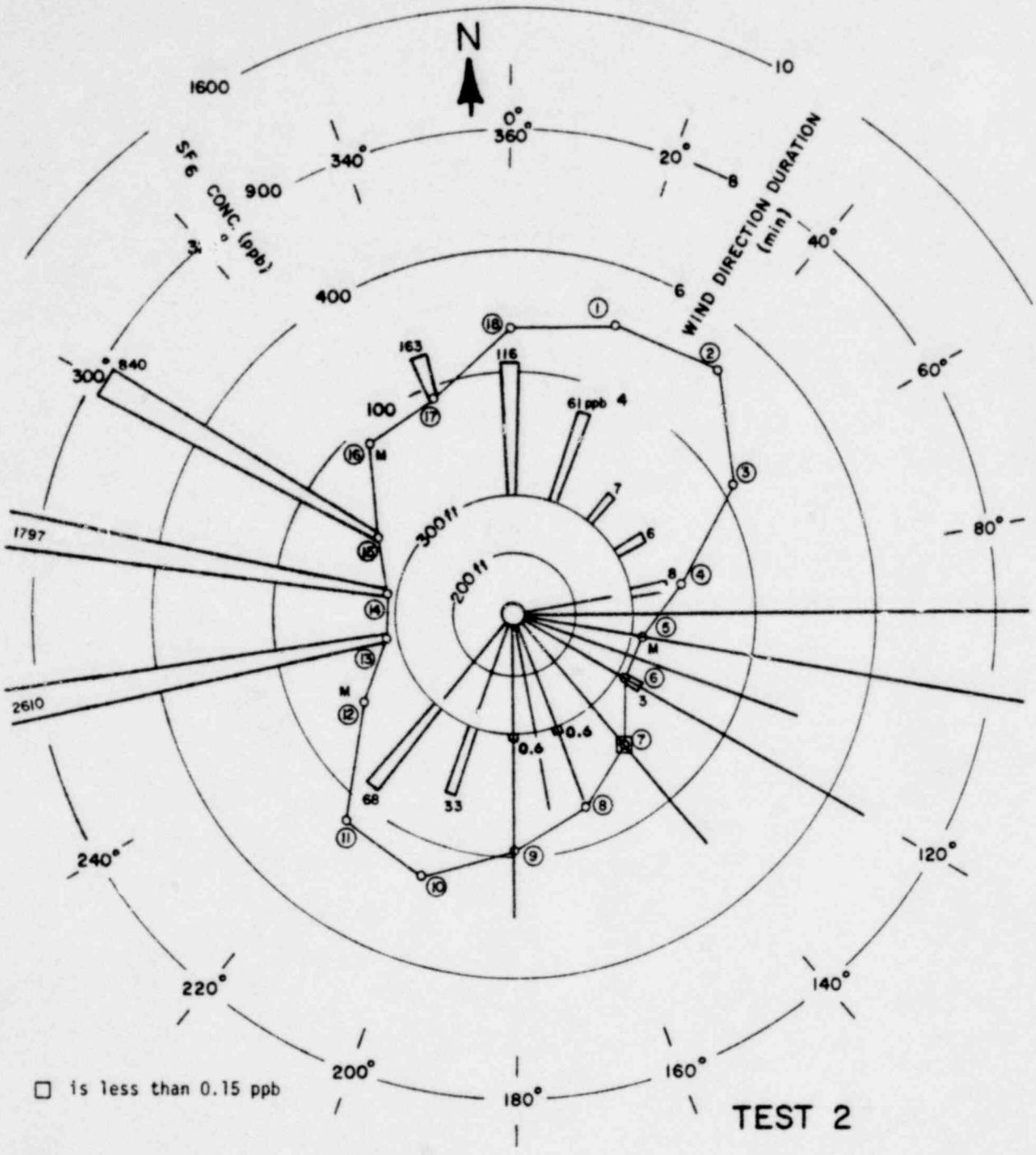

Figure 8
SF_6 Concentrations and Wind Direction Durations: Test 2

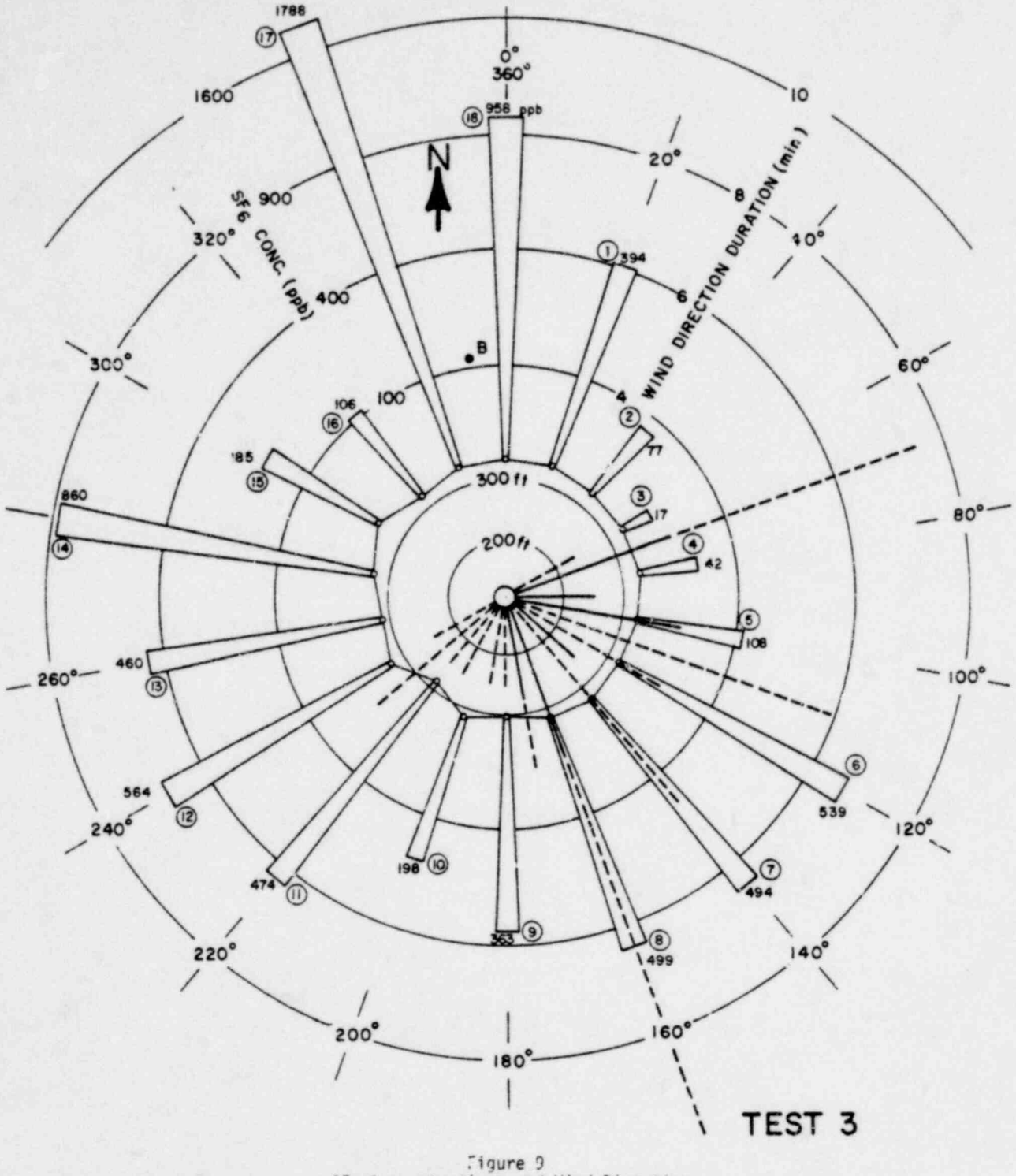

Figure 9
SF_6 Concentrations and Wind Direction Durations: Test 3

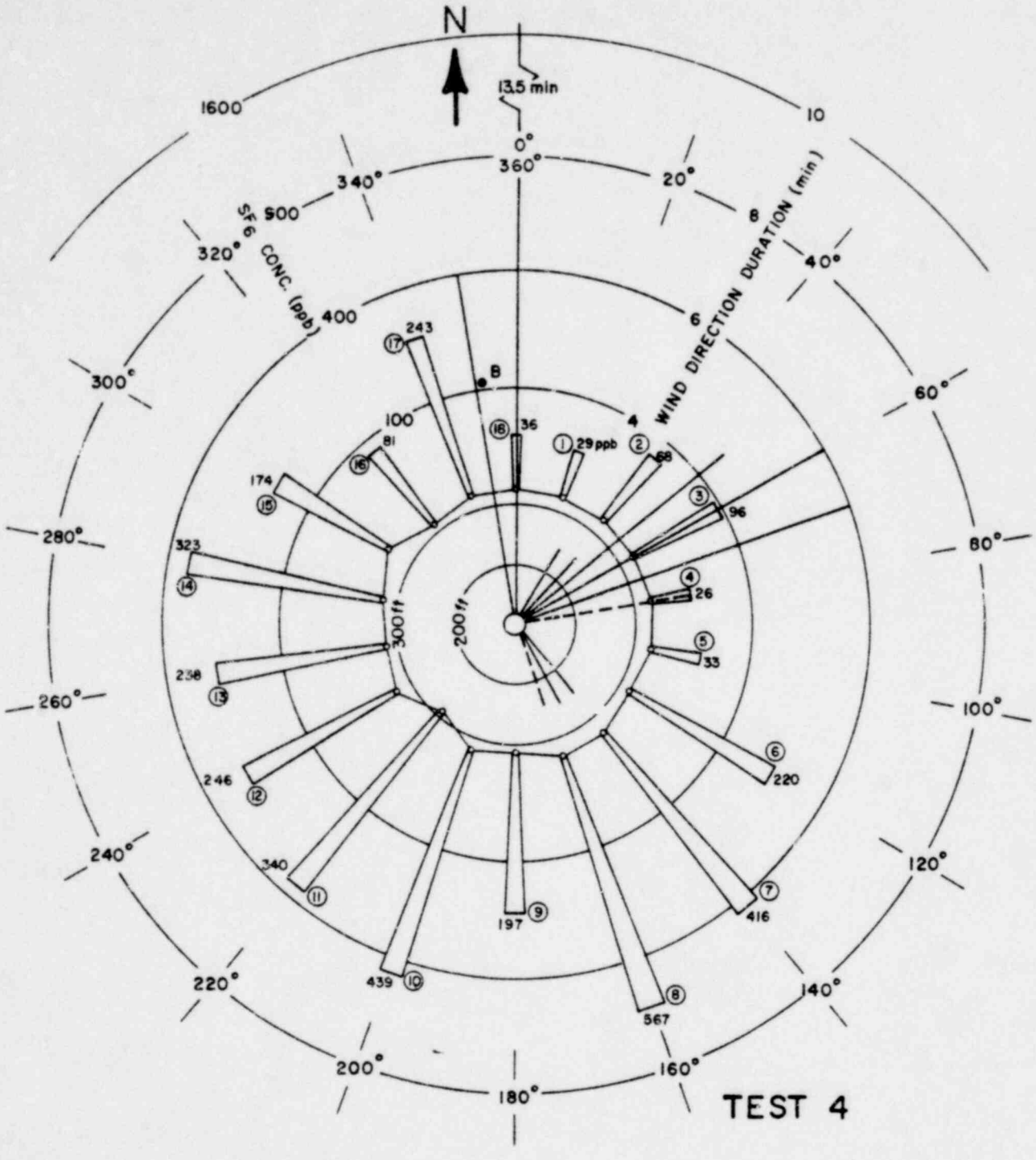

Figure 10
SF_6 Concentrations and Wind Direction Durations: Test 4

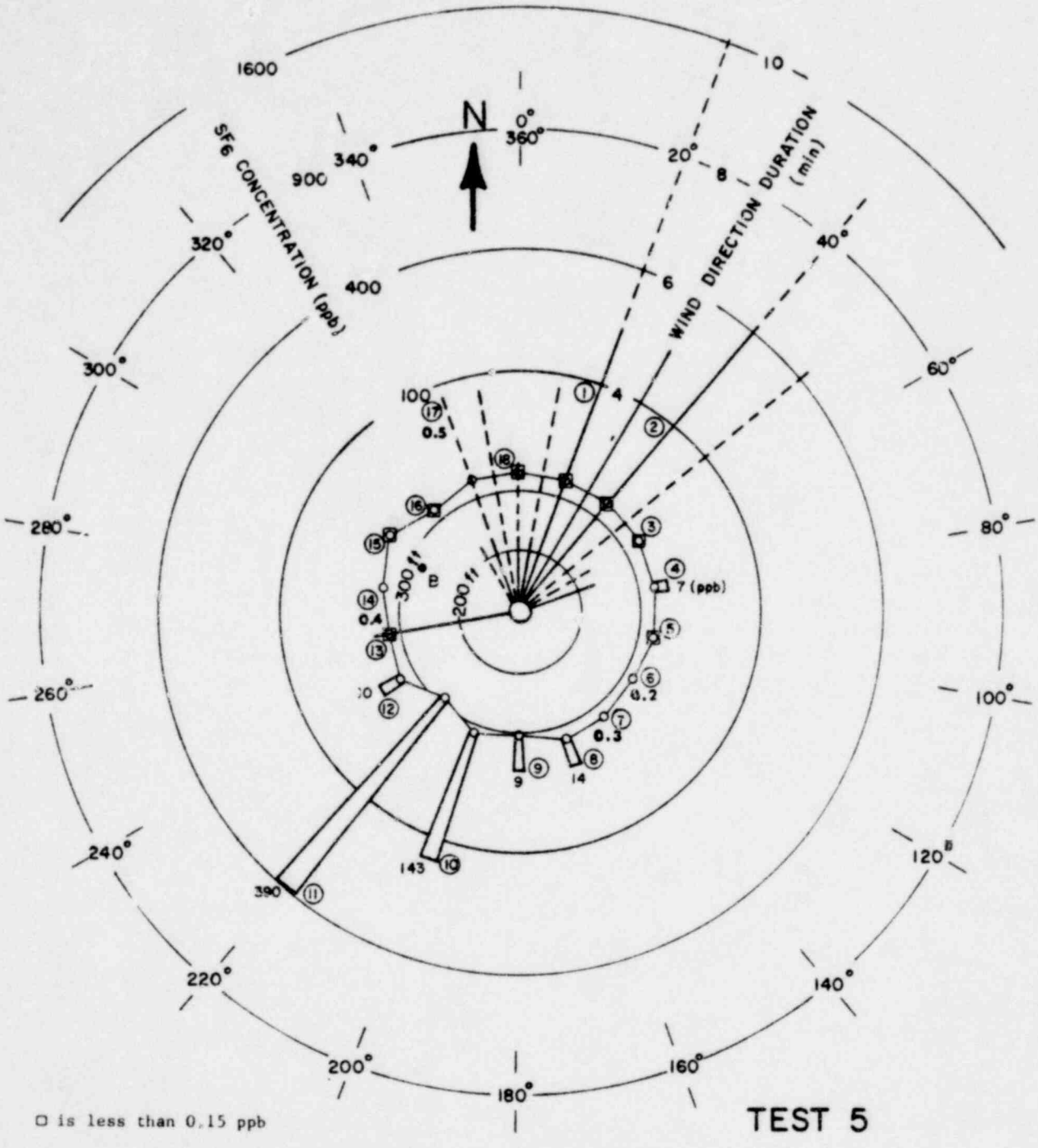

□ is less than 0.15 ppb

Figure 11
SF_6 Concentrations and Wind Direction Durations: Test 5

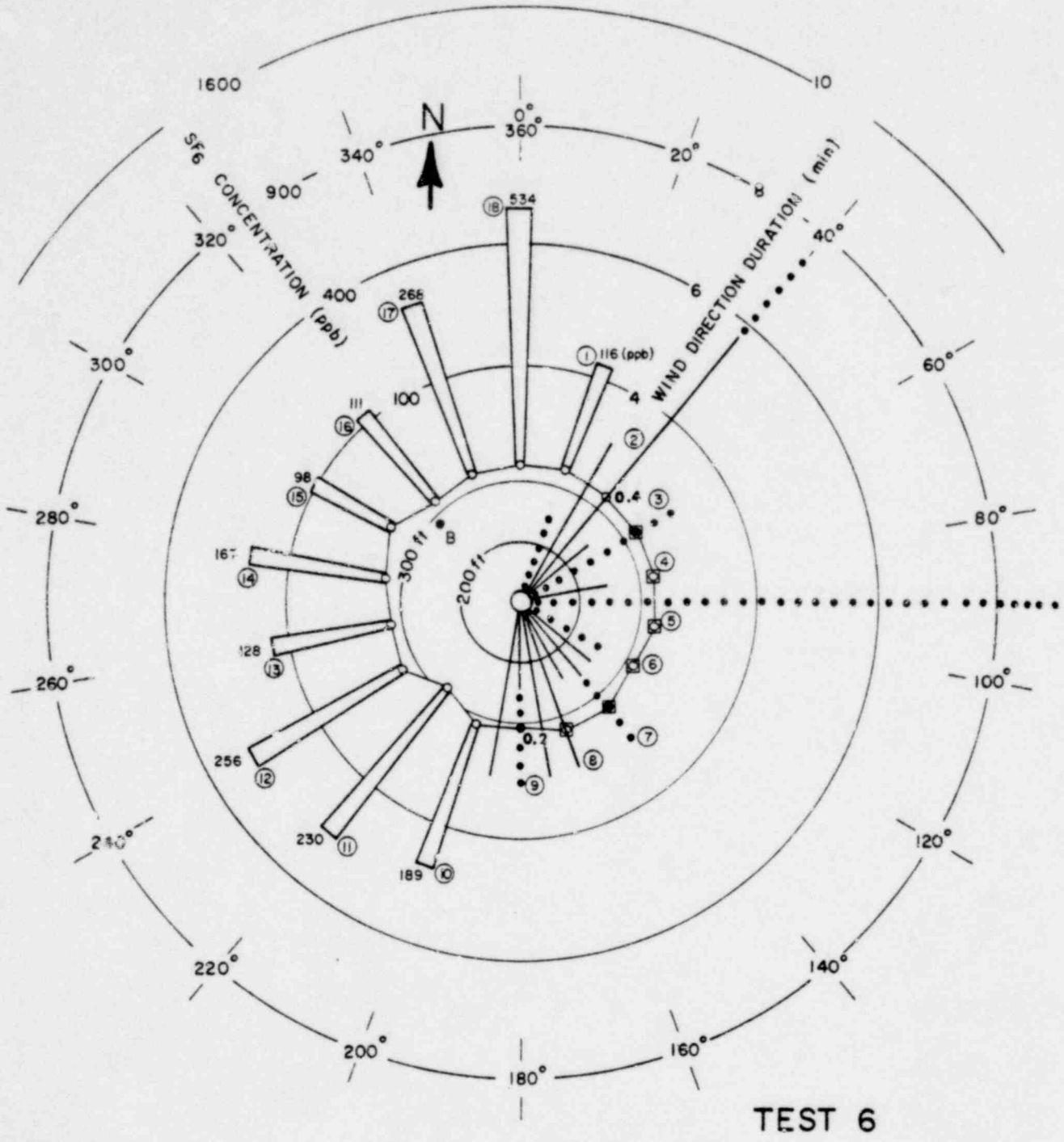

Figure 12
SF_6 Concentrations and Wind Direction Durations: Test 6

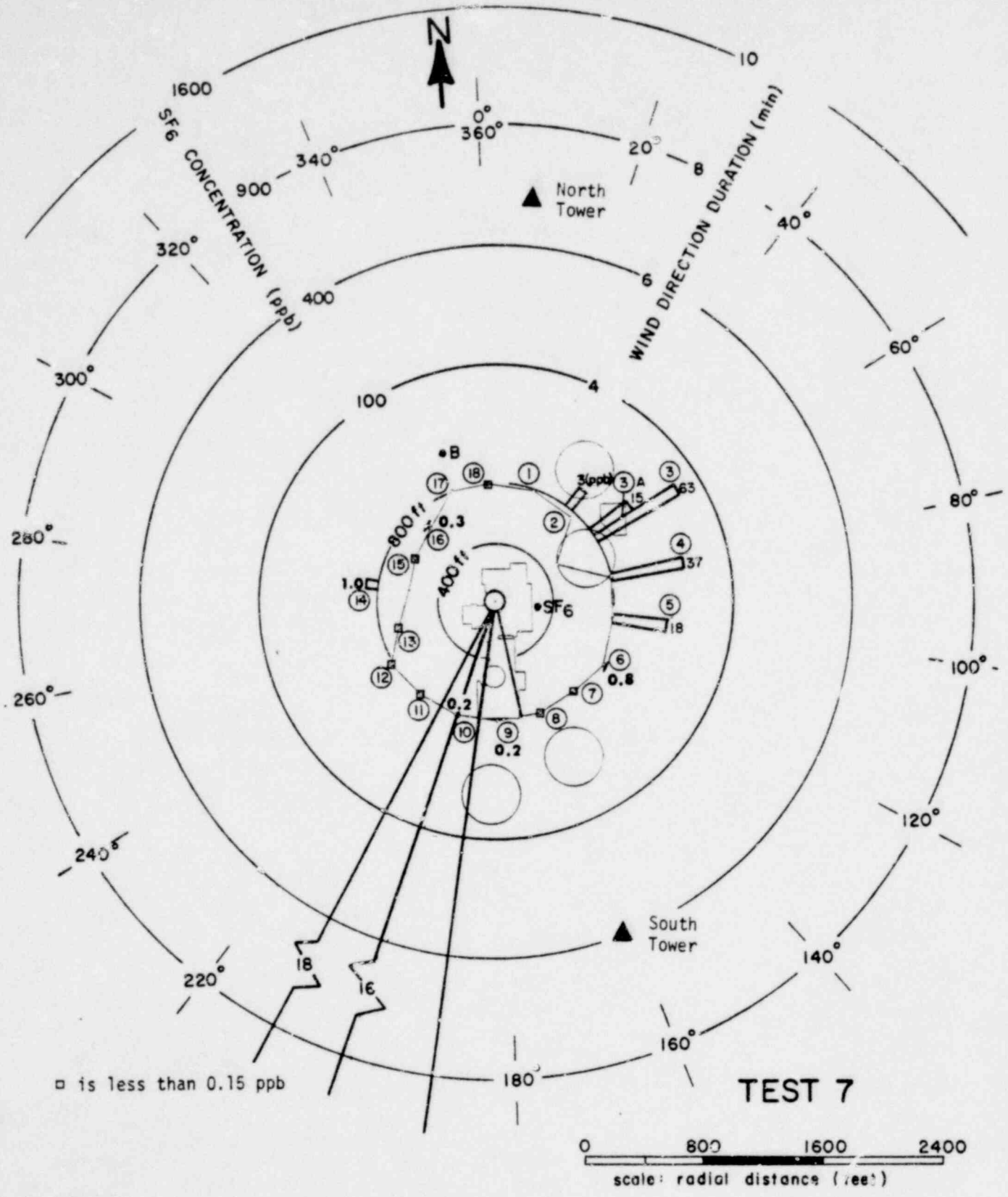

Figure 13
SF_6 Concentrations and Wind Direction Durations: Test 7

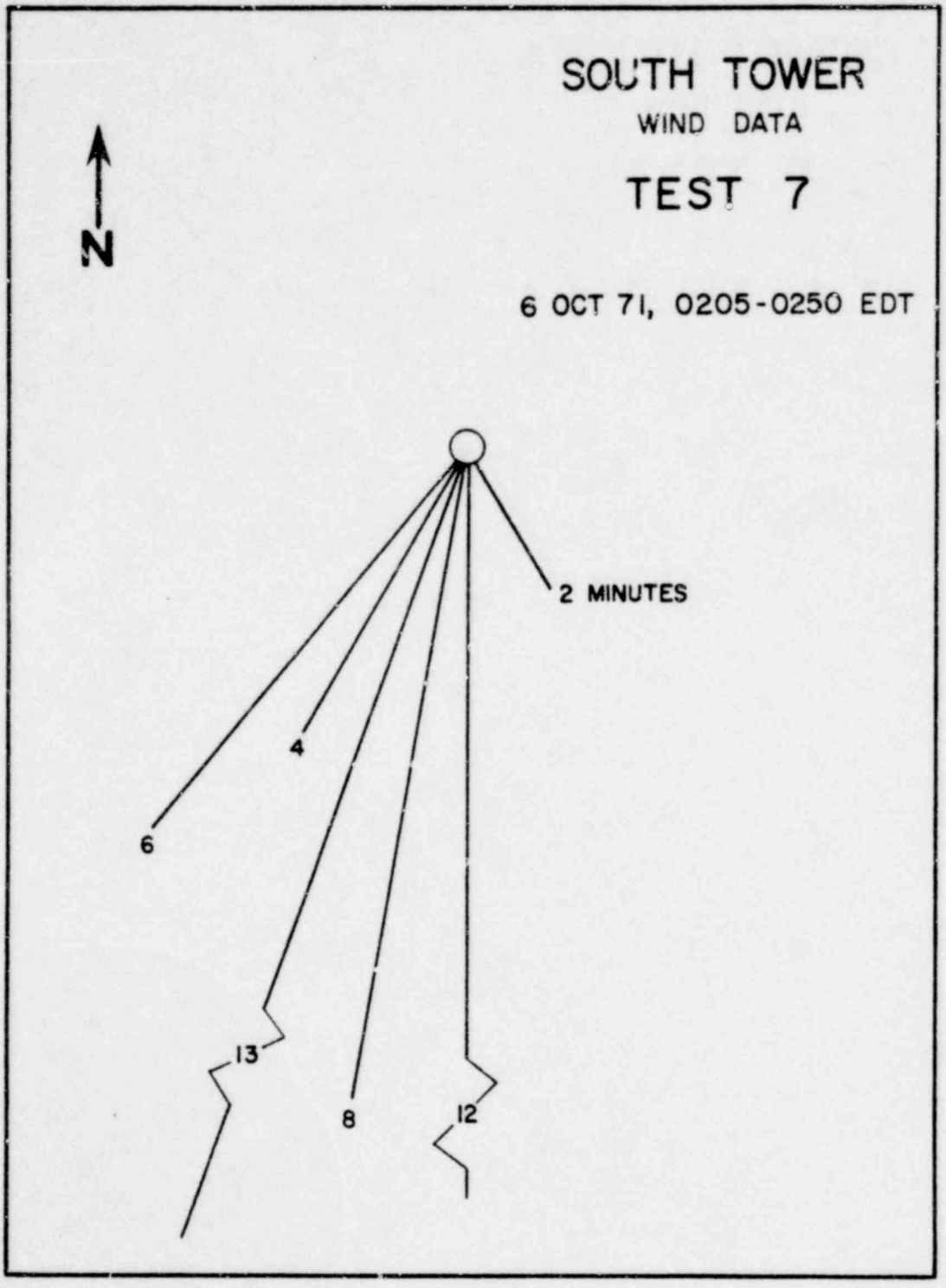

Figure 14
South Tower Wind Direction
Durations: Test 7

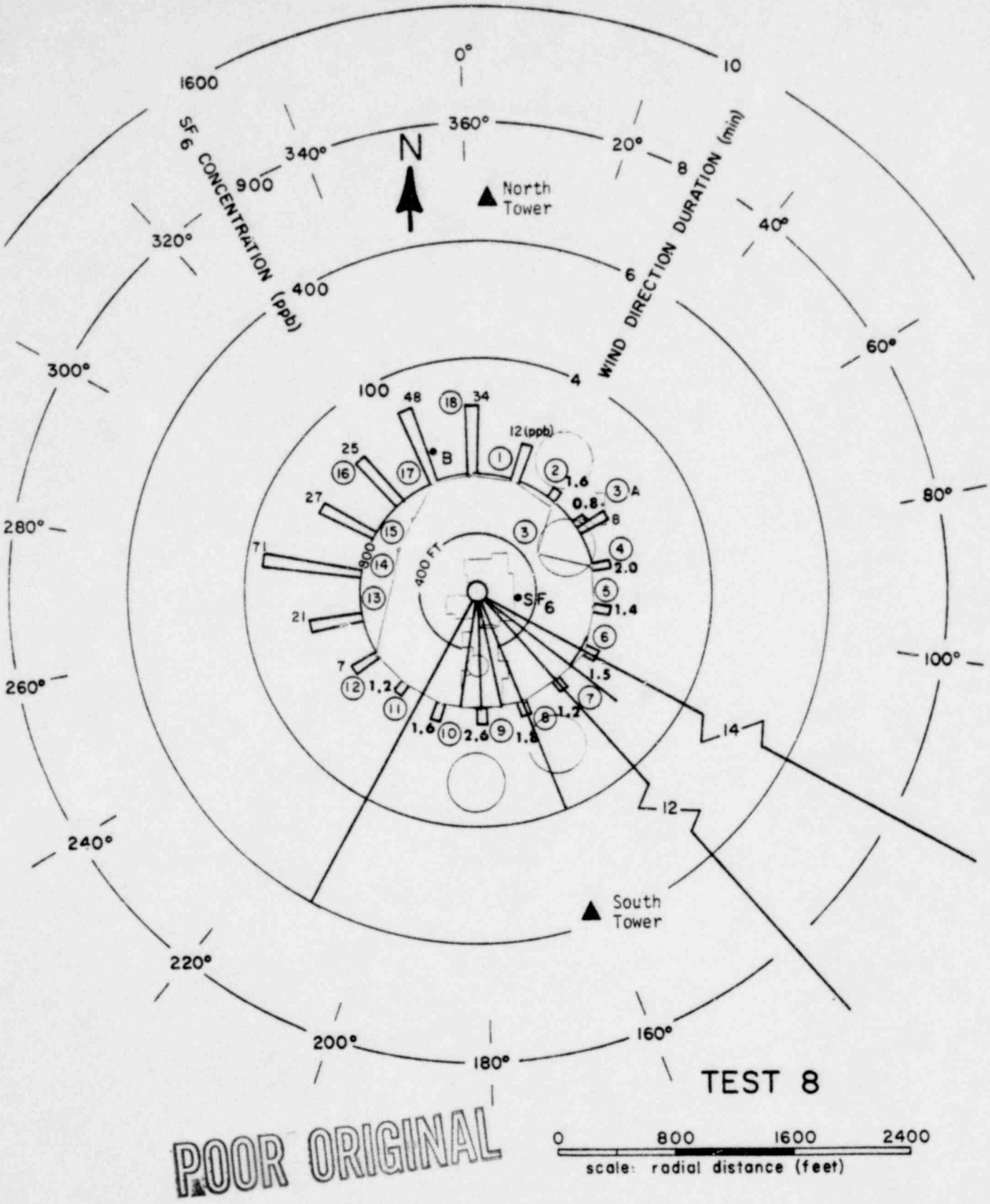

Figure 15
SF_6 Concentrations and Wind Direction Durations: Test 8

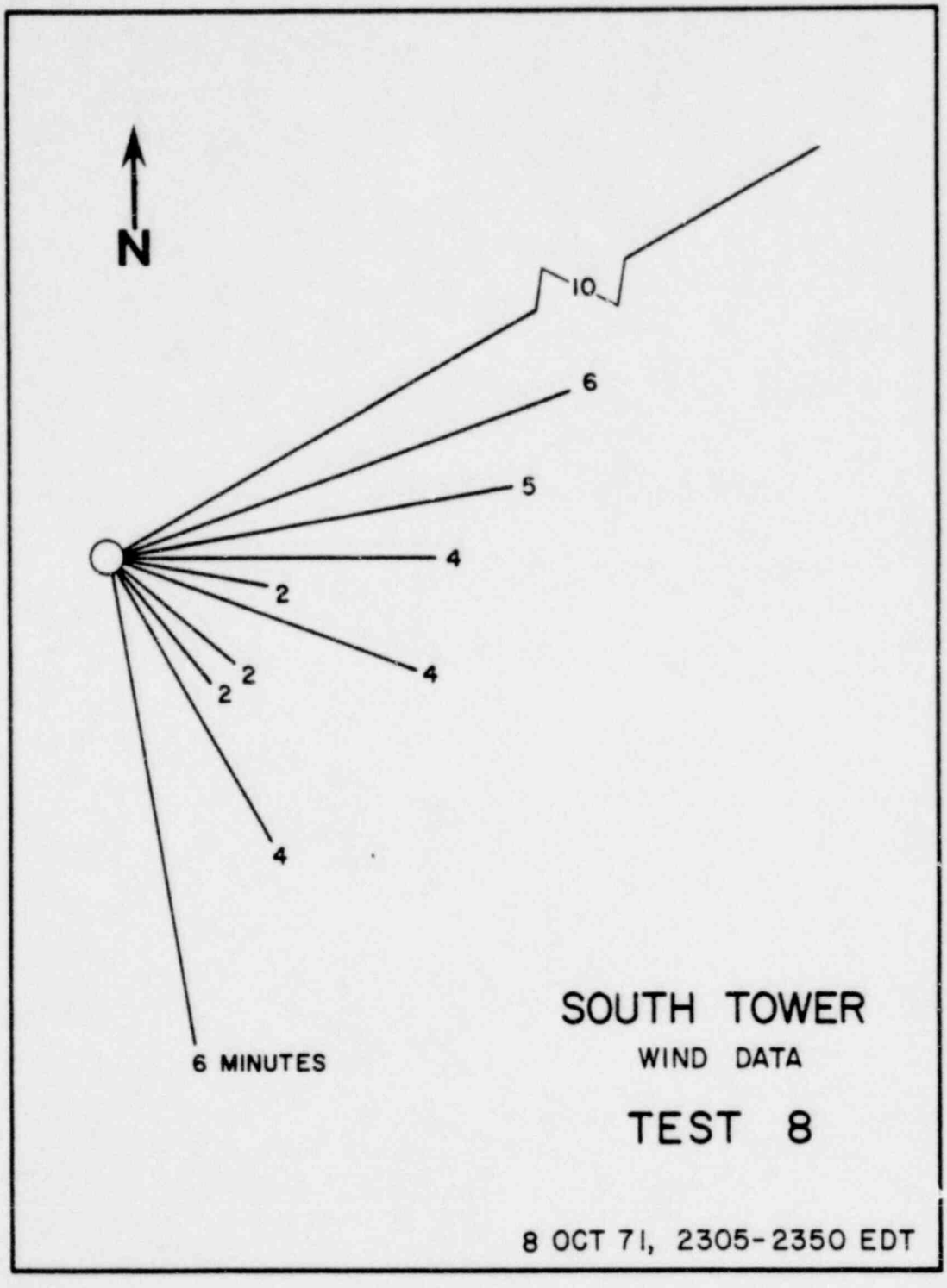

Figure 16
South Tower Wind Durations: Test 8

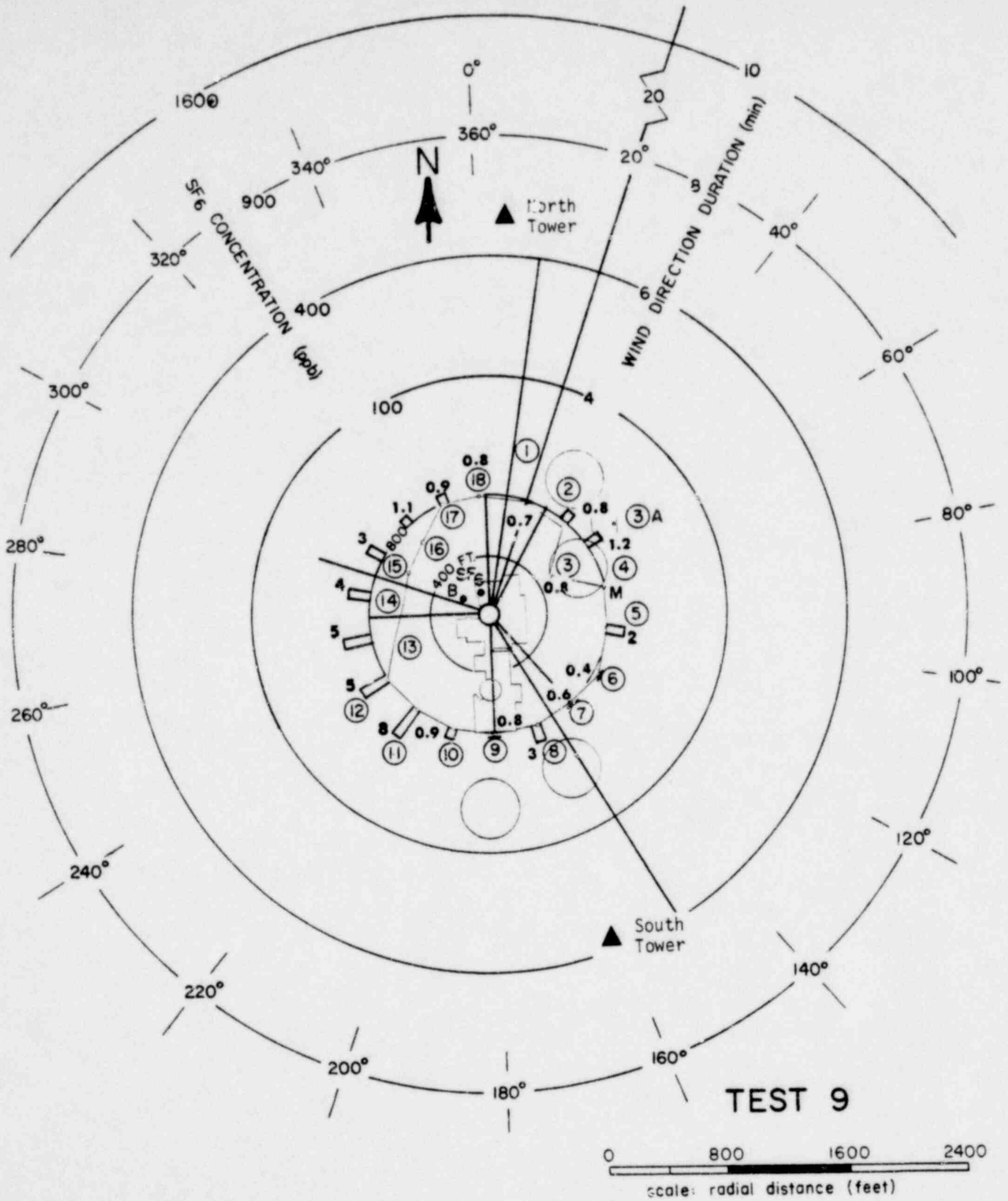

Figure 17
SF_6 Concentrations and North Wind Direction Durations: Test 9

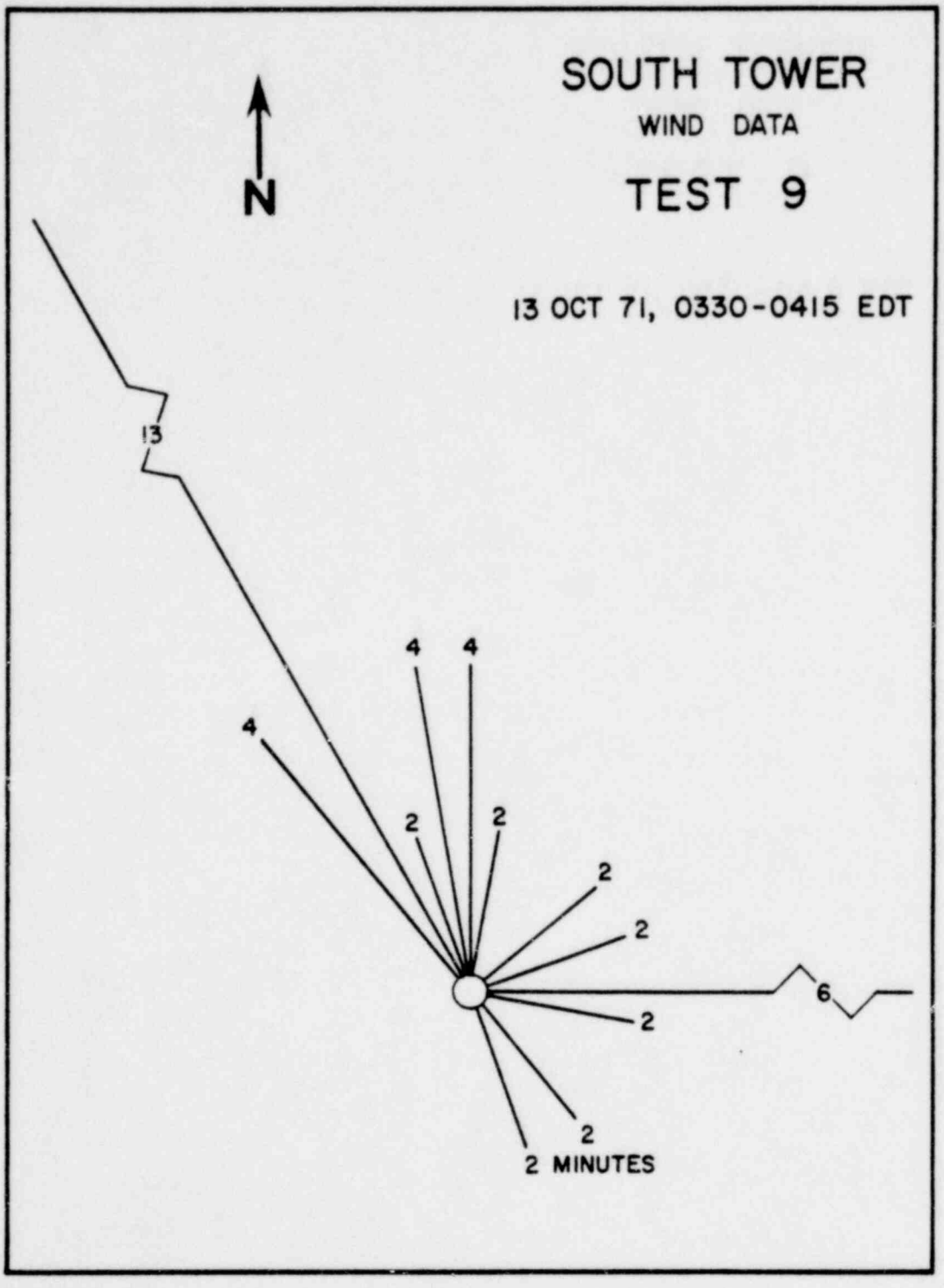

Figure 18
South Tower Wind Direction
Duration: Test 9

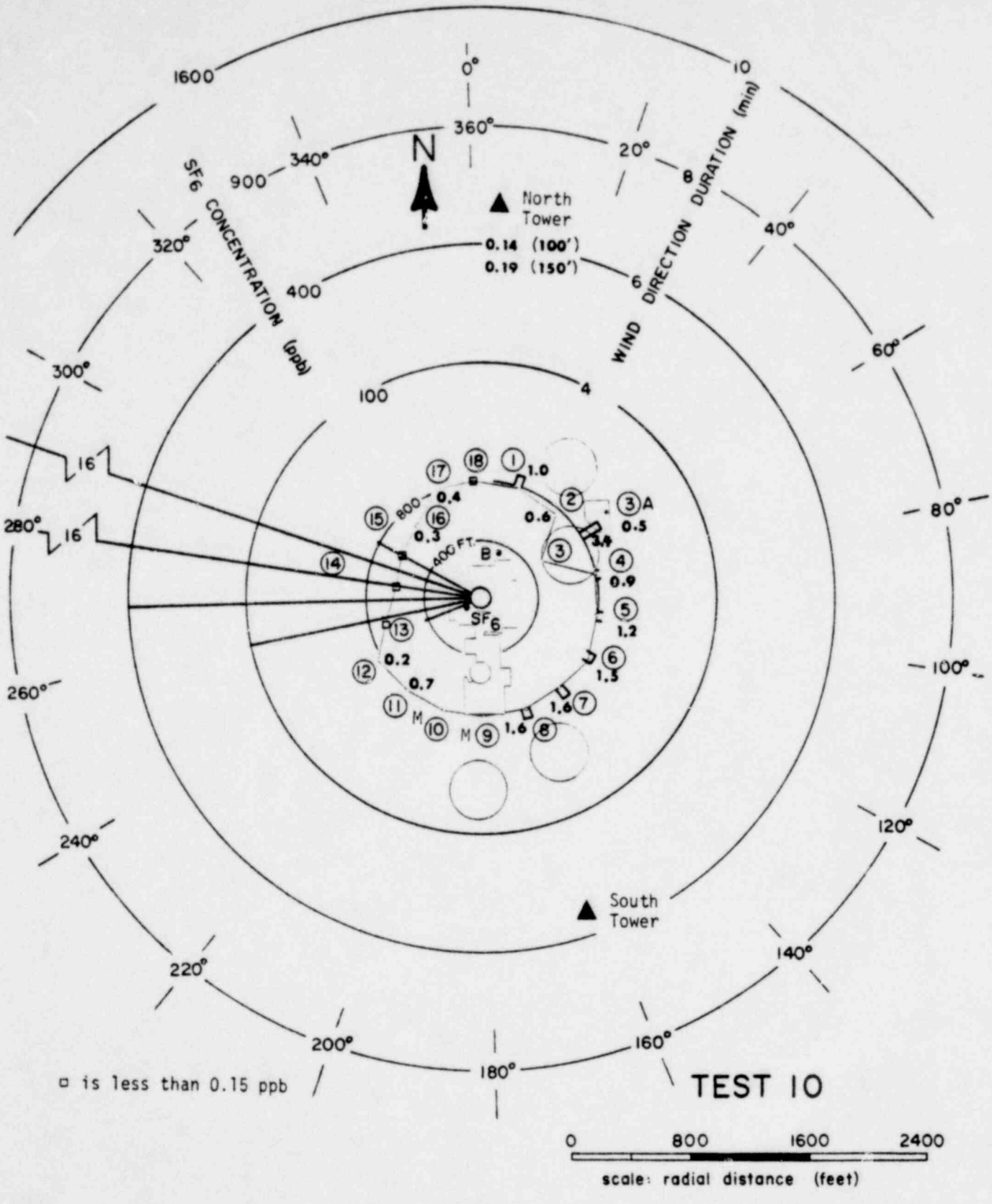

Figure 19
SF_6 Concentrations and North Wind Direction Durations: Test 10

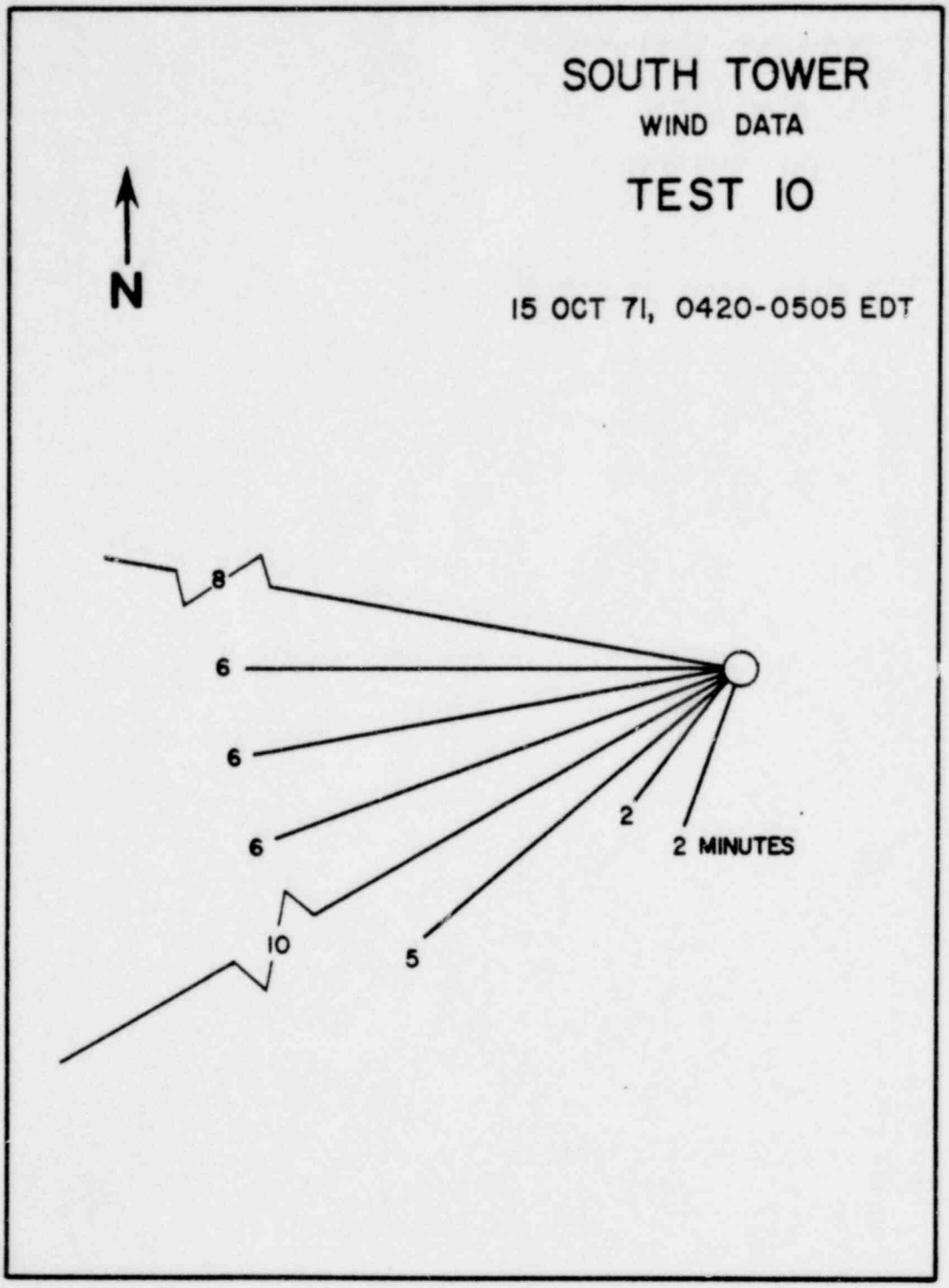

Figure 20
South Tower Wind Durations: Test 10

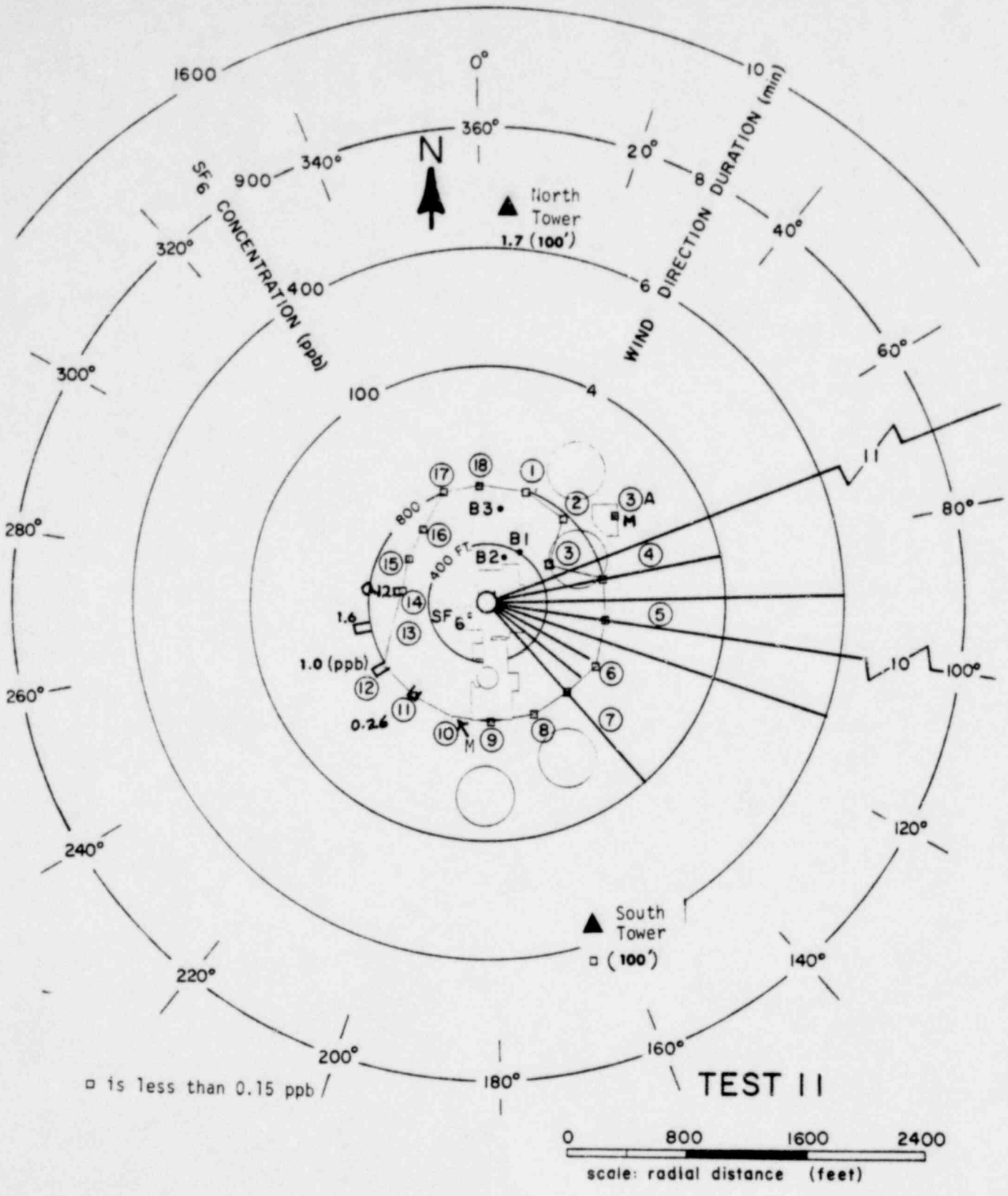

Figure 21
SF_6 Concentrations and North Wind Direction Durations: Test 11

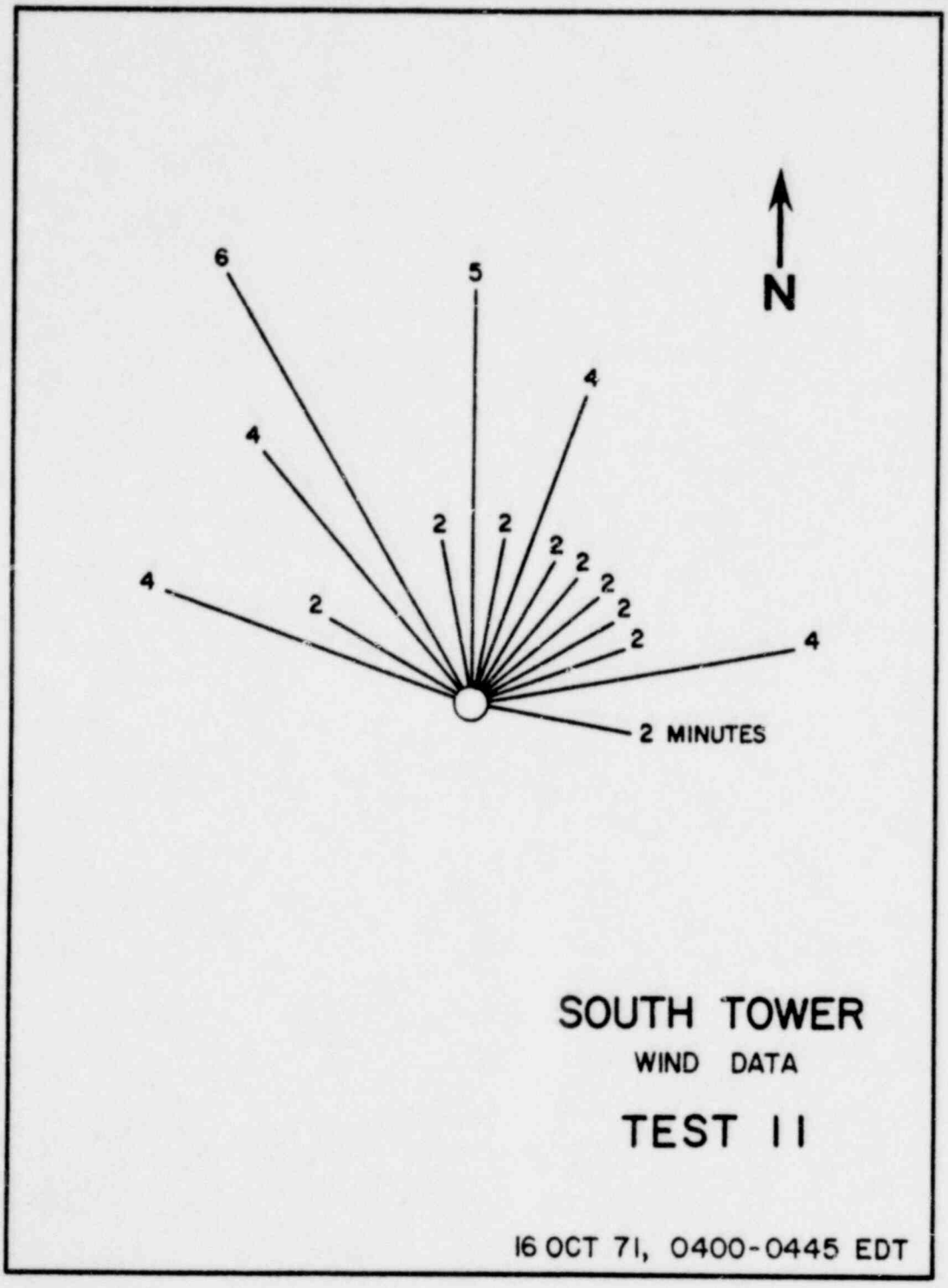

Figure 22
South Tower Wind Durations: Test 11

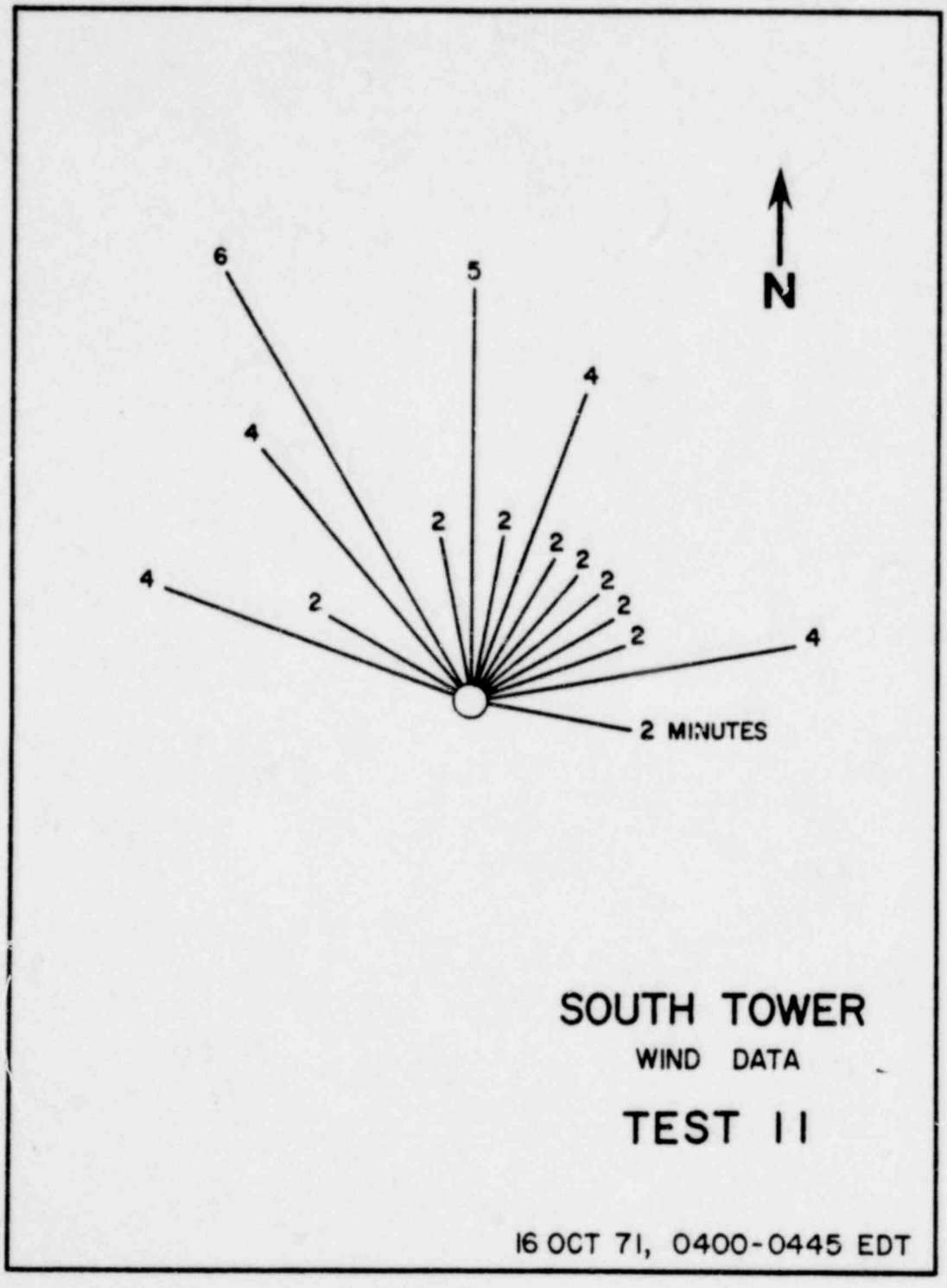

Figure 22
South Tower Wind Durations: Test 11

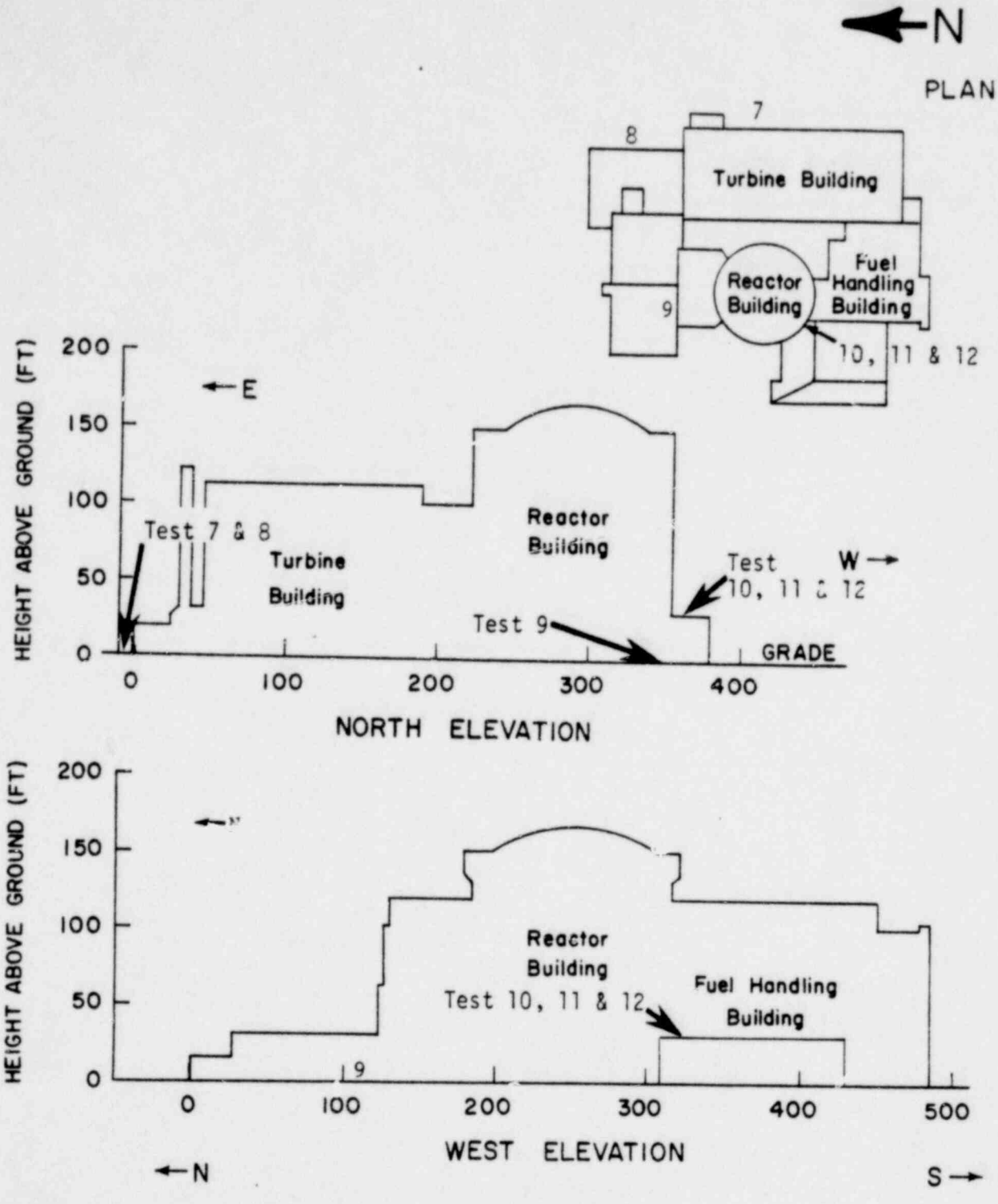

Figure 23

Building Structures Profile as Seen From the North and West

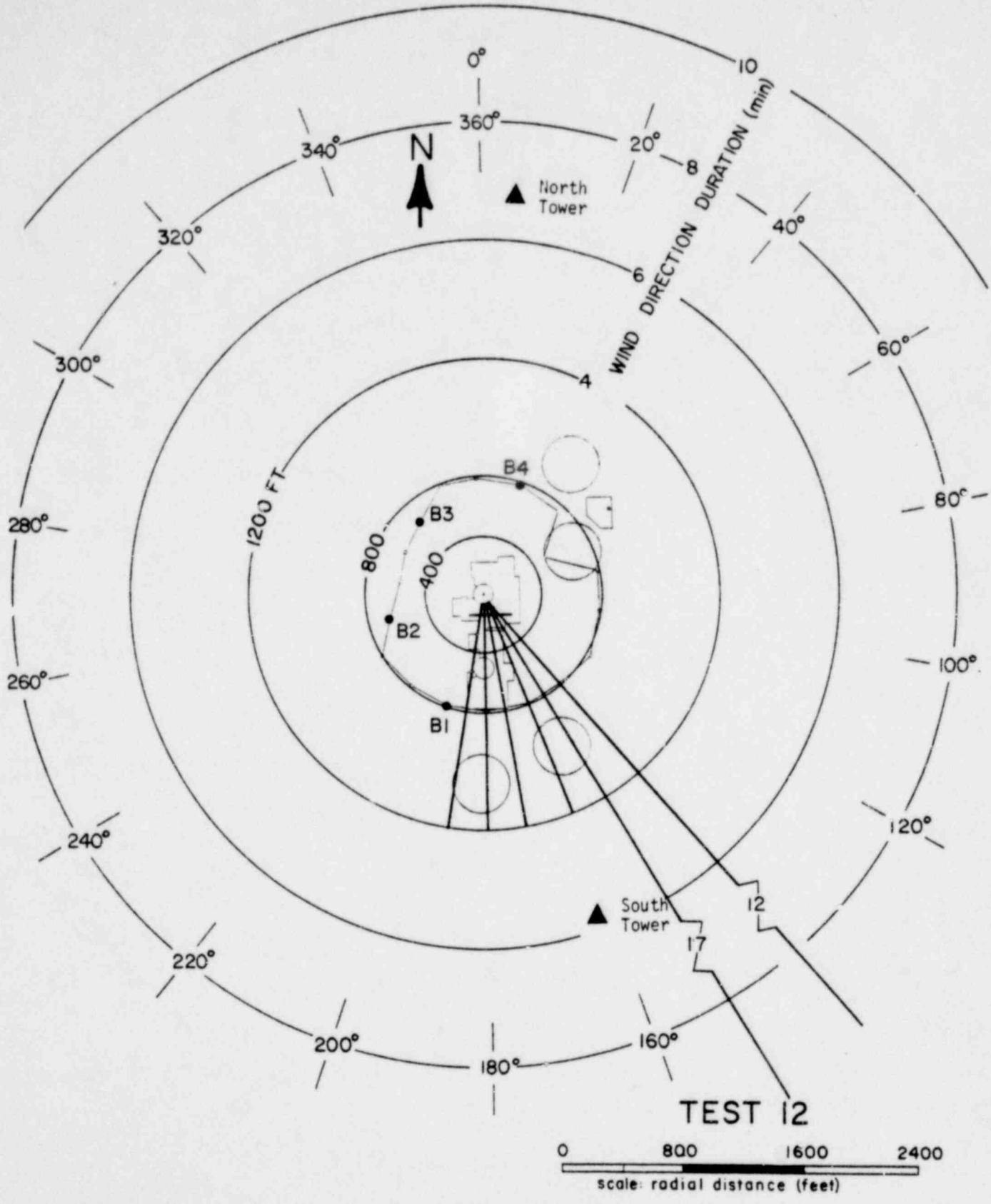

Figure 24

Balloon Locations and North Wind Direction
Durations: Phase 3 (Test 12)

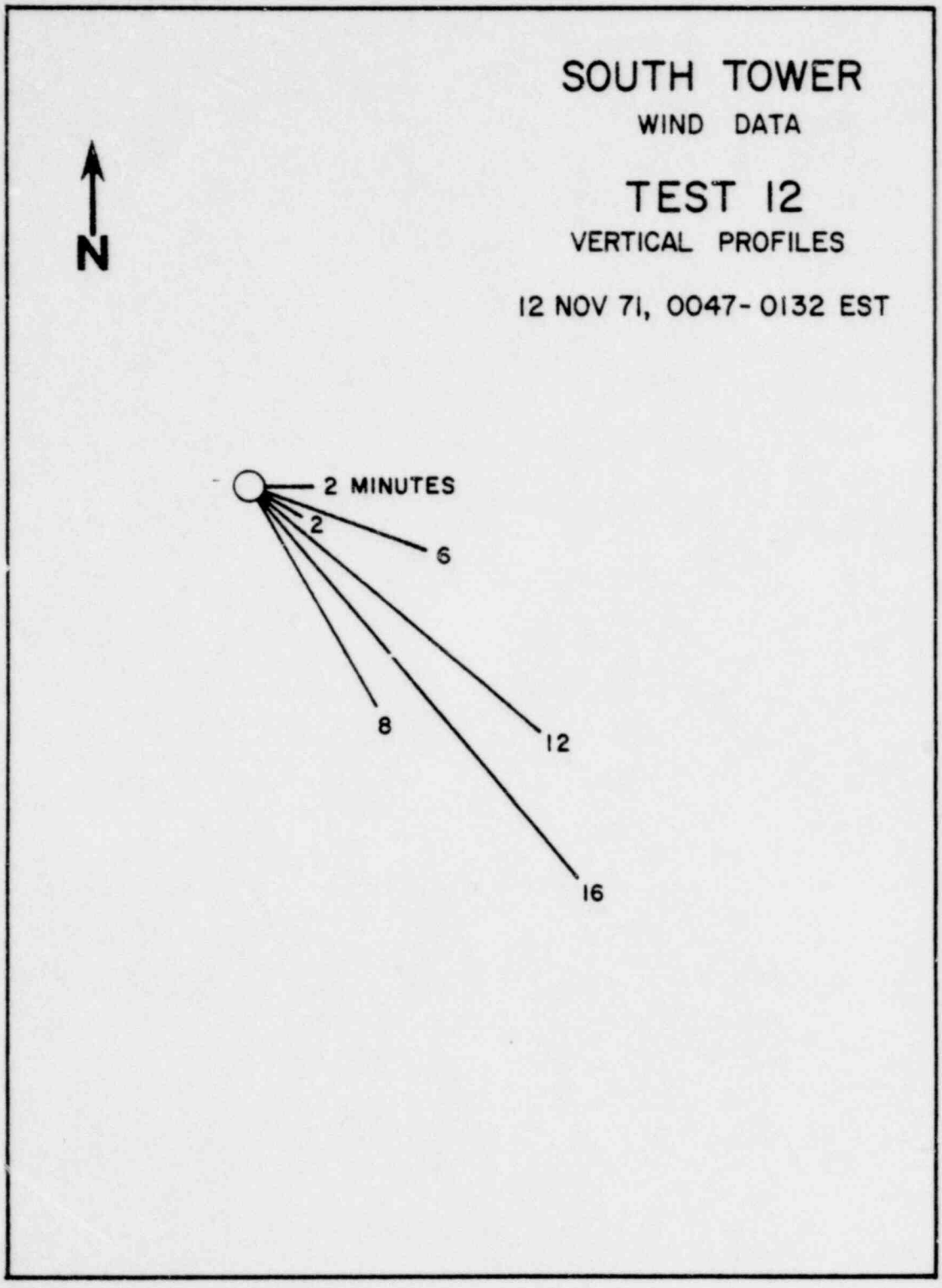

Figure 25
South Tower Wind Direction Durations:
Phase 3 (Test 12)

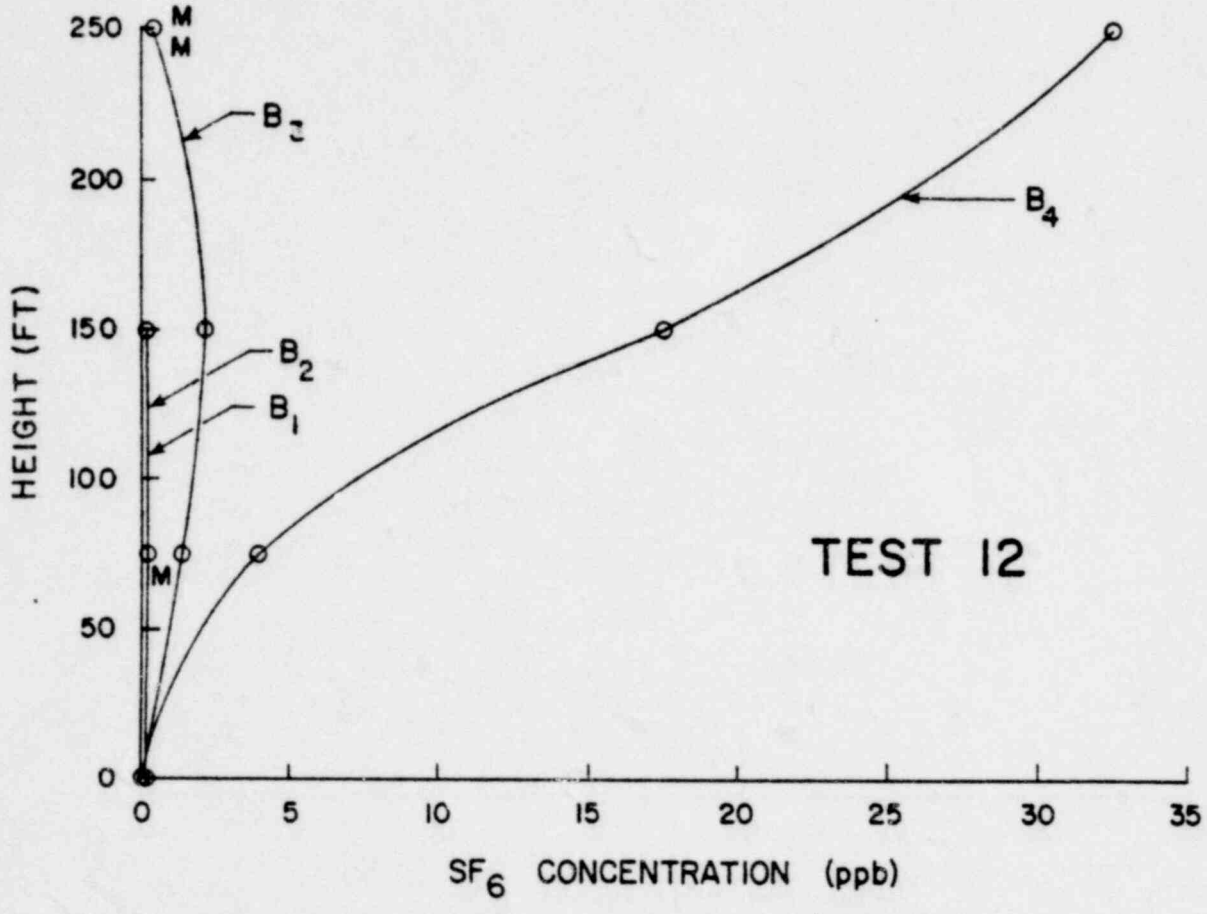

Figure 26
Average Vertical Concentration Profiles:
Phase 3 (Test 12)

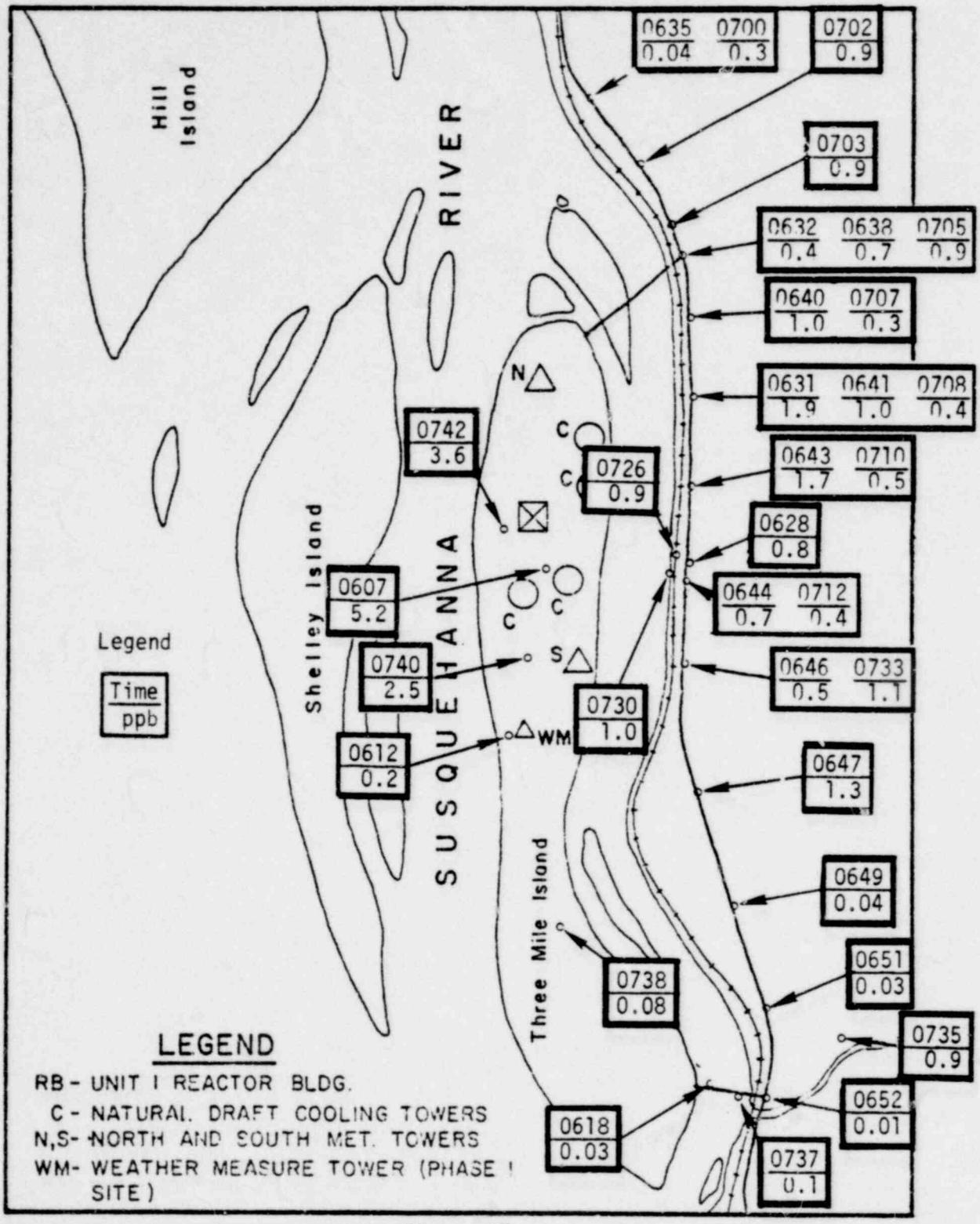

Figure 27
Concentrations Along Rt 441:
Test 10 Road Traverse

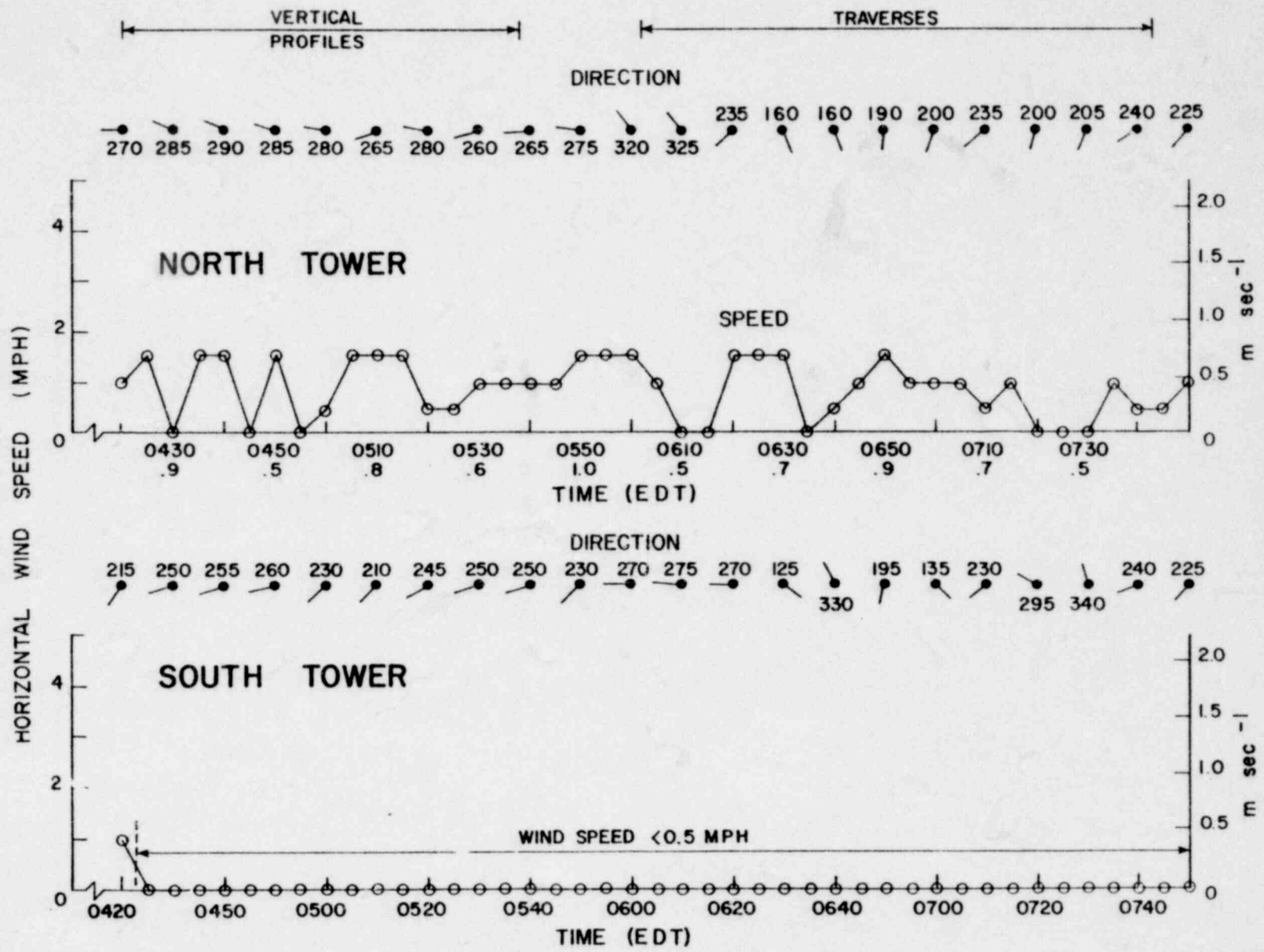

Figure 28
North and South Tower Winds: Test 10 Traverse

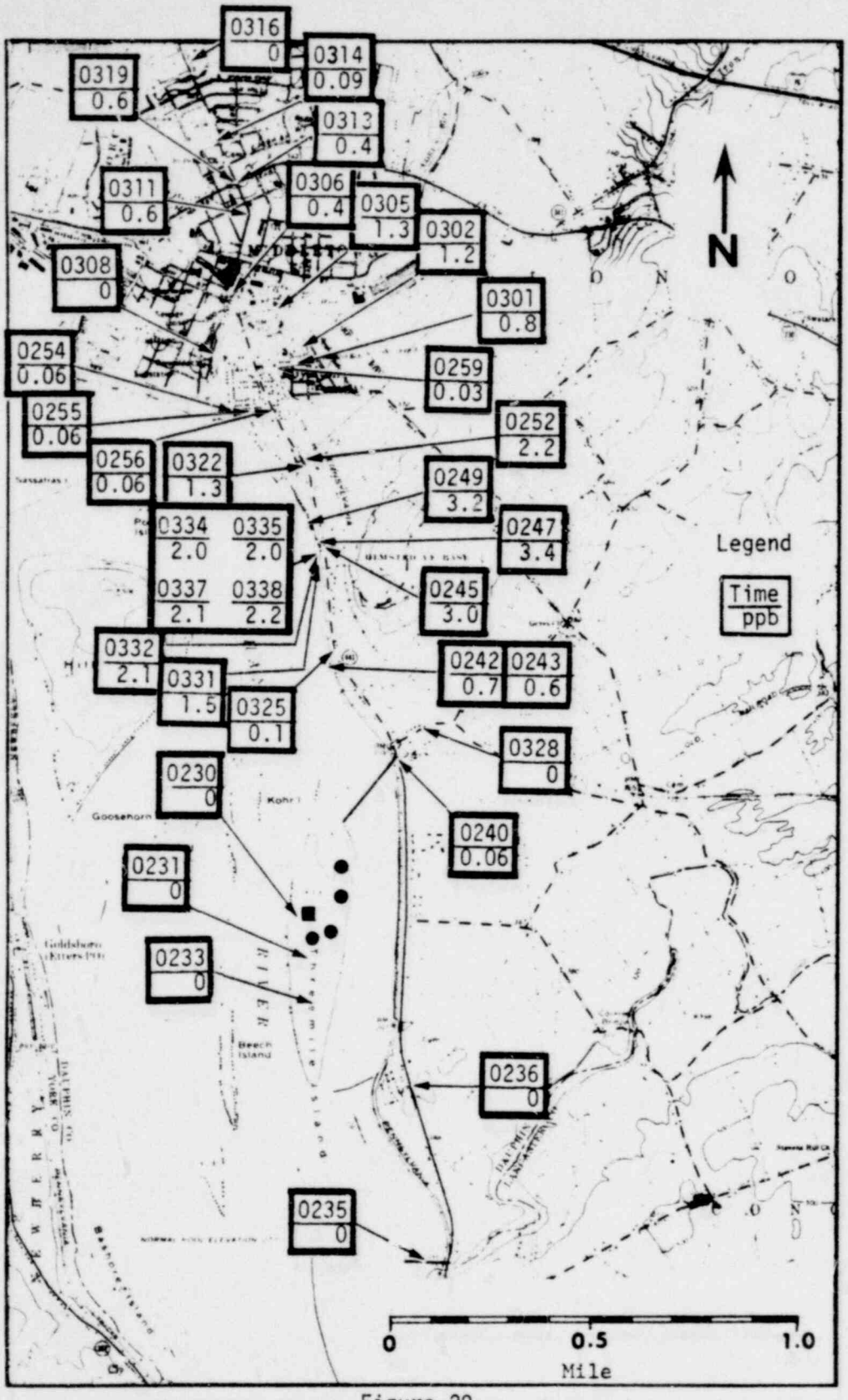

Figure 29
Off-site Downwind Concentrations:
Test 12 Road Traverse

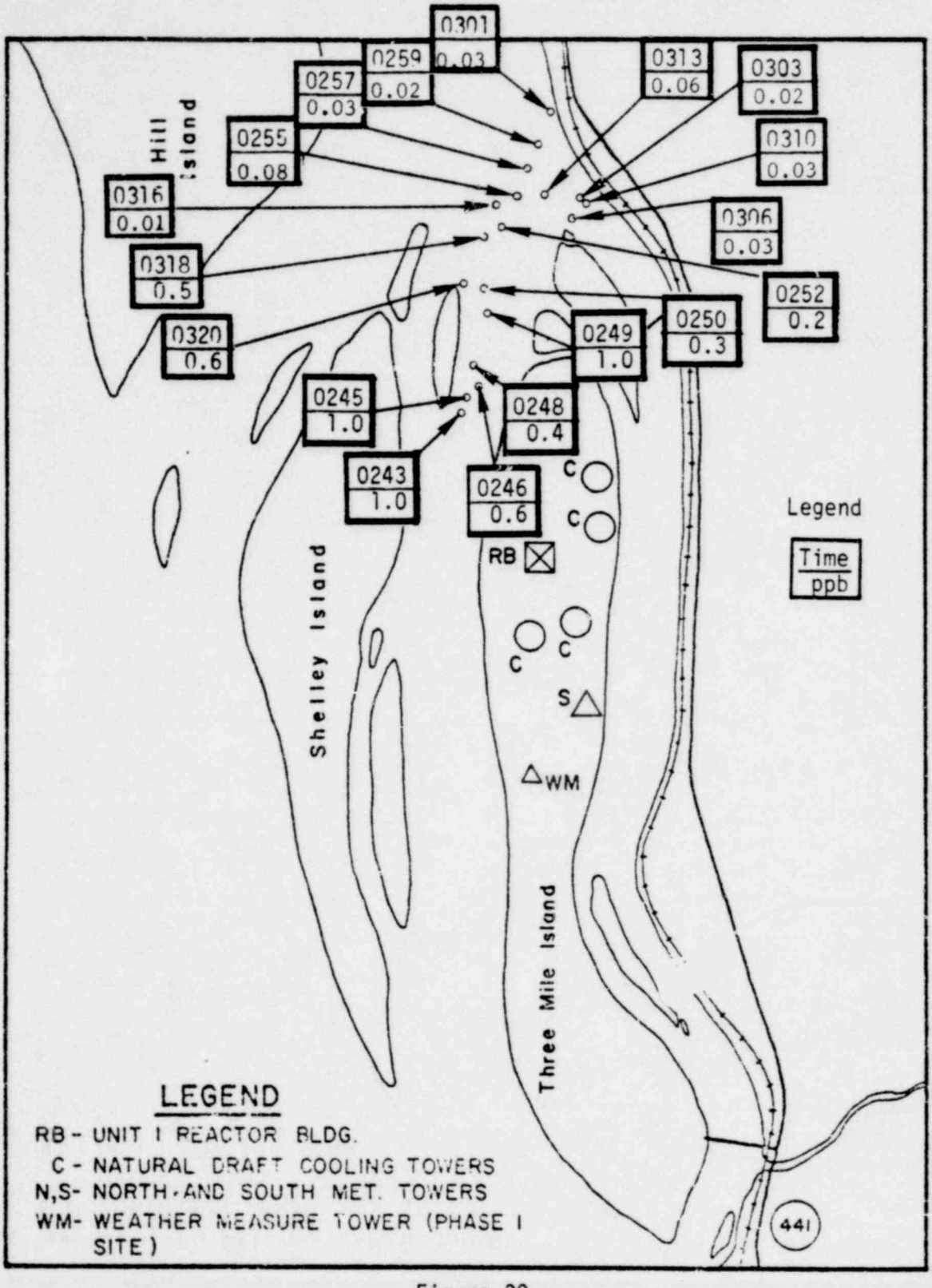

Figure 30
Off-site Downwind Concentrations:
Test 12 River Traverse

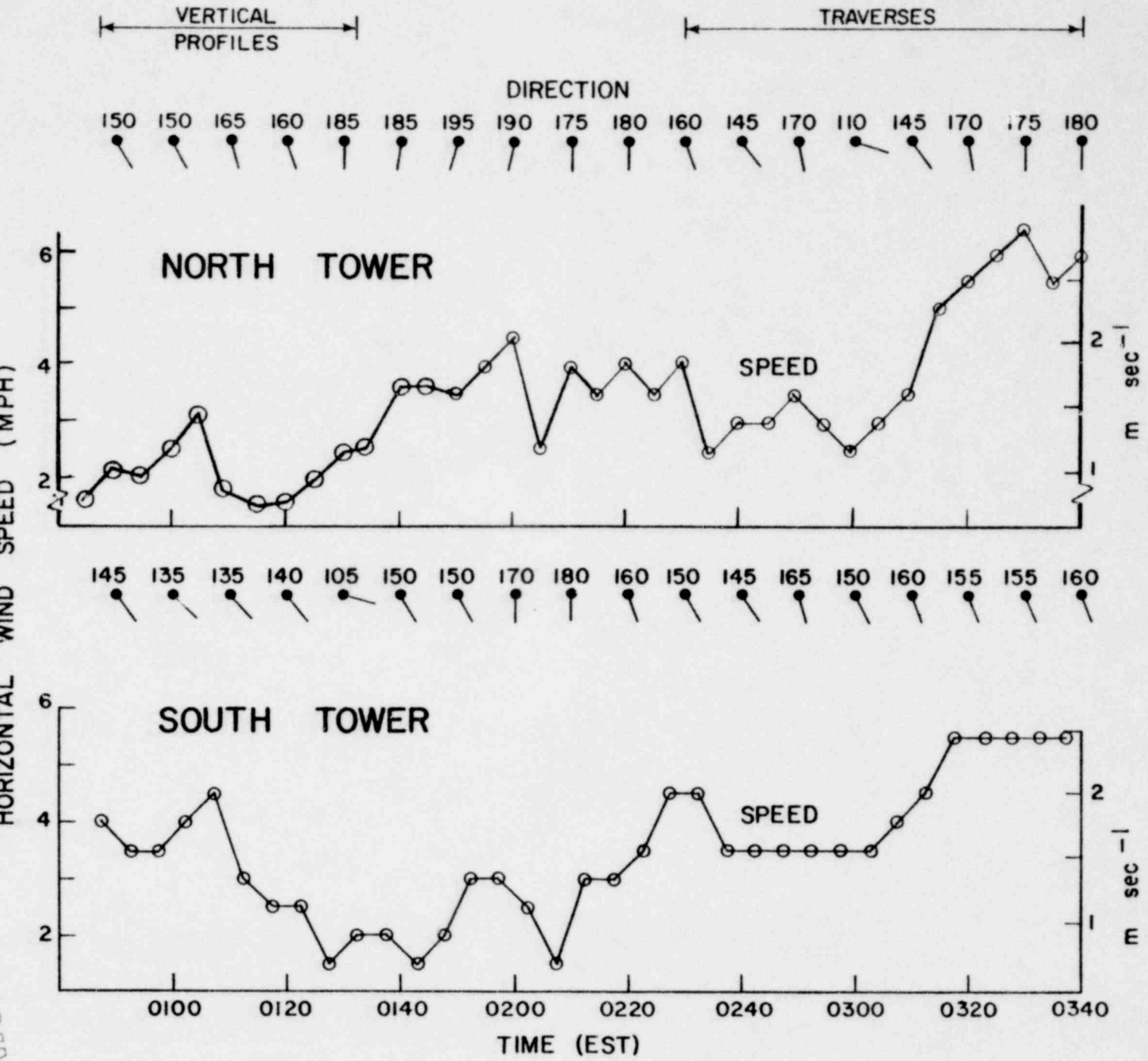

Figure 31
North and South Tower Winds: Test 12 Traverses

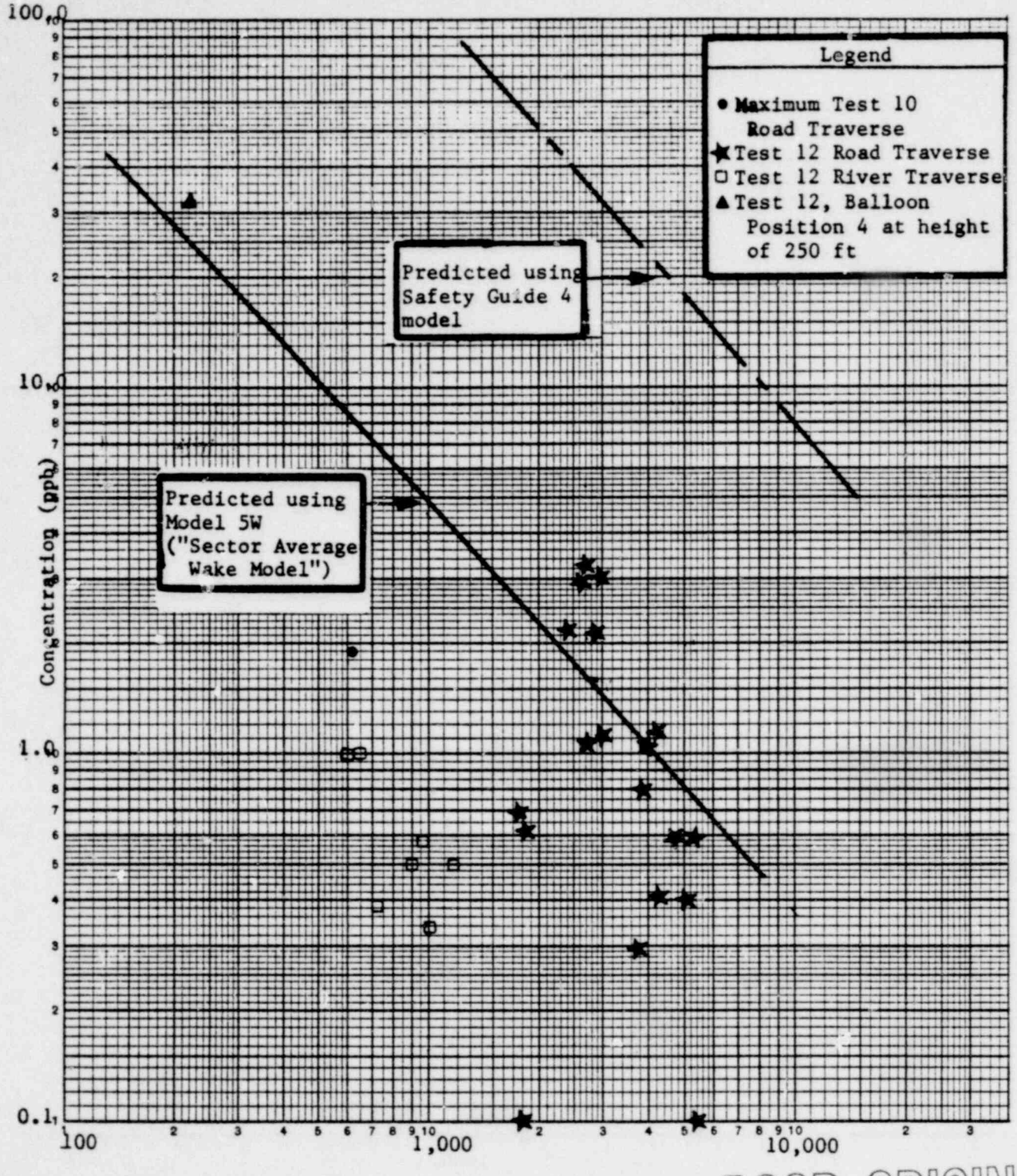

Figure 32
Comparison of Measured Downwind Concentrations
With Model 5W ("Sector Average Wake Model")

APPENDIX A

SF_6 Sampling and Analytical Procedure

LIST OF SYMBOLS

C_s	True concentration of SF_6 in the collected sample.
C_t	Concentration of SF_6 in the tank (diluted sample).
F	Sampling flow rate into tank through needle Valve.
P	Sampling period (time).
R	Dilution ratio of sample.
V_e	Volume corresponding to maximum evacuation of the sampling tank.
V_m	"Make-up" volume, added after sample is collected.
V_s	Volume of collected sample.
V_t	Total (net) volume of tank (tank capacity).

APPENDIX A

SF_6 Sampling and Analytical Procedure

A.1 INTRODUCTION

As outlined previously in Sections 1.1 and 5, SF_6 tracer gas is released under controlled conditions; resultant concentrations are determined at 18 discrete circumferential points based on air samples collected in evacuated tanks over a finite sampling period. The apparatus and procedures are described in detail below.

A.2 APPARATUS AND PROCEDURES

A.2.1 The Sampling Tanks

The sampling tanks used are low pressure oxygen cyclinders with a nominal internal volume of 16 liters. Although 18 such tanks are used for any given test, 20 are readied such that 2 extra are available as spares. Each tank is fitted at one end with a 0-30 in-of-mercury vacuum gauge and a valve. The other end is fitted with a Moore Products Model No. 63SU Constant Differential Flow Controller, a fine-adjustment needle valve, and a quick-release valve. (All fittings are rendered air-tight with Teflon tape.) (See Figure 4).

A.2.2 Tank Capacity

The first step was to accurately determine the actual capacity of each tank, V_t. This was accomplished by filling each tank (without fittings) with water by submersion. The tank was then slowly allowed to drain. The compensating air entered the opposite end through a wet test meter which thus yielded the net volume. The average capacity of the

tanks is 16.1 liters each.

A.2.3 Sampling

The samples of air are obtained by first evacuating the tanks to a pressure of 1 to 2 inches of mercury, and then slowly allowing the tanks to fill through the needle valve at a controlled rate. It was determined experimentally that, if about 8 in or more of vacuum is maintained in the tank, the cylinder will fill at a constant flow rate. If this rate is set at 0.20 liters min^{-1}, the corresponding sampling time is in excess of one hour. However, to provide a margin of safety, a sampling period of about 45 minutes was used.

The flow rate was set on each tank first at the TRC lab, and then again at the TMI site as a check before each test; this is done by evacuating the tanks and monitoring their filling through a 0-1 liter min^{-1} range rotameter.

Although the product of the flow rate and the sampling period should yield the volume of the sample, a more accurate approach is taken as follows.

A.2.4 Sample Volume

First the volume corresponding to a fully evacuated tank, V_e, is measured using the wet test meter. This differs from the net volume, V_t, because of the residual air which remains after the evacuation. However, at the end of the sampling period, the tanks are returned to the on-site lab in a still partially evacuated state. In order to ensure against possible leakage which might introduce SF_6 from the contaminated environmental air, the cylinders are immediately filled with "clean" bottled air.

This "make-up" volume, V_m, is also measured with the wet test meter. Since a direct connection between the tank and the nitrogen bottle might cause the sampling cylinder to over-pressurize, a balloon is used as an intermediate. We may now calculate the sample volume from the expression

$$V_s = V_e - V_m . \qquad (1)$$

The amount of dilution of the sample is thus given by the dilution ratio:

$$R = \frac{V_t}{V_s} . \qquad (2)$$

A.2.5 Tracer Gas Concentration

We come now to the determination of the quantity of SF_6 in the tank. After the cylinder has been brought to zero vacuum, the vacuum gauge apparatus at one end of the tank is removed. (This leaves only a 1/4-in opening to the room air, which permits negligible exchange during the short measurement time.) A probe is then inserted into the cylinder such that sample air is drawn into an Analog Technology Corp. Model 112B Tracer-Gas Leak Detector. This instrument produces a voltage output which is recorded in an Esterline Angus Model T171B strip chart recorder. The detector offers four sensitivity ranges which adequately span the concentrations of SF_6 encountered in this study. Operated in the "column mode", the minimum detectable concentration is 0.01 ppb. Each tank is measured twice on each of two detector-recorders such that instrument malfunction can be immediately discovered; this also provides a real-time check on possible operator error.

Both of the detectors used in this study were calibrated by the manufacturer. However, the instruments were recalibrated at the TRC labs using

purchased concentrations of SF_6 certified correct at 2.5, 250, and 2500 ppb.

A.3 PURGE PROCEDURES

Following measurements of all tank concentrations, the contents were purged using clean bottled air until the gas detector probe measured a background level in the tanks. The valves were closed and the tanks stored until the next test.

A.4 SAMPLE CALCULATION

Total tank capacity, V_t = 16.1 liters

Volume evacuated, V_e = 14.2 liters

Preset flow rate = 0.20 liters min^{-1}

Make-up volume, V_m = 5.3 liters

Therefore, the sample volume

$$V_s = V_e - V_m$$

$$= 14.2 - 5.3 \text{ liters} \quad (1)$$

$$= 8.9 \text{ liters.}$$

Now, the dilution ratio

$$R = \frac{V_t}{V_s}$$

$$= \frac{16.1}{8.9} \quad (2)$$

$$= 1.8 .$$

Thus, if the tank concentration, C_t, of SF_6 is 50 ppb, then the true concentration of the sample is

$$C_s = RC_t$$

$$= 1.8 \times 50 \text{ ppb} \quad (3)$$

$$= 90 \text{ ppb.}$$

If the sample period P was 50 minutes, the flow rate F through the needle valve would be

$$F = \frac{V_s}{P}$$

$$= \frac{8.9 \text{ liters}}{50 \text{ min}} \qquad (4)$$

$$= 0.18 \text{ liters min}^{-1}.$$

Hence, this indicates that the flow rate as initially adjusted in the lab was set (0.20 - 0.18 =) 0.02 liters min^{-1} too low. Figure A-1 shows one of the work sheets that were used during the tests to perform the above calculations.

Location Weather Measure Open Field Test No. 3

Tank No. 2 Position No. 15

Flow Rate 0.20 liters/min. Tank Capacity 15.45 liters

Time	Vacuum (Inches Hg)	
4:46	28½	(Take Reading, OPEN Valve)
4:55	25¼	
5:05	22	
5:15	18¾	
5:25	15	
5:34	12	
		(CLOSE Valve, Take Reading)

Vacuum at time makeup air added: 12 inches Hg.

Time makeup air added: 6:40

Volume corresponding to initial vacuum: 14.15 liters

Volume of makeup air: 5.5 liters

Sample Volume: 8.6 liters

SF_6 concentration in tank: 103 ppb

Dilution ratio: 1.8

True SF_6 concentration 185 ppb

Figure A-1
Example of Work Sheets Used to Compute
Tank Concentrations

1407 128

APPENDIX B

Reduction of Meteorological Data

APPENDIX B

Reduction of Meteorological Data

On-site meteorological measurements are described in Section 6.0. Wind at 100 feet above ground at both the north and south tower is measured continuoisly by Beckman and Whitley short vane anemometers. Typical traces are shown in Figures B-1 and B-2. Wind at 30 ft above ground was recorded only during the Phase 1 SF_6 release periods from a Weather Measure Model W1034-540 anemometer situated in the center of the Phase 1 sampling grid. This is the same location as the SF_6 gas release point for Phase 1 tests. A typical trace is shown by Figure B-3.

Temperature differences between 150 and 25 feet on the north tower are measured by matched thermistors housed in Geotech aspirated radiation shields and recorded continuously. A typical ΔT trace is shown in Figure B-4.

Average wind speed ($\bar{u}$), average wind direction ($\bar{\theta}$), and directional range (θ) were taken over each minor chart division (Figure B-3). When the chart drive was non-uniform, periodic time checks were made manually and a linear time scale assumed between marks. Average one-minute values were estimated from the Analog chart. Direction data were also extracted in a similar manner. During periods of calm or chart drive problems correction for true direction was made on the basis of smoke plumes from Federal H-C 3-minute smoke candles.

North and south tower wind data (used primarily with Phase 2 and 3 tests) were extracted every minute. From these data, values of average direction and average speed were computed during the test interval. The total wind direction meander (or range θ) and the standard deviation σ_θ were also computed. Values of σ_ϕ were also computed from the bivane

located on the north weather tower.

Temperature difference between 150 and 25 feet was averaged over the entire period of SF_6 sampling (usually 40-50 minutes). Since this difference is expressed in °F per 125 ft, it was multiplied by 1.45 to convert to °C/100m.

All pertinent extracted weather data from the three tower locations are presented in Table B-1.

APPENDIX B

FIGURES

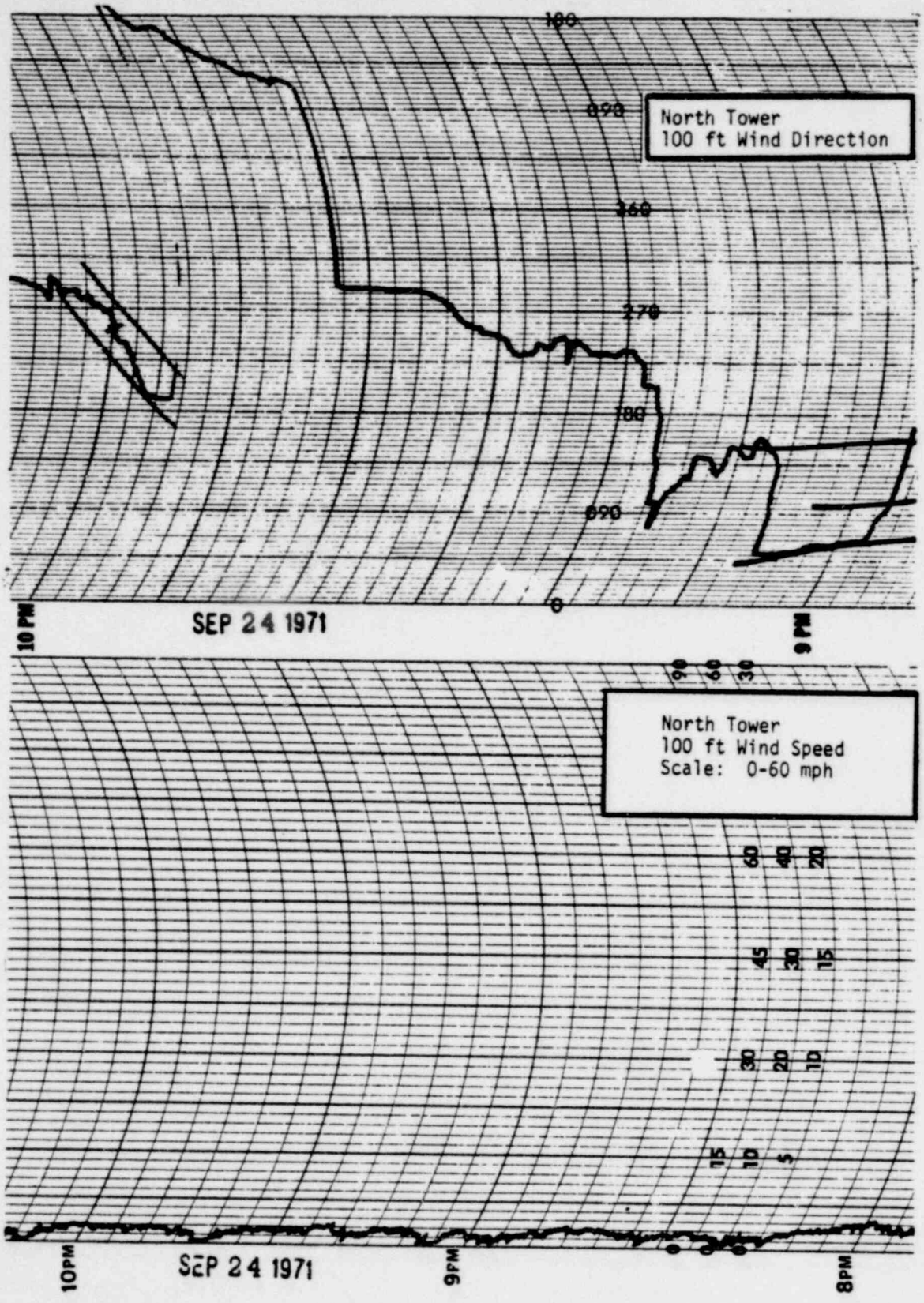

Figure B-1
Example of Wind Speed and Direction
Charts: North Tower

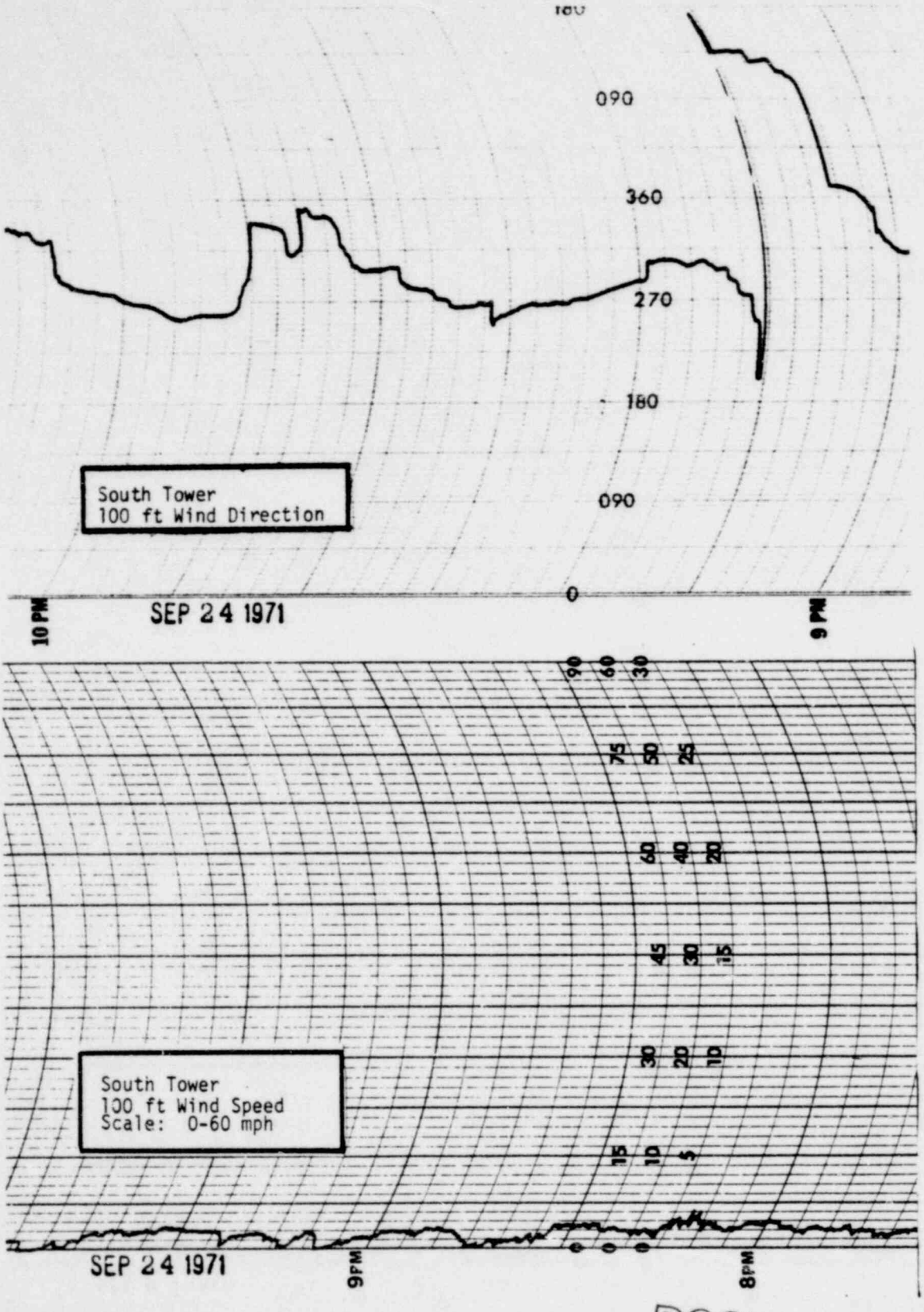

Figure B-2
Example of Wind Speed and Direction
Charts: South Tower

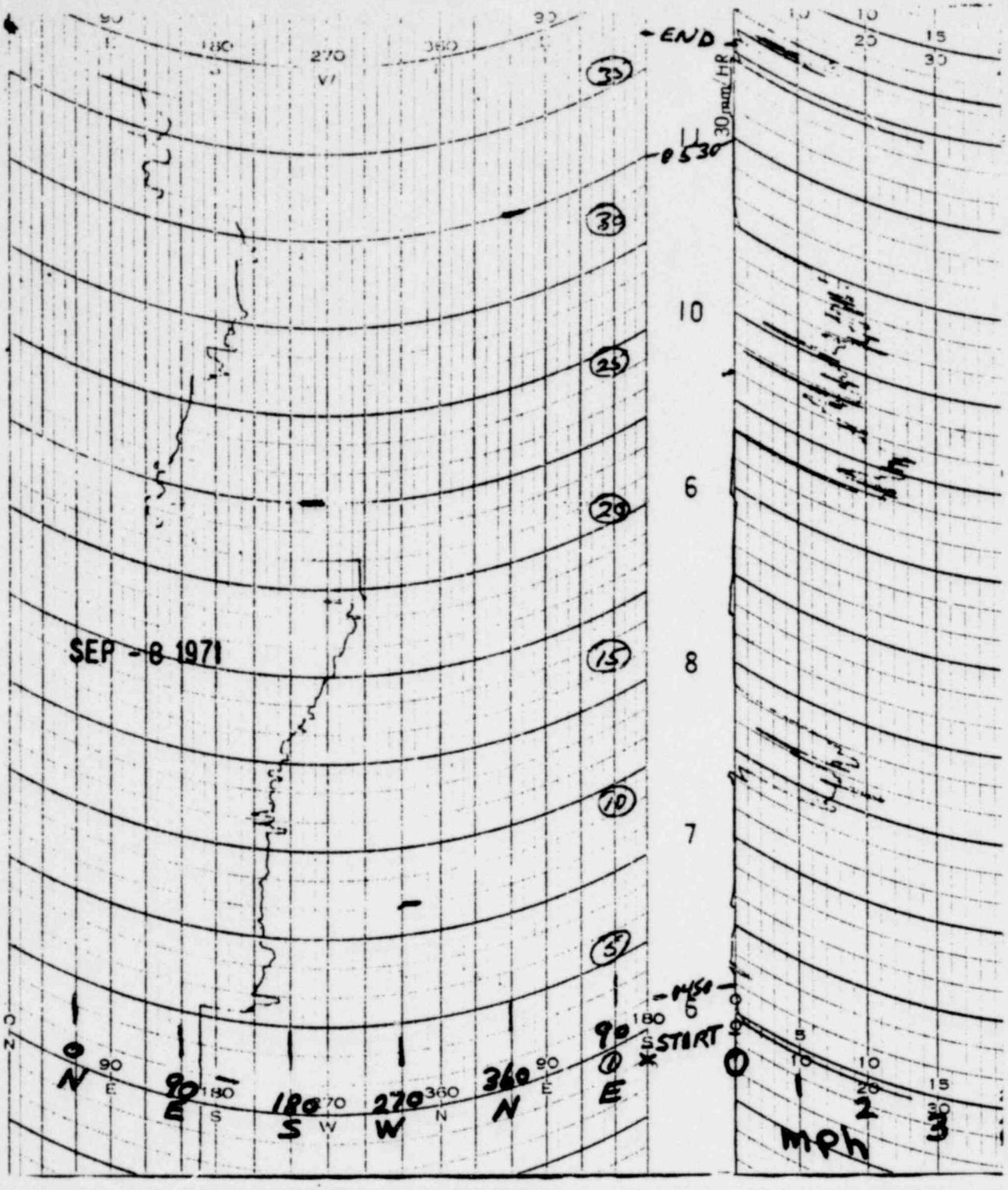

Figure B-3
Example of Wind Speed and Direction Charts
from the 30 ft Weather Measure

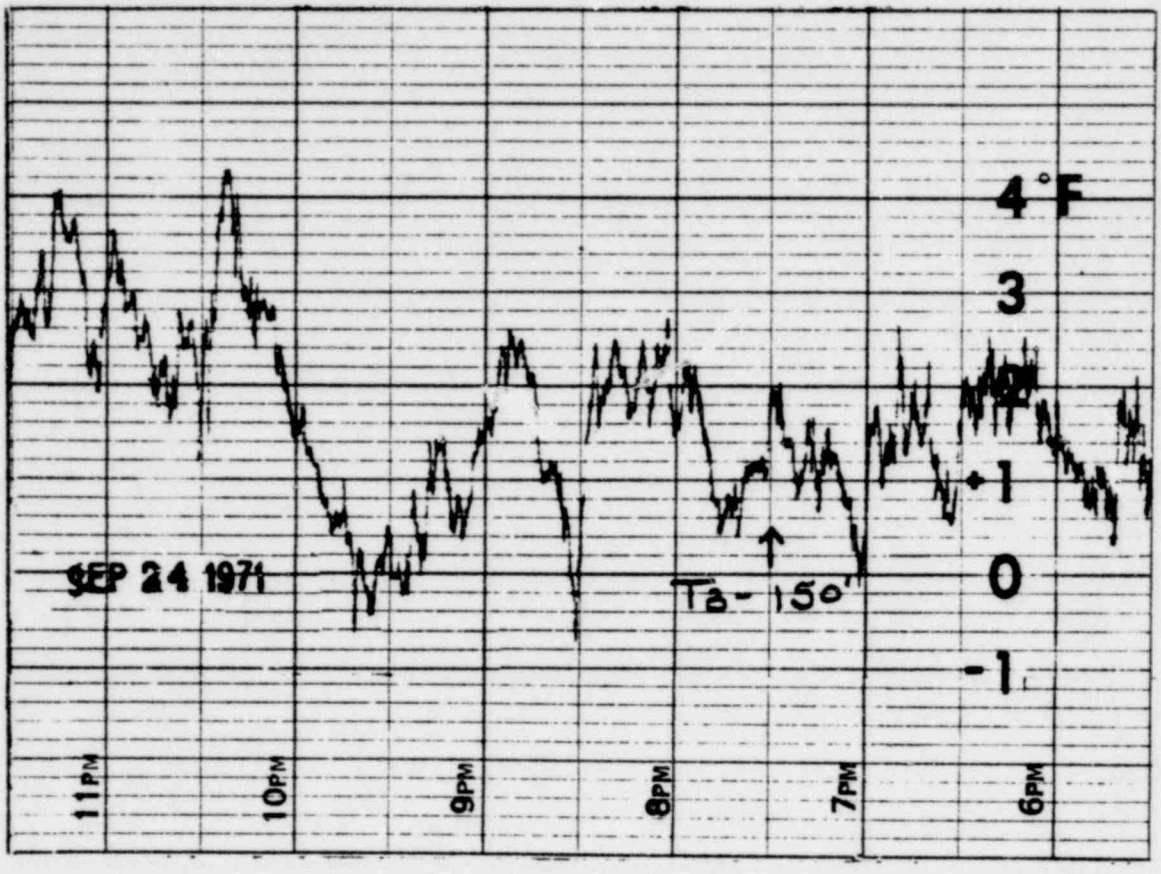

Figure B-4
Example 150 ft-25 ft ΔT Strip Chart

Table B-1

Weather Data Summary

Test	30 ft Weather Measure (South Field)					North 100 ft Tower											South 100 ft Tower				
	Speed	$\bar{\theta}$	R_θ	σ_θ	R_θ/σ_θ	Speed	ΔT_2	θ	R_θ	σ_θ	R_θ/σ_θ	R_ϕ	σ_ϕ	R_ϕ/σ_ϕ	T_{amb}	RH	Speed	$\bar{\theta}$	R_θ	σ_θ	R_θ/σ_θ
2	0.62	132	150	37.3	4.0	1.25	4.26	119	43	10.7	4.0	29	7.4	3.9	46.6	70.0	1.2	93	95	26.6	3.6
3	0.20	142	168	49.4	3.4	1.65	2.97	93	95	26.6	3.6	28	6.1	4.6	66.8	76.3	1.51	84	213	74.1	2.9
4	0.19	41	175	46.7	3.7	0.58	2.83	276	190	48.1	3.6	LW	LW	LW	67.8	76.6	1.2	270	112	19.4	5.8
5	0.15	9	167	40.1	4.2	1.20	0.7	34	30	6.3	4.8	18	4.2	4.2	BD	BD	0.98	0	65	12.5	5.2
6	0.37	131	162	55.4	2.9	0.76	2.05	102	195	73.3	2.7	LW	LW	LW	52.5	56.5	0.67	266	140	47.2	3.0
7	2.0	210	85	NR	NR	1.12	4.4	196	31	7.6	4.1	31	6.3	4.9	62.0	85.0	1.54	195	65	14.2	4.6
8	1.5	100	130	NR	NR	1.79	0.78	130	56	14.2	4.0	26	5.1	5.1	50.0	60.0	1.3	80	85	22.7	3.8
9	1.0	95	70	NR	NR	0.9	5.2	40	165	67.8	2.4	LW	LW	LW	43.5	91.5	0.65	19	150	63.0	2.4
10	NM	NM	NM	NM	NM	0.6	11.6	282	35	9.6	3.6	LW	LW	LW	50.8	76.5	0.15	251	82	21.6	3.8
11	NM	NM	NM	NM	NM	0.87	11.6	97	60	18.2	3.3	LW	LW	LW	50.8	89.8	0.56	11	175	54.3	3.2
12	NM	NM	NM	NM	NM	0.91	3.14	178	75	19.1	3.9	60	15.1	4.0	35.0	67.0	1.8	151	11	3.8	2.9

Note: NM = No measurement taken
NR = Not reduced
BD = Bad data
LW = Wind speed too slow for response

REFFRENCES

1. Slade, D. H., Editor, 1968: Meteorology and Atomic Energy, 1968. AEC, TID-24190, CFSTI, p. 153.

2. Ibid, p. 251.

3. Ibid, p. 112.

4. Safety Guide 4, 1970: Safety Guides for Water Cooled Nuclear Power Plants. U. S. AEC, Division of Reactor Standards, Washington.

5. Collins, G. F., F. E. Bartlett, A. Turk, S. M. Edmonds and H. L. Mark, 1965: A Preliminary Evaluation of Gas Air Tracers. Jour. Air Polln. Control Assoc., 15, 1965, p. 109-112.

6. Turk, A., S. M. Edmonds, H. L. Mark, and G. F. Collins, 1968: Sulfur Hexaflouride as a Gas-Air Tracer. Env. Sci. and Tech., 2, p. 44-48.

7. Turner, D. B.: Workbook of Atmospheric Depression Estimates, PHS Publication No. 999 AD-26, 1967, p. 37.